AN EXPERIMENTAL INVESTIGATION OF THE MAXIMUM KNEE JOINT LOADING DURING LEVEL WALKING

A Thesis Submitted
In Partial Fulfilment of the Requirements
for the Degree of
DOCTOR OF PHILOSOPHY

ME

By
SHRI DAYAL

to the

DEPARTMENT OF MECHANICAL ENGINEERING
INDIAN INSTITUTE OF TECHNOLOGY KANPUR
JANUARY, 1978

I.I.T. KANPUR
CENTRAL LIBRARY
Acc. No. 56205

1978

ME-1978-D-DAY-EXP

TO THE CAUSE OF

BIOENGINEERING RESEARCH IN INDIA

CERTIFICATE

This is to certify that the thesis entitled AN EXPERIMENTAL INVESTIGATION OF THE MAXIMUM KNEE JOINT LOADING DURING LEVEL WALKING by Shri Dayal for the award of the degree of Doctor of Philosophy is a record of bonafide research work carried out by him under my supervision, and has not been submitted elsewhere for a degree.

SSRao

(Dr. S.S. Rao)
Assistant Professor
Department of Mechanical Engineer
Indian Institute of Technolog
Kanpur

JANUARY, 1978.

POST GRA[illegible]TE OFFICE
This th[illegible]is has been approved
for th[illegible]ward of the Degree of
Docto[illegible] Philosophy (Ph.D.)
in acco[illegible]ance with the
regulations of the Indian
Institute of Technology [illegible]anpur
Dated: 10/1/78

ACKNOWLEDGEMENTS

I am grateful to my supervisor, Dr. Samba Siva Rao, for allowing me to work on a problem of my interest; and for initiating me to the computational aspects in finite element analysis. The work of the experimental project was like setting-up a new laboratory; and I am grateful to the Head of the Mechanical Engineering Department for providing the necessary facilities for carrying out the work. I am also thankful to the staff of various laboratories and Fabrication Shop of the Mechanical Engineering Department, for their cooperation in my effort.

My sincere thanks are due to:

Dr. Y.C. Das of the Civil Engineering Department, for allowing prolonged use of the multi-channel recorder along with recording paper from his laboratory;

The Soil Mechanics Laboratory, for allowing use of the input connectors for the balancing unit;

The T.V. Centre, for providing the cameramen and films for cine-photography;

The Head of the ACES for allowing use of electronic components for the operational amplifier;

Mr. and Mrs. D.K. Trivedi, for help in providing the tailor made design of the OP-AMP circuit;

Dr. J.K. Dwivedi, of the Health Centre for useful discussic regarding the anatomical structure of the lower extremity;

I am especially thankful to the following faculty of the Mechanical Engineering Department:

Dr. G.K. Lal, for allowing use of his laboratory equipment, for access to his collection of papers on Dynamometry and useful discussions on the subject, and also for acting as a subject during the experiments

Dr. Raminder Singh, for his keen interest in my work and many fruitful discussions; and also for volunteering to act as a subject;

Dr. B.D. Agrawal, for useful discussions and help in my work and also for acting as a subject;

I am also thankful to the following post-graduate students of the Mechanical Engineering Department for volunteering to act/acting as a subject:

Mr. Kultar Singh, Mr. Sumant Bhattacharya and Mr. V.N. Chandorker.

I also express my gratitude to the following professors abroad for providing copies of relevant papers/useful suggestions:

R.M. Kenedi and J.P. Paul of the Bioengineering Unit, University of Strathclyde, Scotland;

C. Radcliffe of the University of California, Berkeley, U.S.A.;

J. Ramond Pearson of the University of Michigan, U.S.A.;

D.P. Garg of the Duke University, Durham, U.S.A.

Last, but not the least, I am thankful to my wife and children for their patience and understanding during the period of my further studies.

- Shri Dayal

TABLE OF CONTENTS

LIST OF TABLES

Tables

Page

Appendix-C

LIST OF FIGURES

NOMENCLATURE

∂	partial derivative
λ	coordinate transformation matrix
ν	Poisson's ratio
ϕ	angular rotation
σ	stress
$\bar{\sigma}$	stress vector
a	direction cosine
A	ankle; area of finite element
b	width of octagonal ring; direction cosine
B	strain matrix
c	coefficient; direction cosine
d	distance
D	elasticity matrix
DCX	X-direction cosine for axis of tibia
DCY	Y-direction cosine for axis of tibia
DCZ	Z-direction cosine for axis of tibia
DCXN	X-direction cosine for normal to axis of tibia
DCYN	Y-direction cosine for normal to axis of tibia
DCZN	Z-direction cosine for normal to axis of tibia
e	strain
$\bar{e}$	strain vector
E	Young's modulus
EMG	electromyography; electromyograph

F	vertical force
g	acceleration due to gravity
G	centre of gravity
GS	force due to muscle gastrocnemius
H	height
i	index
I	moment of inertia
j	index
k	radius of gyration; element stiffness matrix in local coordinates
$\bar{k}$	element stiffness matrix in global coordinates
K	knee; stiffness matrix of structure
l	direction cosine
L	direction cosine; length of stride
m	direction cosine
M	direction cosine; moment; point of attachment of muscle
n	direction cosine; normal stress component
N	direction cosine; normal stress component matrix
P	force vector; horizontal force on octagonal ring; force in patella ligament
s	shear stress component
S	shank of leg; shear stress component matrix
t	thickness

u	displacement
$\bar{u}$	displacement vector for element
U	displacement vector for structure
V	resultant vector
W	weight
x	axis; coordinate along x-axis
$\bar{x}$	axis; coordinate along $\bar{x}$-axis
X	axis; coordinate along X-axis
y	axis; coordinate along y-axis
$\bar{y}$	axis; coordinate along $\bar{y}$-axis
Y	axis; coordinate along Y-axis
z	axis; coordinate along z-axis
$\bar{z}$	axis; coordinate along $\bar{z}$-axis
Z	axis; coordinate along Z-axis

SYNOPSIS

AN EXPERIMENTAL INVESTIGATION OF THE MAXIMUM KNEE JOINT LOADING DURING LEVEL WALKING

A Thesis Submitted in Partial Fulfilment
of the Requirements for the Degree of
DOCTOR OF PHILOSOPHY
by
SHRI DAYAL
to the
Department of Mechanical Engineering
Indian Institute of Technology, Kanpur
January, 1978

The December 1971 Indo-Pakistan war resulted in a large number of amputees among the army personnel. Consequently the problem, of providing artificial limbs of modern design to the limb fitting centres, attracted the attention of the Defence Ministry, Government of India. The foundation for an "Artificial Limbs Manufacturing Corporation" was laid by the Prime Minister, adjacent to the I.I.T. Campus at Kanpur, in November 1973. It was planned that in the beginning designs borrowed from various countries would be indigenously manufactured; and a research and development centre would be established later on. This research project was motivated by the desire to make some advance towards a national cause.

The consideration of muscle force, in the analysis for maximum loading of the knee joint, had been made by Paul and Morrison of the Bio-Engineering Unit, University of Strathclyde, Scotland, U.K., in 1967. The variation of

resultant knee joint force with time was found to be a three peaked curve, for the stance phase of the gait cycle; and the experimental results indicated that the highest peak was either the first or the third. This aspect was also investigated, in 1974 by Harrington, who also worked at the Bio-Engineering Unit and found that the second peak was the highest. The question regarding timing of the highest peak is related to the identification of the muscle group which would be active during the maximum loading of the knee joint. A unique answer for the order of the highest peak is likely to be of great utility in tackling some of the bio-mechanical aspects like evaluation of muscle fatigue and identification of tibio-femoral contact zone at the instant of maximum loading. The present investigation was made in order to obtain greater insight into the problem.

It had been shown by Paul that the maximum resultant knee joint force increases linearly with the increase of a physical dimensional factor. Since the present investigation was expected to be the first of its kind in India, it was considered desirable to compare the results of the present investigation with those of Paul and to determine if they are influenced to any significant extent by the tropical climate of our country.

The force-plate dynamometers used until now, for measuring the foot-to-ground force actions, had tubular columns

as the elastic deformation elements. As compared to the tubular column, an octagonal ring element proposed by Cook of M.I.T., U.S.A., has the advantage of providing a non-dimensional sensitivity and stiffness characteristic for horizontal versus vertical loading. The octagonal ring elements were, therefore, used in the design of the force-plate which was fabricated for the purpose of experimentation. Based on photoelastic results, Cook had given empirical formulae for determining the deformation characteristics of the octagonal ring element. A more accurate solution for the deformation characteristics was obtained by using the finite element technique. The deflection and strain, due to a central vertical load, were found to be about 13.8 and 27 per cent higher than the values given by Cook's formulae, respectively.

The elastic deformation was sensed by electrical resistance strain gauges; and bridge circuits were formed to measure three force components along and three moment components about a set of reference axes, having their origin at the centre of the top surface of the force-plate. An operational amplifier was developed to amplify the output, before recording the six force components on an ultraviolet light-galvanometer recorder. The effect of cross-sensitivity between different channels was considered while calibrating the force record. The cine-photographic technique, for time and motion study, was used to obtain the displacement pattern of anatomical landmarks on the limb segments during a walk

cycle. A dynamic analysis of the left lower extremity upto the knee joint was performed, considering the effects of external, gravitational, inertial, and muscle force components. The resultant force at the knee joint was calculated for specific timings, which corresponded to the second and the third peaks.

The experiment was performed with three normal adult male subjects, who walked without shoes on a level surface at their natural stride length, which was maintained constant during all the four test runs. A summary curve was prepared for each subject, on the basis of results for all the four test runs, and the average value of the maximum resultant knee joint force was noted. The magnitude of the muscle force at the peaks was also noted and the average values corresponding to the activity of quadriceps femoris and muscle gastrocnemius were found to be 2.33 and 1.92 times the body weight, respectively. The test results indicated that a single muscle or muscle group cannot be identified for the instant of maximum knee joint loading, though in a majority of cases it was the quadriceps femoris. The average value of the maximum resultant knee joint force was found to be 3.59 times the body weight. The general trend of the experimental results compared favourably with that of Paul and suggested no significant influence of the climatic conditions.

The present investigation, as reported above, is of the nature of basic research. It is expected that it would provide greater insight for the design of artificial limbs.

CHAPTER 1

INTRODUCTION

1.1 Motivation

The December 1971 Indo-Pakistan war resulted in a large number of amputees among the army personnel. As a consequence the problem, of providing artificial limbs of modern design to the limb fitting centres, attracted the attention of the Defence Ministry, Government of India. The foundation for an Artificial Limbs Manufacturing Corporation was laid by the Prime Minister, adjacent to the I.I.T. Campus at Kanpur, in November 1973. To begin with, 87 different designs of Limbs, Braces, and Rehabilitation Aids were obtained from other countries for indigenous manufacture. Provision was, however, made for setting-up a Research and Development Centre, to cope with the future needs. Kanpur was selected as the place for setting-up the project because of the existence of a number of industries, which could supply the ancilliary equipment; and also because of the presence of the Indian Institute of Technology, which could effectively interact in the Research and Development effort.

This research project was motivated by the desire to make some advance towards a national cause.

1.2 Historical Developments in the State of Art

The human body may be considered as a complex three-dimensional mechanism. The upper and lower extremities may be likened to a system of levers, different segments of which are connected together by super-universal joints. The system of levers is energized by a large number of muscle-motors and is controlled, to perform a specified task, by an elaborate network of the nervous system.

Walking happens to be one of the primary activities performed by this living mechanism and, therefore, a scientific study of the mechanics of locomotion had attracted attention of the investigators in many countries, during the past. The Weber brothers (1836), in Germany, made a study of human gait, based on experimental evaluation of cadavers and live subjects. Their most significant findings were that the leg behaves as a simple pendulum during the swing phase of gait cycle, and that there is no muscular action involved during this period. They also found that the tension developed by a muscle is proportional to the shortening in length it undergoes. Braune and Fischer (1872) made a study of the kinetic properties of human body segments. Marey (1873 and 1887), in France, conducted experiments for determining the locus of the centre of pressure at the sole of the foot and vertical displacement of the body during walking. He also made computations of the

energy output during locomotion; and developed the technique of chro no-photography, in which successive exposures were made on the same photo-graphic plate by means of a rotating disk in front of the camera.

Bernstein (1935 and 1936), in the U.S.S.R., improved upon the results obtained by Fischer in respect of the mass properties and centroids of limb segments. Elftman (1934 to 1941), in the U.S.A., made a study of the various aspects of locomotion, like the distribution of pressure in human foot, the function of arms in walking, the rotation of body in walking, the force exerted by the ground in walking, the forces and energy changes in walking, the function of muscles in locomotion and the action of muscles in the body. He is credited for the development of a "force plate" for measuring the foot-to-ground force actions. The force plate was spring supported and had a mechanical system to magnify the spring deflections. In the U.S.A., a research effort on a national level was started, in the late forties, for conducting fundamental studies on locomotion at the University of California, Berkeley (1947). The need for information on the loading pattern at the joints, useful for the orthopaedic surgeon as well as the designer of artificial legs and braces, shifted the emphasis on the analysis of joint reactions.

A force plate dynamometer was developed by Cunningham and Brown (1952), for the measurement of foot-to-ground force

actions. It was a device using strain gauges mounted on four tubular columns, kept between the top and bottom plates. The dynamometer could measure forces along the three reference axes with origin at the centre of the force plate, the torque about the vertical axis, and also the position of the centre of pressure of foot on the force plate. The quantities under measurement were recorded, as an electrical signal, on an oscillograph tape. Using this force plate and the cine-photographic technique to obtain a simultaneous record of the position of leg in space, Bresler and Frankel (1950) evaluated the three force components and the three moment components acting at the ankle, knee and hip joints during level walking. They could not, however, consider the muscle forces in the analysis and determine the joint reactions.

An evaluation of hip joint force, by direct measurement, was made by Rydell (1965, 1966). He implanted an artificial femoral device (modified Austin-Moore prosthesis) carrying strain gauges, in the thigh of two patients who had suffered fracture of the neck of the femur. The maximum value of joint force for the two subjects, during normal walking, was found to be 3.3 times the body weight. One of the subjects was a male and the other a female. The joint forces were higher in the later case, in general. The peak value of the joint force during all the tests was 4.33 times the body weight, which occurred while the female subject was running.

The knowledge that muscle activity in the human body is controlled by communication of electrical impulses from the central nervous system, led to the developments in electromyography, which is subsequently referred to as EMG. Various attempts were made to collect the myoelectric signals from individual muscles by means of implanted as well as surface electrodes; and to co-relate these signals to the force developed by the muscles [Lippold (1952), University of California (1953), Bigland and Lippold (1954), Close and Todd (1959), Joseph and Battye (1966), and Paul (1971)]. The findings indicated that the intensity of EMG signals was dependent upon the type of electrodes used and their placing; that there happens to be a time lag between the maximum muscle force and the peak value of myoelectric signal; that the signal intensity depends on the instantaneous length and rate of change of length of the muscle; and also that the calibrating procedure cannot be designed in such a way that the entire load is taken up by a single muscle. The EMG signals can, at best, be taken as an indicator of the phasic activity of the muscles.

This information was used, to advantage, by Paul (1967) and Marrison (1968, 1970) of the Bio-Engineering Unit, University of Strathclyde, Glasgow, Scotland. They assigned the external moments at the hip and knee joints to the balancing moments due to action of probable muscles, and

calculated the joint reactions. Using the cine-photographic technique, as used earlier by Bresler and Frankel, they obtained data on the displacement pattern of anatomical landmarks on the limb segments, during a walk cycle. The foot-to-ground force actions were measured by a modified version of the force plate developed earlier by Cunningham and Brown. This force plate also had four tubular columns, on which strain gauges were applied to sense three force components along and three moment components about the reference axes. The force components were recorded on a six-channel, ultraviolet light, galvanometer recorder. Using the equations of equilibrium and making some simplifying assumptions, the joint reactions were calculated. Normal subjects, both male and female, in the age group of 18 to 36, were examined during 15 tests on level walking. The resultant knee joint force was found to have a three peaked curve during the stance phase of the walk cycle. The results indicated that the highest peak was either the first or the last, which occurred during activity of the hamstrings and muscle gastrocnemius, respectively. The average maximum values of the resultant forces at the hip and knee joints were found to be 3.9 and 3.4 times the body weight, respectively. The peak values of these ratios, during all the tests, were 6.4 and 4.46, respectively.

Paul (1970) proposed a linear relationship between the average maximum joint force and a factor, consisting of the

product of body weight with the stride length per gait cycle and divided by the subject height.

Paul and Poulson (1974) extended the analysis to cover more activities than normal walking. The rates of change of loading were calculated. The presence of antagonistic muscle activity, and the fact that it could result in considerably higher magnitudes of joint reactions, was recognized. It was argued, however, that the antagonistic muscle activity occurs in regions which are 10% of the cycle before and after heel strike; and that the maximum values of joint loads do not occur during these periods. It was also indicated that the experimental techniques employed could cause the overall result to be in error by 50%.

Harrington (1974), working at the Bio-Engineering Unit, University of Strathclyde, made a study of the knee joint loading for normal adults, normal children and pathological subjects. He also used the force plate cum cine-photographic technique during his experimentations. A summary knee joint force curve was reported for the four normal adult males, which shows that the second and third peaks are the highest and the next lower. The timings for these peaks were about 30% and 80% of the stance phase; and occurred during activity of quadriceps femoris and muscle gastrocnemius, respectively. The ratio between the maximum joint force to body weight was found to be 3.5.

Winter et al. (1974) developed a Television-Computer system, for the measurement and analysis of kinematics of locomotion, at the University of Manitoba, Canada. The use of accelerometers (Ryker and Bartholomew, 1951) or goniometers (Lamoreux, 1971) was considered prohibitive in view of the time required to fit and align them; and because of their interference with normal gait. Circular reflective markers were applied at anatomical landmarks, whose space coordinates were to be obtained. The kinematic data was supplemented by an EMG telemetry system for muscle activity and phasic signals from the micro-switch shoe (Winter et al., 1972). A statistical study, based on data collected during 3 or 4 strides of the subject, was made. Velocities and accelerations in many ranges, not covered previously, were reported. The advantage of the system was the automatic reduction of kinematic data, but the data collection was limited to the sagittal plane. Also the accuracy of measurements could not be as high as in the cinephotographic technique.

Spolek et al. (1975) developed an instrumented shoe system, which could be used to obtain the lower leg loading envelopes during non-laboratory situations. The elastic deformation members were two rectangular cross-bars, each of which was held between two mounting plates, under the sole of the shoe. One of the cross-bars was kept under the heel

while the other under the toe. Strain gauges were applied on the cross-bars to sense three force components – fore and aft shear, medial-lateral shear and axial compressive component; and one moment component – the axial torque. Rotary potentiometers were also mounted to obtain anterior-posterior and medial-lateral angular motions of the leg relative to foot. The principal design aim of the device was to obtain the magnitude of torque on the tibia during sharp turns. The system would not, however, be suitable as a general purpose device, owing to its interference with the normal gait characteristics.

Numerous mathematical models can be found in the literature for analysis of human body dynamics, using rigid body idealization with active controls at the different joints.

A synthesis of biped locomotion machines was reported by Frank and Vukobratovic (1969). Townsend and Seireg (1972a, 1972b and 1973) developed a computer based procedure for the trajectory synthesis and control of bipedal locomotion for optimum stability and energy expenditure. The procedure, however, could not consider the individual muscle actions and load sharing between them. The problem of determining the load sharing between the different muscles, in order to maintain a particular posture, was investigated by Seireg and Arvikar (1973). Using a linear programming procedure, the

model could be let to predict without prior selection, the participating muscles and the forces carried by them. Only a criterion for muscular load sharing was to be selected beforehand. The criterion used, during static posture and quasi-static locomotion, was the minimization of a weighted sum of all the muscle and ligament forces. These forces were assumed to provide any unbalanced moments at the joints. The problem of quasi-static locomotion was tackled by Seireg and Arvikar (1975) and the joint forces were predicted. Locomotion under fully dynamic conditions could not be investigated because of lack of dynamic data for all body segments and the corresponding ground reactions. Recent developments in the technique of "interactive computer graphics" (Newman and Sproull, 1973) have enabled reformulation of an existing model of the human musculo-skeletal structure. In a project carried out at the University of Wisconsin, Williams and Seireg (1977) have developed an interactive computer model which can study a variety of complex dynamic activities. The muscle load sharing, as obtained from the model, is compared with the pattern of EMG signals from various muscles and the model is modified to match the existing trends. A significant weakness of this technique lies in the fact that the EMG signals represent only the phasic activity of muscles and not the magnitudes of load shared by them.

1.3 Discussions, and Objectives of the Present Investigation

Although the experimental evaluation of the resultant knee joint force during normal level walking was reported by Paul (and Morrison) in 1967 and by Harrington in 1974, a basic question, regarding the timing and muscle participation during maximum loading of the knee joint, has remained unanswered. The variation of resultant knee joint force with time was shown to be a three-peaked curve by Paul; and on the basis of 15 tests, which also included female subjects, it was concluded that the highest peak was either the first or the last. Harrington reported a summary curve, for four adult males, from which it was observed that the second peak was the highest and the next lower one was the last.

Since different results were reported for the highest peak, in the earlier two investigations, it was considered desirable to make further investigation in this regard. It would be noted that the question about timing of the highest peak is related to the identification of a specific muscle or muscle group which would be active during maximum loading of the knee joint. In case of a unique answer, it would be of great utility in tackling some of the bio-mechanical aspects like evaluation of muscle fatigue and identification of tibio-femoral contact zone at the instant of maximum loading.

It was shown by Paul that the resultant knee joint force increases linearly with the increase in the value of a physical dimensional factor. Since the present investigation was expected to be the first of its kind in India, it was considered desirable to compare the results of the present investigation with those of Paul and to determine if they are influenced to any significant extent by the tropical climate of our country. It would be worthwhile to observe in this connection that, by habit, inhabitants of cold climate walk faster than those belonging to the tropical climate.

The force plate cum cine-photographic technique for experimental measurements, though used by Bresler and Frankel as early as 1950, is considered to be the most accurate even now. It was noted, however, that very little developments have taken place in the design of the force plate during the past. After the development of the force plate, at the University of California, by Cunningham and Brown in the early fifties, only minor design modifications were made by the University of Strathclyde team in the late sixties. In both the designs, the spring elements undergoing elastic deformation, which was sensed by strain gauges, were four tubular columns. Cook et al. (1954 and 1963) have shown the utility of octagonal ring elements for use in multi-component dynamometers. As will be shown later, in Section 2.2, the horizontal load to vertical load ratio between sensivity and stiffness for an

octagonal ring is independent of the physical dimensions, while it does not hold good for the tubular column. Based on the results of photo-elasticity, Cook had proposed empirical formulae for the deformation characteristics of the octagonal ring.

It was decided to use octagonal ring elements in the design of the force-plate; and to work out a more accurate solution for the deformation characteristics of the octagonal ring, by using the present day technique of finite element analysis.

1.4 Outline of the Experimental Analysis

It was proposed to obtain test results, on maximum knee joint loading, for three normal adult male subjects. The subjects were to walk without shoes on a level surface at their natural stride length. The natural stride length of a subject was to be ascertained prior to the test runs. A method was to be devised such that there was minimum variation in the stride length of a subject during different test runs. The advantage seen in so doing was to obtain a reduction in the amount of scatter for magnitude of maximum resultant knee joint force, while comparing, the results of different test runs by a subject. Each subject was to have four test runs.

The foot-to-ground force actions, during the stance phase, were to be measured by a force plate dynamometer. The force plate was to be positioned, in a portion of the walk platform, to receive the left foot of a subject on its top surface. Octagonal ring elements were to be used in the design of the force plate; and the electrical circuitry was to be matched for obtaining a record of the six force components on an ultraviolet light-galvanometer recorder. The dynamometer was to be calibrated for determining the magnitudes of the six force components. The effect of cross-sensitivity, between different force channels, was to be taken into account during calibration.

Circular adhesive markers were to be placed over anatomical landmarks of the left lower extremity and the position of the limb was to be simultaneously recorded, in the anterior/posterior and medial/lateral planes, by using cine-photography. After each test run, a large size illuminated graph was to be placed on the surface of the force plate such that a vertical line of the graph was positioned over its centre. The graph was also to be recorded in the field of view of the two movie cameras, without any alteration in their position. The cine films were to be projected on a stop-action projector and the position of markers, in each frame, was to be noted with reference to the lines of the graph. The marker positions

were to be used for establishing the reference coordinates of the ankle and knee centres, during the stance phase. The required kinematic data, for analysis, was then to be calculated from the reference coordinates.

The analysis, for knee joint loading, was to be performed in the regions of the second and third peaks during the stance phase. The musculature active during these periods was to be assumed on the basis of conclusions derived from a comparison between the EMG results of a number of investigators and the variation of extending/flexing knee moment with time. It was also to be assumed that there was no antagonistic activity between different groups of muscles. A dynamic analysis of the limb segment upto the knee joint was to be performed for determining the maximum values of muscle force and the resultant knee joint force. The overall result, regarding the maximum resultant knee joint force for a subject, was to be obtained by averaging the values for different test runs, corresponding to a particular instant of time, and plotting a summary curve. The summary curves, for all the three subjects, were then to be compared to determine if there was any consistency, regarding the order of the highest peak, for maximum knee joint loading.

CHAPTER 2

MEASUREMENT OF FOOT-TO-GROUND FORCE ACTIONS

2.1 Introduction

The analysis of resultant force at the knee joint requires consideration of all the force actions, either external or internal, which may be acting on the free body of the limb segment upto the position of the joint. The ground-to-foot reactions form a part of the external force actions; and are equal in magnitude but opposite in sign to the force actions imparted by the foot to the ground. Therefore, the measurement of foot-to-ground force actions is a basic necessity for the problem at hand. In the past, a dynamometer designed to measure these force actions was conventionally called a 'force plate'. This chapter is devoted to the development and calibration aspects of a force plate, which was used to measure three force components along and three moment components about a set of reference axes, having their origin at the centre of top surface of the force plate.

2.2 Generalised Scheme of Measurement

In the context of the measurement of six force components, a generalised scheme for the measurement of a

single force component is depicted in the block-diagram of Figure 2.1. The force component, when applied to a spring element, causes elastic deflection which may be sensed by a transducer to render it in the form of an electrical signal. The electrical signal may require amplification or attenuation before being displayed/recorded. The output signal has to be calibrated, by application of a known magnitude of the force component, before an unknown magnitude of the force component can be measured.

2.3 Review and Relative Merits of Spring Elements in Use

The basic physical form of the spring elements used in various force measuring devices may be classified according to the nature of force applied to them and the resulting deformation. The elastic element may carry a tensile/compressive force; or be subjected to bending/twisting moment. The bending element may be either a cantilever, a simply supported beam, or a fixed beam. An elastic element is sometimes made of hollow cross-section, in order to enhance sensitivity to the applied force. However, the element should not only be sensitive to the applied force but must also be sufficiently stiff, so as to resist undue deflection.

In the course of development, special elements have been identified which provide a high ratio of

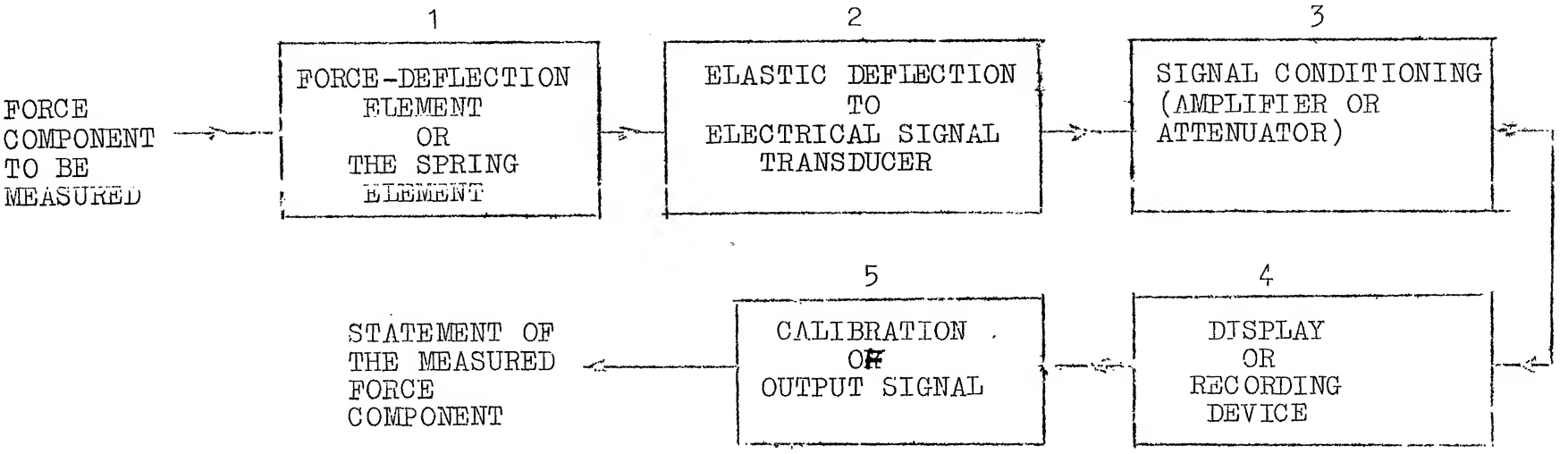

Figure 2.1 Block Diagram for the Generalised Scheme of Measurement

sensitivity to stiffness i.e. for the same stiffness of the two elements, the strain due to load is considerably higher for the special element. The circular and octagonal rings shown in Figure 2.2, fall in the catagory of special elements. Their principal dimensions and load directions are also indicated in Figure 2.2. When a single force component is present, the circular rings have been extensively used for fabricating load cells and proving rings. The elastic deformation of a circular ring may be found by using curved beam theory. There are strain nodes, i.e. points of zero strain, due to the vertical and horizontal loads at orientations of 39.6° and 90° from the vertical, respectively. This property helps in separating the force components by suitably positioning the transducer elements of block 2, Figure 2.1. The electrical resistance strain gauges have been widely used as the elastic deflection to electrical signal transducers. Their principal advantages are the high sensitivity, very small size and weight, and suitability for use in static as well as dynamic measurements. Two additional advantages, which result from the use of Wheat Stone's bridge circuit, are the elimination of temperature effects, and the adding together of signals due to tensile and compressive strains. The circular ring has, however, a tendency to roll due to action of the horizontal force, P. The ring, therefore, cannot be

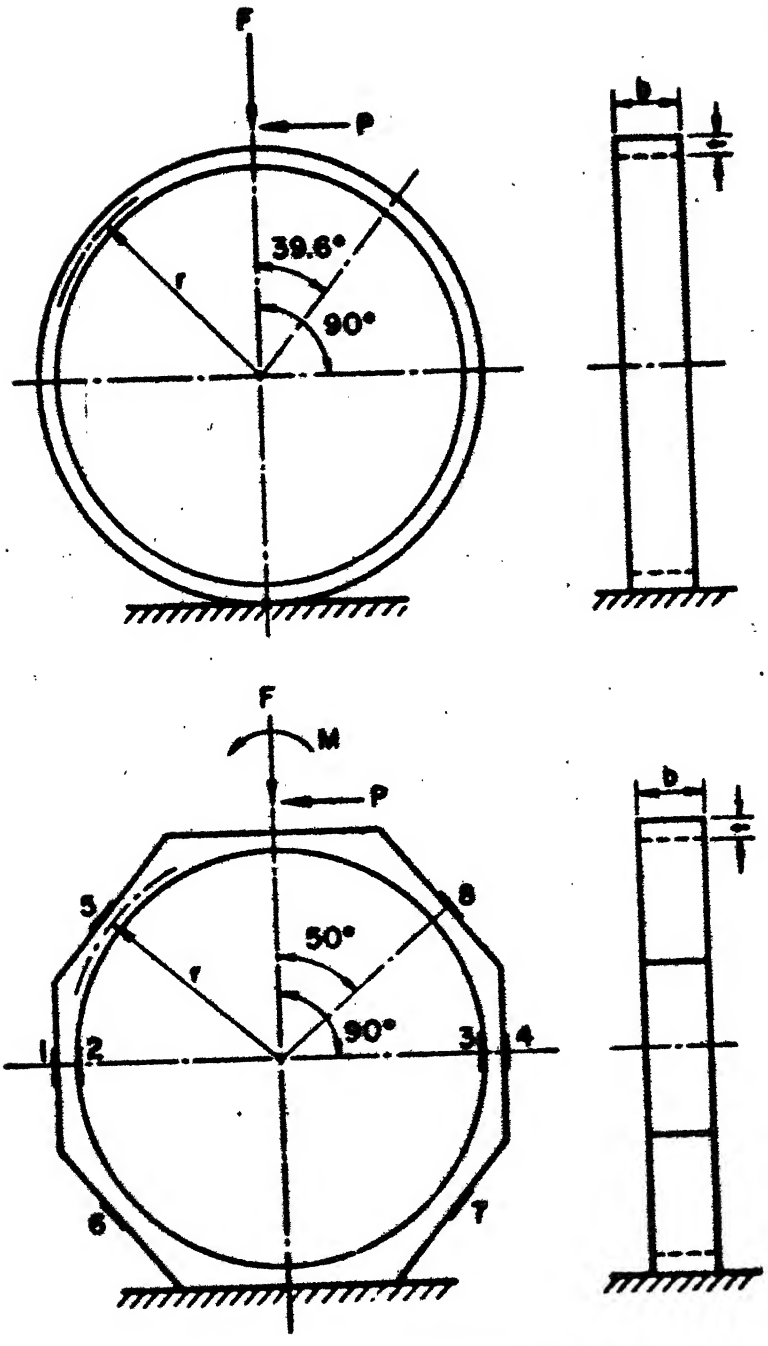

Fig.2.2 Circular and Octagonal Ring Elements

perfectly fixed at the base, resulting in lack of stability. This shortcoming was overcome by providing flat faces at the top and bottom; and using an octagonal shape, which also results in increased stiffness of the ring. However, on account of changed boundary conditions, there is no elasticity solution. Using photoelasticity, it was found that the strain nodes now occur at orientations of 50° and 90° from the vertical (Loewen and Cook, 1955). The following empirical formulae were proposed by Cook, for the strain and deflection due to the vertical and horizontal loads (Cook and Rabinowicz, 1963):

$$\text{Strain}_{90^\circ} = 0.7\,\frac{Fr}{Ebt^2} \qquad \text{Strain}_{50^\circ} = 1.4\,\frac{Pr}{Ebt^2}$$

$$\text{Deflection}_{90^\circ} = 1.0\,\frac{Fr^3}{Ebt^3} \qquad \text{Deflection}_{50^\circ} = 3.7\,\frac{Pr^3}{Ebt^3}$$

Since the stress pattern was found symmetrical about the vertical axis through the centre of the ring, a half-octagonal ring could also be used to sense the vertical and horizontal loads.

The performance of a spring element, as a force sensing unit, is assessed on the basis of sensitivity as well as stiffness under loading. Both these quantities should be as high as possible. If e denotes the strain magnitude and d denotes the deflection associated with the

application of a force component F, the strain sensitivity and stiffness to the force component can be expressed as e/F and F/d, respectively. Therefore, the product $\frac{e}{F} \cdot \frac{F}{d}$ of $\frac{e}{d}$ i.e. strain per unit deflection, should have a high value.

As mentioned in Section 1.2, the spring elements used in the earlier force plates were four tubular columns. For a tubular column, if d_o and l are the outside diameter and length, respectively, the value of the ratio $\frac{e}{d}$ can be shown to be $\frac{1}{l}$ for the vertical load along the axial direction. For the horizontal load, assuming the tube to be a cantilever fixed at the lower end, the value of the ratio can be worked out as $\frac{3}{2} \frac{d_o}{l^2}$. The relative sensitivity and stiffness ratio, for the horizontal versus vertical load, can therefore be seen to be $\frac{3}{2} \frac{d_o}{l}$. The magnitude of this relative ratio depends on the physical dimensions of the tube. For the University of California force plate, designed by Cunningham and Brown (1952), where the values of d_o and l were 0.688 in. and 5.25 in., respectively, the value of $\frac{3}{2} \frac{d_o}{l}$ works out to 0.196. In comparison, in case of an octagonal ring, the values of $\frac{e}{d}$ can be shown to be $0.7 \frac{t}{r^2}$ for the vertical load and $0.378 \frac{t}{r^2}$ for the horizontal load. In this case, the relative sensitivity and stiffness ratio works out to 0.54. Thus, in case of an octagonal ring, not only the sensitivity to stiffness ratio is higher,

there is an additional advantage that the relative sensitivity and stiffness ratio is independent of the physical dimensions. This is a unique advantage from the design point of view, since there is no limitation on the size of rings to be used.

2.4 Force Components Sensed by An Octagonal Ring

Referring to Figure 2.2, the vertical force component, F, can be sensed by strain gauges placed in positions 1, 2, 3 and 4. The strain gauges in positions 5, 6, 7 and 8 can be used to sense the horizontal force component, P. The Wheatstone's bridge circuits for sensing F and P are shown in Figure 2.3(a). Also shown in this figure is the bridge circuit for sensing the moment M, which can be obtained by simply interchanging two arms of the circuit for F. The bridge circuits can be easily grasped if the strain gauges which undergo tension and compression, due to action of a force component, are identified. This aspect has been explained in Figure 2.3(a), by stating the strain gauge position numbers against T or C. It can be verified that the bridge circuits are insensitive to any other force component than for which they have been assigned.

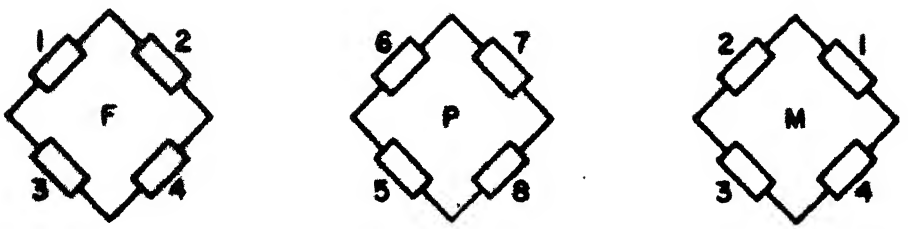

T - 1,4
C - 2,3

T - 6,8
C - 5,7

T - 2,4
C - 1,3

Fig.2.3(a) Bridge Circuits for Force Components sensed by an Octagonal Ring

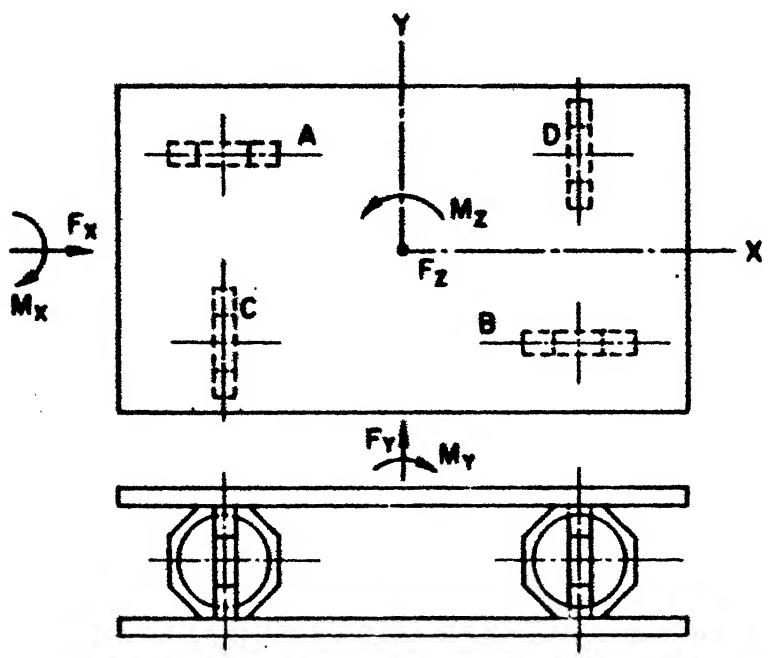

Fig.2.3(b) Schematic Ring Arrangement in a Six Component Dynamometer

2.5 Arrangement of Octagonal Rings in a Six-Component Dynamometer

The schematic arrangement of rings, for sensing six force components is shown in Figure 2.3(b). It consists of four octagonal rings A, B, C and D, placed between the bottom and top plates. Strain gauges are mounted on all these four rings at suitable orientations, in accordance with the basic scheme outlined in Section 2.4. The force component along the X-axis can be sensed by the rings A and B; while the force component along the Y-axis can be sensed by the rings C and D. The force component along the Z-axis can be sensed by using all the four rings A, B, C and D. The moment components about the X and Y axes can be sensed by using the ring sets C-D and A-B, respectively. The moment component about the Z-axis can be sensed by using either of the ring sets A-B or C-D. In each of these schemes, a force component can be sensed irrespective of its position on the top plate and, in an ideal case, without influence of the other force components.

2.6 Design of the Octagonal Rings

The octagonal rings, used in the six component dynamometer, were designed as part of a laboratory project even before the present research project was taken up. The problem assigned at that time was to measure only four

force components – the three forces along the reference axes, and a moment component about the vertical axis. The strain gauge bridge circuits were also formed to sense the four force components. Later on, when some papers from the Bio-engineering Unit, University of Strathclyde, Scotland, were available, it was felt that a generalised approach to analysis can be made by measuring all the six force components.

The ring dimensions were chosen to ensure sufficient stiffness of the ring under maximum loading. At the same time, it was also checked that the strain due to minimum loading was large enough to be sensed by strain gauges. An estimate of the magnitude of loading was made in accordance with the description of force components by Klopsteg and Wilson (1968). The maximum value of the vertical force component was taken as 500 lb., which could result if the subject was running and all the foot pressure was concentrated on a single ring. The minimum value of the force component in the horizontal plane was taken as 10 lb. The deflection of the ring under a central vertical load was assumed as 0.05 in.; and, with reference to Figure 2.2, it was also assumed that r = 1.5 in. and b = 3t. Using Cook's empirical formula for deflection under a central vertical load, the thickness of a steel ring was found to be 0.1386 in. The strain due to minimum horizontal load was found to be 60 micro in./in., which was considered

adequate. The dimensions of the ring, which were finally adopted, were the following:

$$r = 38 \text{ mm}; \qquad t = 4 \text{ mm}; \qquad b = 12 \text{ mm}$$

2.7 Physical Form of the Dynamometer

The six component dynamometer made use of the octagonal rings described in Section 2.6. Full as well as half octagonal rings were used in order to utilize the rings on which strain gauges had already been mounted. The structural arrangement of the dynamometer fabricated is shown in Figure 2.4. The natural frequencies of the structural system for vertical and horizontal oscillations were about 364 c/s and 134 c/s, respectively. The basic structure, of Figure 2.4, was supported on a base plate which was bolted to the bottom plate of the dynamometer. Four levelling screws were provided on the base plate, close to the corners of the bottom plate. The particular utility of the base plate was in mounting the dynamometer on a stand, for the purpose of calibration. The pulley systems used for loading the dynamometer could also be supported on the base plate. A connection panel, for the strain gauge circuits, was provided in the front portion, and aluminum cover plates were provided on the remaining three sides. The connection panel and the cover plates

Sl. No.	No.Off.	Description	Material	Size
5	1	Bottom Plate	MS	360X200X6
4	1	Top Plate	MS	360X200X6
3	4	Octagonal Ring	MS	80 Face to Face, 4 Thick
2	4	Half Octagonal Ring	MS	80 Face to Face, 4 Thick
1	24	CSK Screw	MS	M5, 12 Long

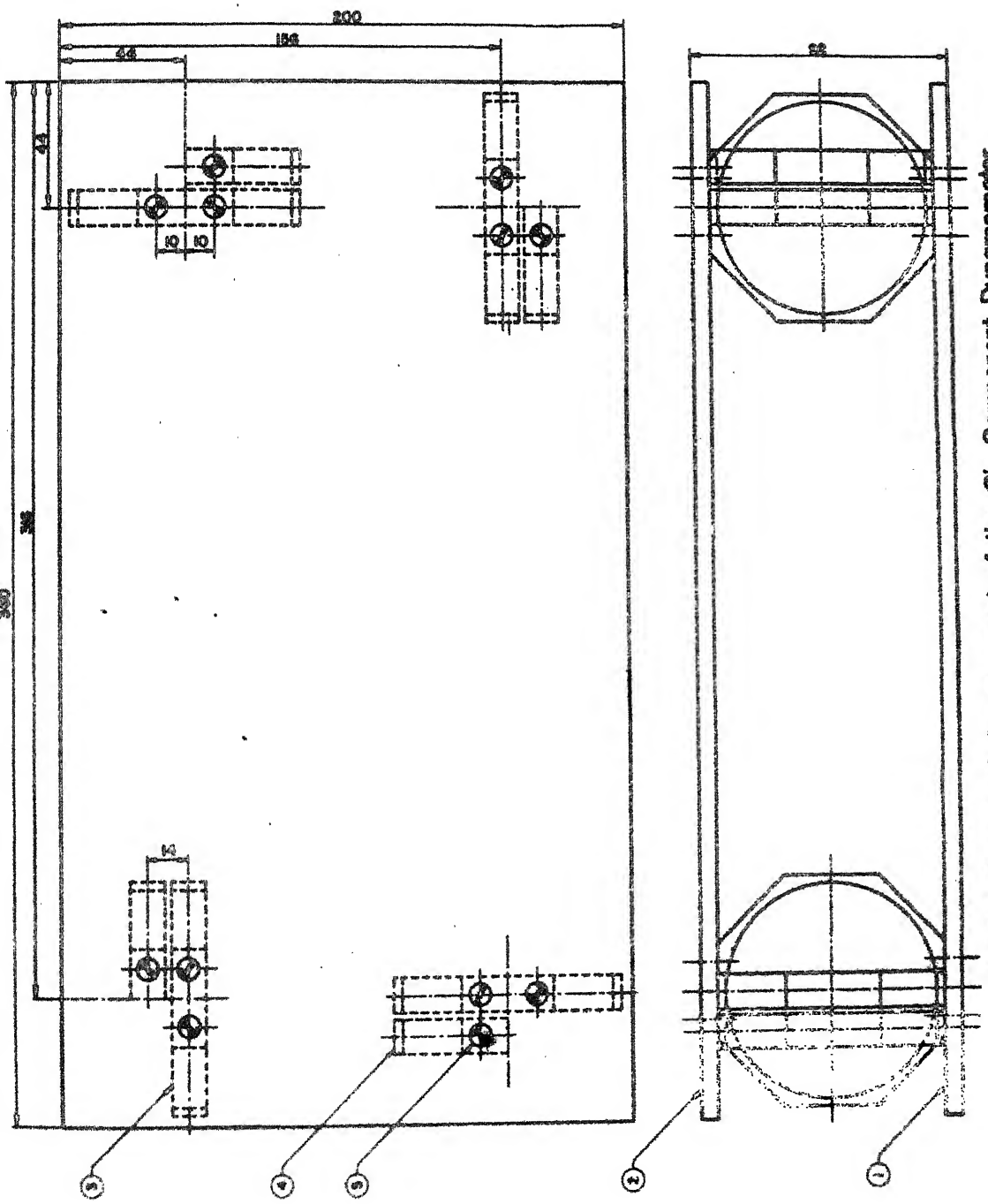

Fig.2.4 Structural Arrangement of the Six Component Dynamometer

were supported on brackets, which were screwed to the bottom plate of the dynamometer.

2.8 Strain Gauge Circuits for the Six Force Components

The strain gauge circuits were formed in accordance with the general principles stated in Sections 2.4 and 2.5. The design of these circuits was also influenced by considerations of impedance matching with that of the galvanometers used in the recorder. The optimum value of the output impedance of a bridge circuit was 120 ohm. The strain gauge circuits for the six force components are shown in Figure 2.5(a). The strain gauges used for forming the bridge circuits had a nominal resistance of 120 ohm and a gauge factor of the order of 2.0. The width of the resistance element was 3 mm and that of paper used for bonding was 6 mm. Thus, on the octagonal rings of width 12 mm, two such gauges could be placed side by side. The strain gauges were of an Indian make and had a very low current carrying capacity, which was not specified by the manufacturer. In the initial stages, considerable difficulty was experienced due to burning out of gauges, when 'Budd' strain indicators were used for the display of output signals. These strain indicators made use of a reference bridge system and 1.5 volt A.C. excitation at a carrier frequency of 1000 c/s. Later on, the bridge circuits were

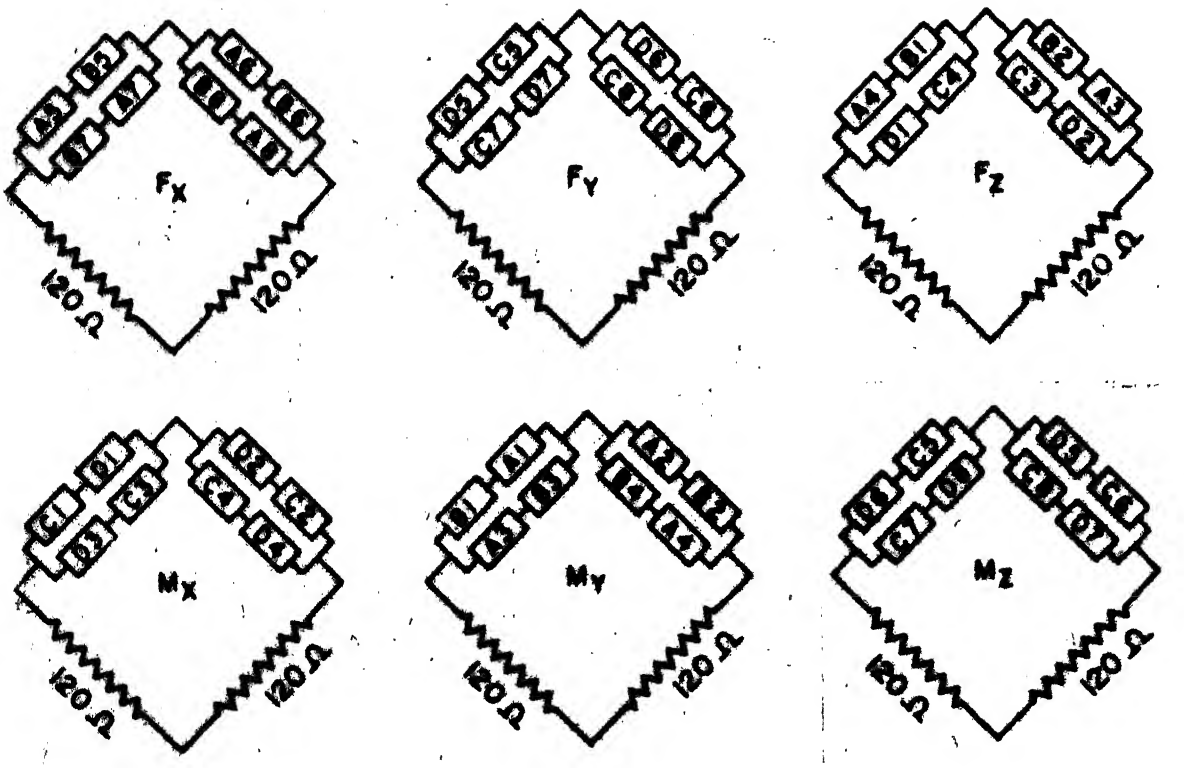

Fig.2.5(a) Strain Gauge Circuits for the Six Force Components

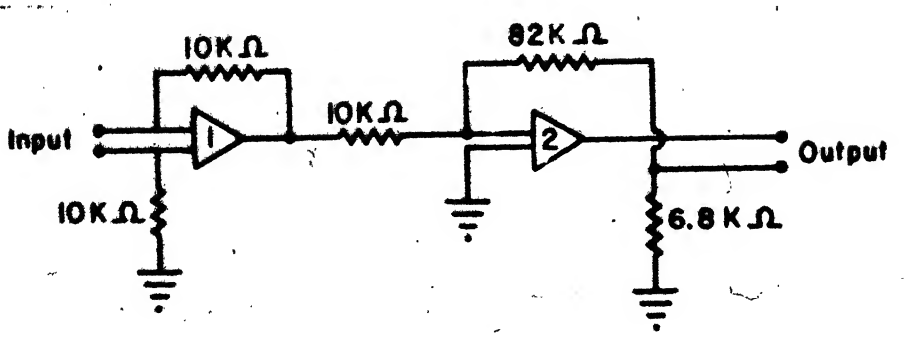

Fig.2.5(b) Operational Amplifier Circuit for one Force Channel

D.C. excited, at a low potential, to keep a very low gauge current in the range of 1.0 mA. A current amplifier was provided to increase the signal amplitude to a convenient level. Each bridge circuit had two active arms; the remaining two arms were provided by 120 ohm resistors, located inside the balancing unit used.

2.9 Description of Associated Electrical Circuitry

A block diagram, representing the electrical circuit elements, for recording the six force components is shown in Figure 2.6; and the equipment used is shown in Figure 2.7. A bank of 1.5 volt accumulators, providing 6 volt D.C. supply, was connected to the input terminals of the 'Bridge Balance Unit', for excitation of the strain gauge circuits. The voltages across each bridge could be adjusted for the required signal sensitivity. Balancing of the bridge circuits could be done by turning the potentiometer knobs, on the panel of the balancing unit. A six channel operational amplifier circuit was tailor made to provide the current amplification for the output signals, such that they could be displayed on the recorder. The circuit for one channel of the operational amplifier unit is shown in Figure 2.5(b). Amplification of the order of five times the input current was required, such that the output current was of the order of 10 mA. I.C. elements,

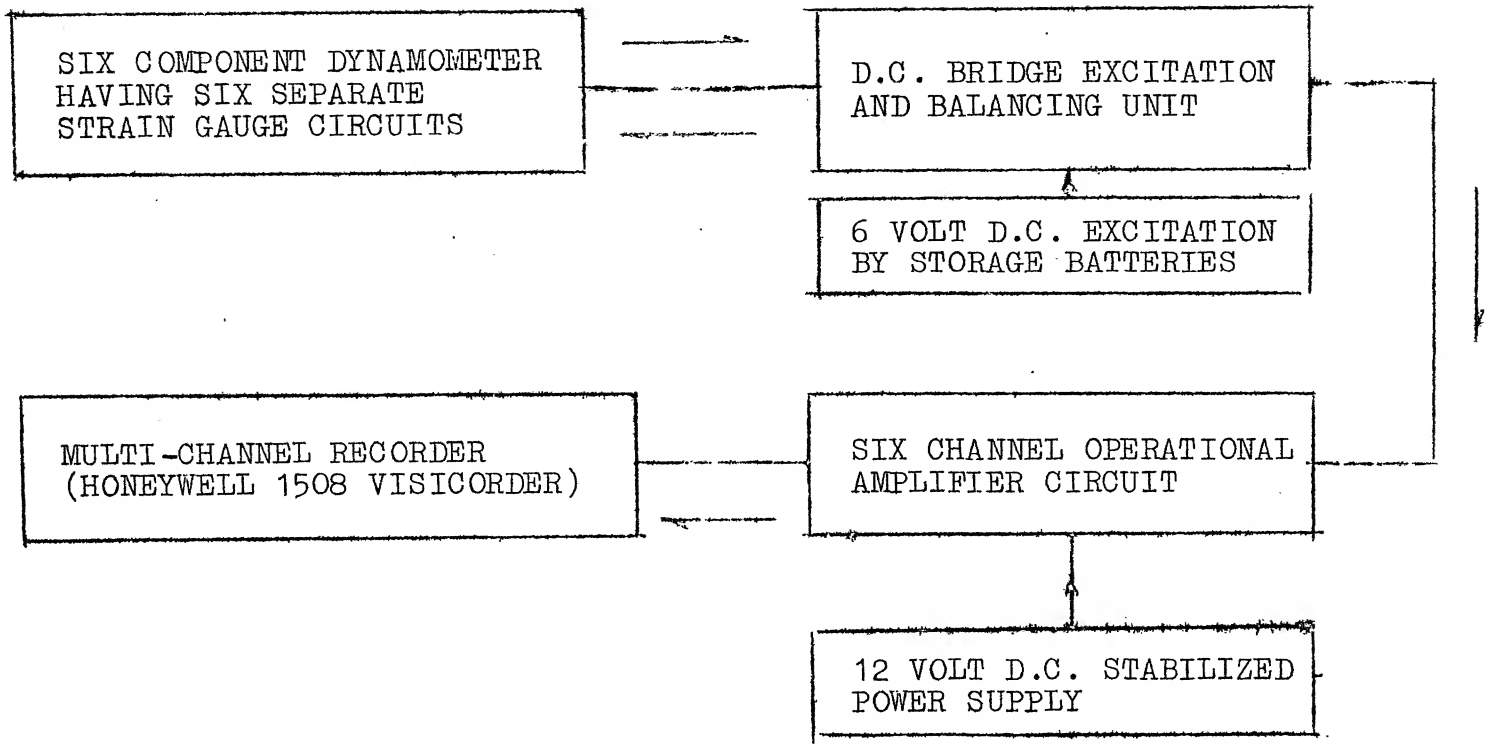

Figure 2.6 Block Diagram for Recording the Six Force Components

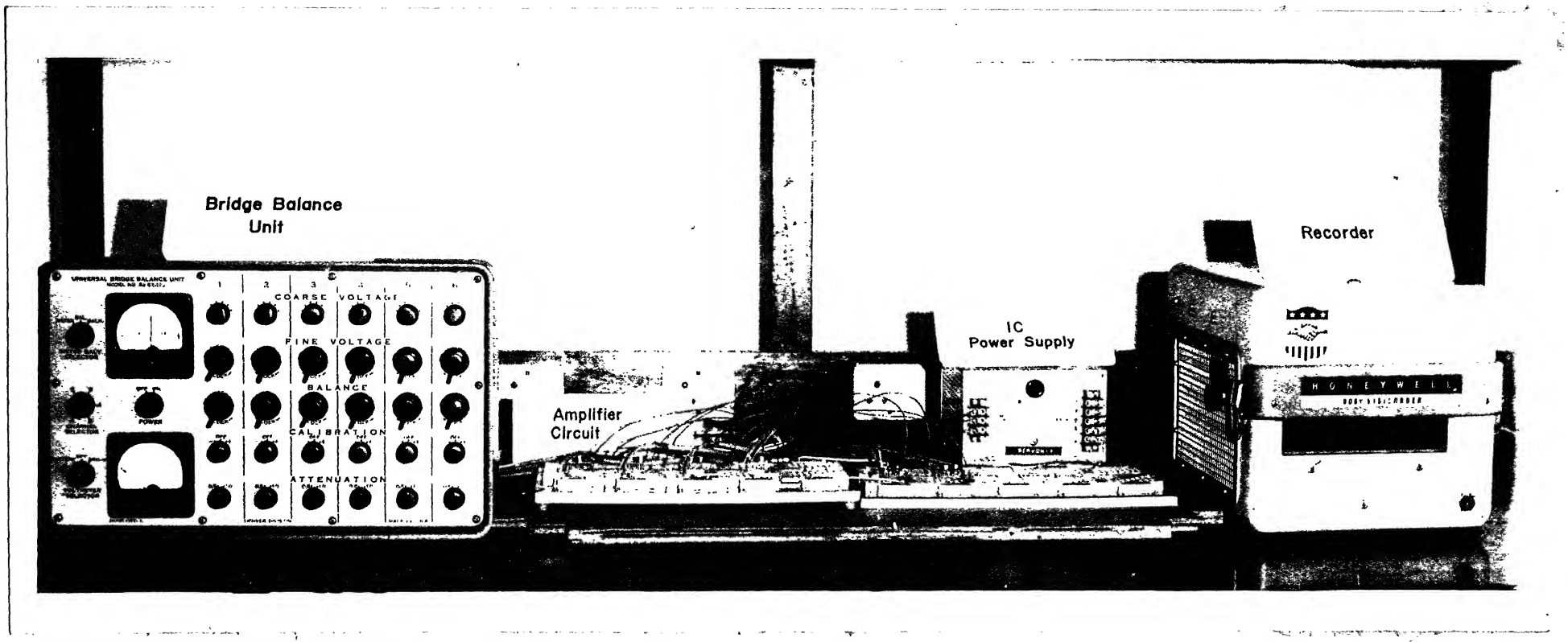

Figure 2.7 Equipment used in Recording the Six Force Components

741 and 741-C, were used in the assembly of the amplifier units. The 12 volt D.C. power supply for the amplifier circuit was provided by a standard power source, energized from the mains. The problem of amplifier drift was not encountered during recording the dynamic signal, which had a duration of less than a second. During static calibration, however, amplifier drift was noted; but could be taken care of, firstly, by noting the change in signal amplitude only at the instant of change in loading and, secondly by stating the measurements in statistical terms. An ultra-violet light reflecting galvanometer type recorder, Honeywell 1508 VISICORDER, was used for recording the output signals. The recorder unit had an electronic flash time marker system, which could print the 'time' lines on the light sensitive recording paper. Time marking at an interval of a hundredth of a second were availed. The unit had also the provision of marking a scale, on the recording paper, with lines spaced at a tenth of an inch. The recording paper speed was set at 4 in/sec, during the experiments. The recorder galvanometers had an undamped natural frequency of 200 c/s. The external damping resistance required was 120 ohm, when a flat frequency response could be obtained for signals upto 120 c/s. The galvanometer coil had a resistance of 62 ohm and could carry a maximum safe current of 15 mA.

In order to eliminate noise from the output signals, shielded cables were used for the output connections – from the strain gauge circuits to the balancing unit, from the balancing unit to the operational amplifier circuit, and from the amplifier unit to the input junction of the recorder. The shields of these cables and the bodies of the dynamometer, the balancing unit and the recorder, were all earthed with the 'earthing terminal' of the mains.

2.10 Experimental Plan for Calibration

The abrupt variations in the force magnitudes, or the transient portion of the force record, occurs just after heel strike on the force plate. Since the second and third peaks of knee joint loading are expected around 30% and 80% of the stance phase (Harrington, 1974), respectively, the force components can be determined by static calibration.

In an ideal case, the output of a force measuring channel should be influenced by that particular component only; and should be uneffected by the remaining force components. However, on account of factors like errors in symmetry of gauge element and placing of strain gauges, a certain amount of cross-sensitivity between different force channels is present in most cases. Thus multi-component

calibration becomes essential. For sophisticated force measuring devices, the output signal versus input load characteristic was expressed in the form of a second order polynomial by Levi (1972). According to this scheme, for a six component dynamometer, at least 21 different load conditions would be needed, requiring a special purpose calibrating jig. While such schemes may be worthwhile for applications like model testing in a wind tunnel, in the present case, a linear calibration model would be sufficient. Thus, if F_Z, F_Y, F_X, M_X, M_Y and M_Z represent the six force components; and G1, G2, G3, G4, G5 and G6 represent the corresponding recorder galvanometer deflections, the calibration model can be expressed as

$$G1 = C_{11}F_Z + C_{12}F_Y + C_{13}F_X + C_{14}M_X + C_{15}M_Y + C_{16}M_Z \quad (2.1)$$

$$G2 = C_{21}F_Z + C_{22}F_Y + C_{23}F_X + C_{24}M_X + C_{25}M_Y + C_{26}M_Z \quad (2.2)$$

$$G3 = C_{31}F_Z + C_{32}F_Y + C_{33}F_X + C_{34}M_X + C_{35}M_Y + C_{36}M_Z \quad (2.3)$$

$$G4 = C_{41}F_Z + C_{42}F_Y + C_{43}F_X + C_{44}M_X + C_{45}M_Y + C_{46}M_Z \quad (2.4)$$

$$G5 = C_{51}F_Z + C_{52}F_Y + C_{53}F_X + C_{54}M_X + C_{55}M_Y + C_{56}M_Z \quad (2.5)$$

$$G6 = C_{61}F_Z + C_{62}F_Y + C_{63}F_X + C_{64}M_X + C_{65}M_Y + C_{66}M_Z \quad (2.6)$$

The calibration coefficients, occurring in the above equations, denote the galvanometer deflections

corresponding to the application of a particular force component. Thus, C_{11} denotes the deflection of galvanometer for channel 1, when a unit force is applied in the F_Z direction; C_{12} denotes the deflection of galvanometer for channel 1, when a unit force is applied in the F_Y direction; and so on. These coefficients can be evaluated by physical loading of the dynamometer.

2.11 Calibration of the Force Components

The vertical force component was applied to the dynamometer while it was resting on the floor, by placing known weights at the centre of top plate. For application of the remaining force components the dynamometer was mounted on a slotted angle iron stand. A load was applied by means of multi-strand steel wire sling, one end of which was fastened to a hole in the top plate of the dynamometer. The sling passed over a pulley and held a loading pan freely suspended from the other end. The pulley was supported on a bracket, bolted to the base plate. The loads were applied in steps of equal magnitude; and galvanometer deflections were noted during loading as well as unloading. The loading sequence was repeated three times for each force component. The mean value and standard deviation of galvanometer deflection corresponding to a loading step were calculated by use of a computer

programme. Chauvenet's criterion was incorporated in the computer programme for rejecting such readings which were dubious. The galvanometer deflections were noted in divisions, each division being of a tenth of an inch and was printed on the photosensitive paper of the recorder. The maximum loading during calibration was decided from an estimate of the likely magnitudes of the force components during the stance phase. A record of observations taken during calibration of the three force components is given in Tables A-(i), A-(ii) and A-(iii) of Appendix A. These tables state the direction and step of loading, the maximum load applied during calibration, and the mean value and standard deviation of the galvanometer deflections. The directions of loading and galvanometer deflection were duly taken into account while forming the final equations for output of a force component.

2.12 Calibration of Moment Components

The galvanometer deflections for moments about the X and Y axes were calibrated by applying a known moment on the top plate of the dynamometer. A steel beam was fastened to the top plate, and two equal and opposite loads were applied at points which were 80 cm apart. One of the loads could be directly suspended from the beam, while the other was applied upwards by use of a pulley

held on an angle iron frame. The physical set-up for applying the moment about the Y-axis, M_Y, is shown in Figure 2.8. The moment about the X-axis was applied, in a similar manner, by fastening the beam to the top plate at right angles to the direction shown in Figure 2.8.

A schematic diagram for the loading, during calibration for M_Y, is shown in Figure 2.9(a). Considering only the force F acting downwards, and assuming it to be shared equally by the two rings A and B, the moments acting on the two rings are indicated in the figure. The sum of these two moments would be $\frac{F}{2}(D + 2y)$. If the load acting (upwards) on the left end of the beam is also taken into account, the resulting moment on the two rings would be $F(D + 2y)$.

During experiment, the centre of pressure of the foot on the force plate may lie outside or between the centres of the two rings. In the former case, the sum of moments experienced by the two rings would be in accordance with Figure 2.9(a). The true value of the moment can be found by

(i) Calculating the 'apparent moment' from the recorded galvanometer deflection by using the calibration coefficient, and

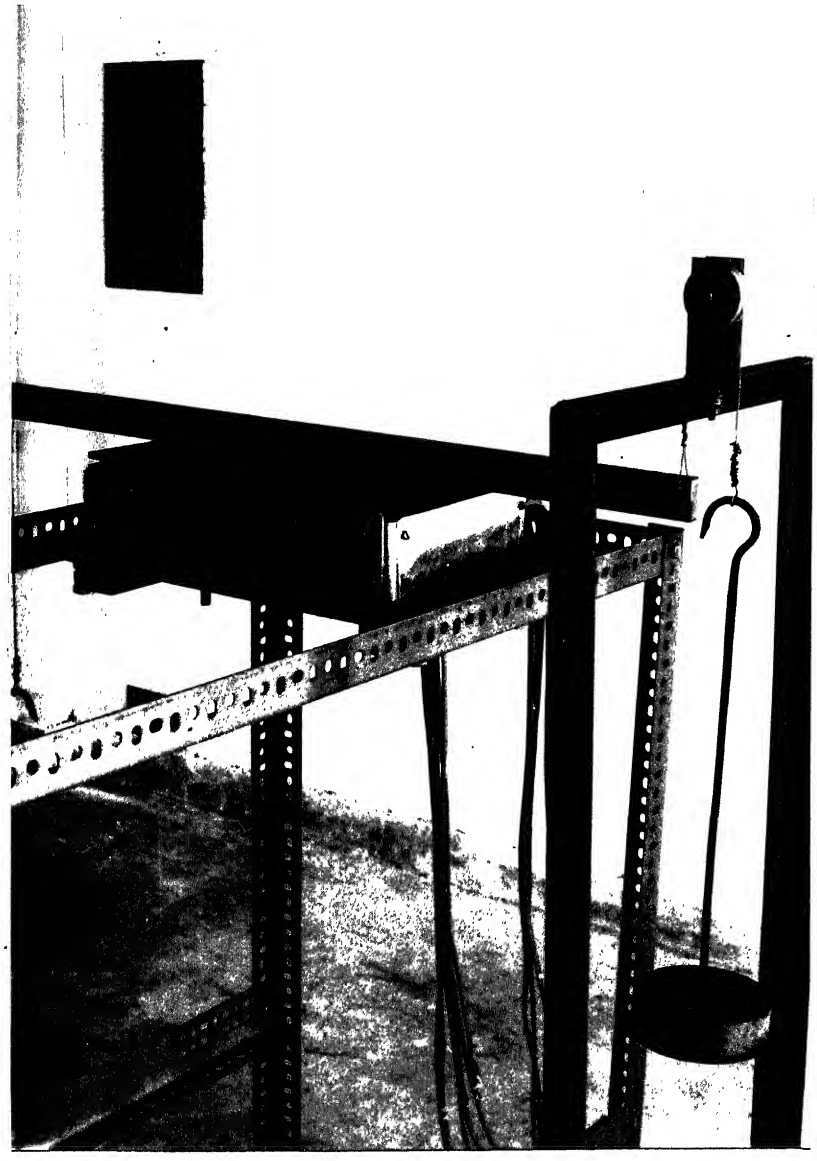

Fig. 2.8 Physical set-up for calibrating the moment about Y-axis

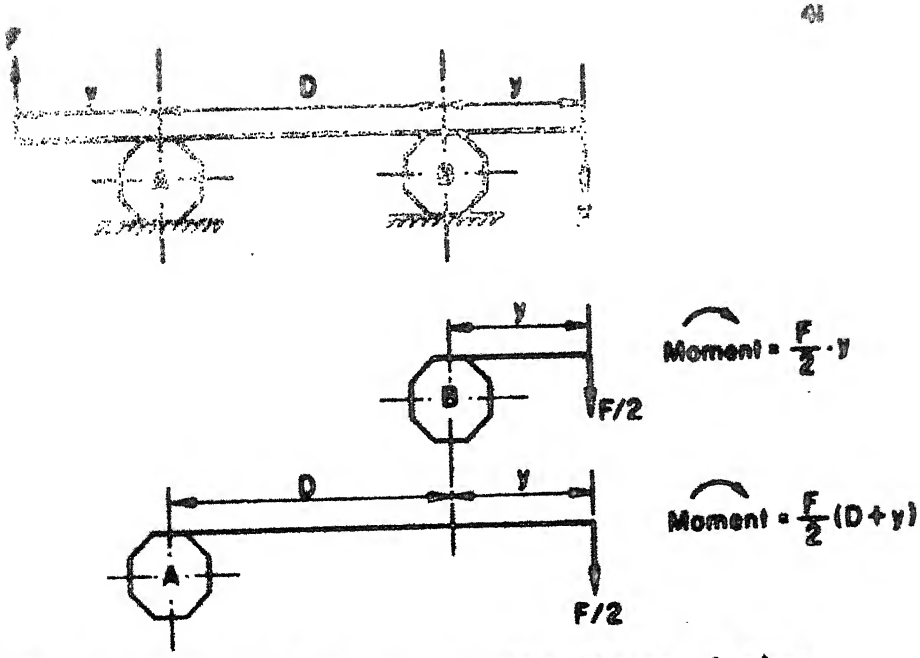

Fig.2.9(a) Moment Actions on the Rings during Calibration

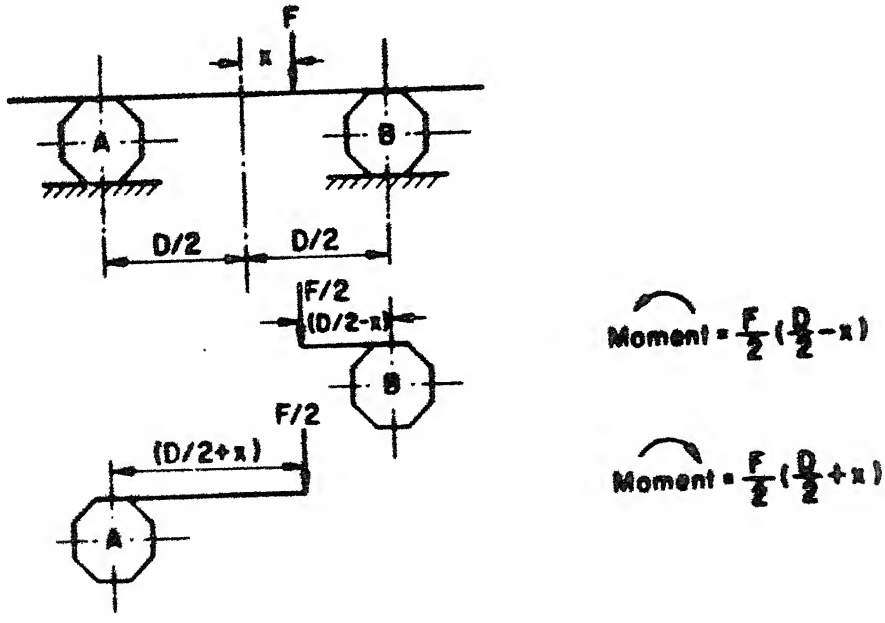

Fig.2.9(b) Moment Actions on the Rings during Actual Loading

(ii) The 'true moment' would be double the value of the 'apparent moment', since the load is acting only on one side of the centre of plate.

The later case is illustrated in Figure 2.9(b). In this case the sum of moments on the two rings would be $\frac{F}{2}(\frac{D}{2} + x) - \frac{F}{2}(\frac{D}{2} - x)$ or Fx, causing an equivalent galvanometer deflection. The calibration coefficient found for the moment component can still be used to determine the value of the true moment, by adopting the following procedure:

(i) Using the calibration coefficient and the recorded galvanometer deflection, an 'apparent moment' output is calculated,

(ii) The constant term, which occurred at the time of calibration, i.e. FD is subtracted from the 'apparent moment', and

(iii) The resulting value of moment is divided by 2, in order to obtain the 'true moment' which caused the galvanometer output.

In fact the method of calibration used for the moment components M_X and M_Y offers a great convenience in application of loading, since it would be much more difficult to apply a point load between the centres of the two rings. The distance between centres of the two rings D, used for detecting M_X and M_Y, was 11.2 cm and 27.2 cm, respectively.

It was noted during calibration of these two moment components that there was a difference in the sensitivity of the channels, with respect to the direction of the moment component. The calibration was, therefore, done for both the directions – positive as well as negative. The observations and results of calibration are reported in Tables A-(iv) and A-(v) of Appendix A. The physical arrangement for calibrating the moment component about the Z-axis is shown in Figure 2.10. Two equal and opposite forces are applied on the top plate of the dynamometer, at a distance of 11 cm apart. The observations and results for calibration of this moment component are given in Table A-(vi) of Appendix A.

2.13 Calibration Coefficients and Check for Performance of the Dynamometer

The following are the values of the calibration coefficients, derived from the results of calibration:

$C_{11} = 0.26$ $\quad$ $C_{22} = 0.96$

$C_{13} = 0.08$ $\quad$ $C_{25} = 0.00406$ (M_Y +ve)

$C_{14} = 0.002875$ (M_X -ve) $\quad$ $C_{25} = -0.001905$ (M_Y -ve)

$C_{33} = 0.478$ $\quad$ $C_{44} = 0.03787$ (M_X +ve)

$C_{34} = 0.00356$ (M_X +ve) $\quad$ $C_{44} = -0.0285$ (M_X -ve)

$C_{34} = -0.00381$ (M_X -ve)

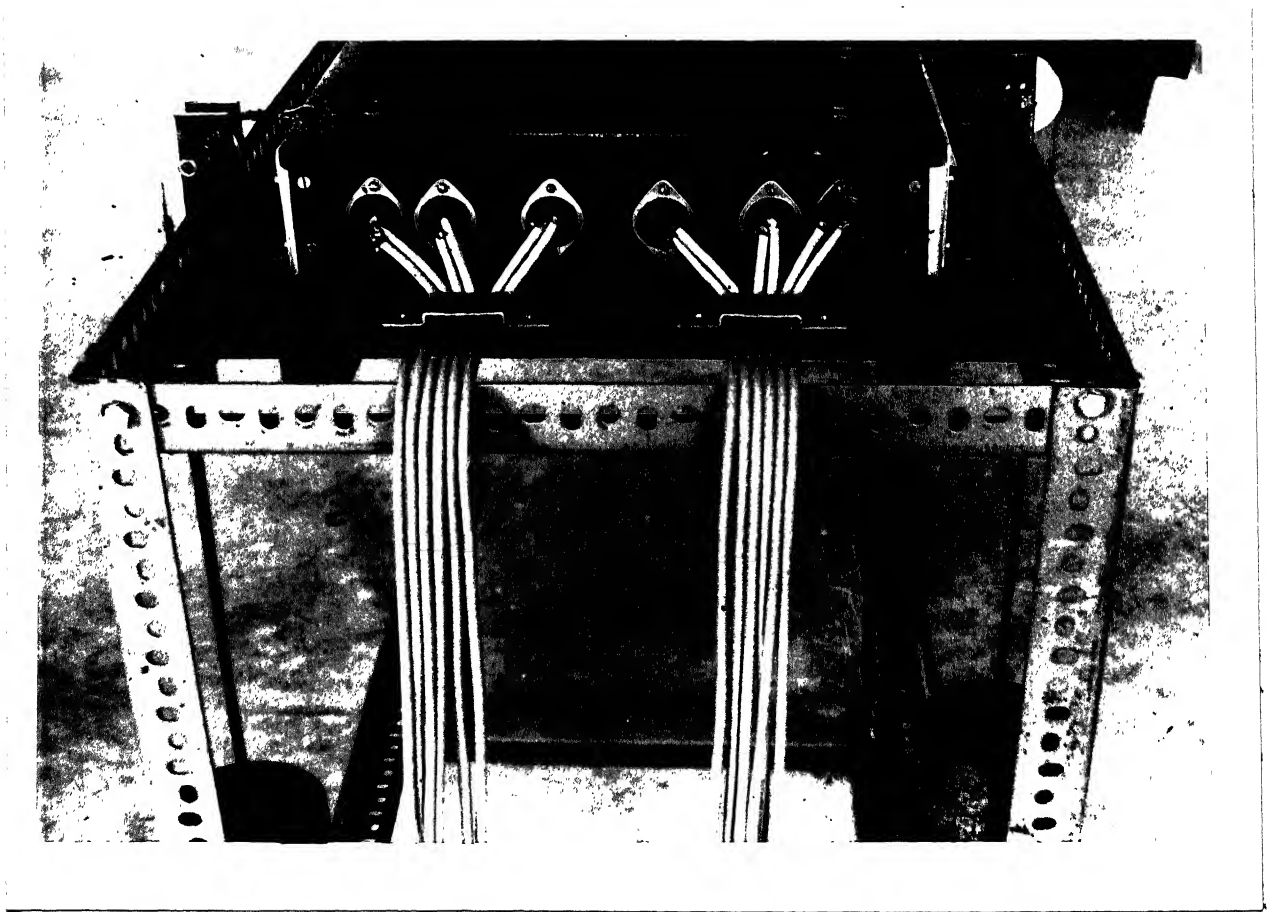

Fig. 2.10 Physical set-up for calibrating the moment about Z-axis

C_{55} = 0.00931 (M_Y +ve)

C_{55} = -0.00843 (M_Y -ve)

C_{54} = 0.004375 (M_X -ve)

C_{66} = 0.048

C_{64} = 0.0065 (M_X +ve)

C_{64} = -0.0065 (M_X -ve)

C_{65} = 0.001685 (M_Y +ve)

C_{65} = -0.004655 (M_Y -ve)

Among the coefficients mentioned above, six relate to the direct influence of the force components on their respective channels, and seven to the effect of cross-sensitivity. The remaining coefficients occurring in equations (2.1) to (2.6), of Section 2.10, are zero.

Simple tests were devised to check the performance of the dynamometer under the action of more than one force component simultaneously. In the first test, the three force components were applied simultaneously. The galvanometer deflections of the three force channels, during the test sequence, are mentioned in Table 2.1. The galvanometer deflections were noted during unloading only, since overshoots of some galvanometer deflections were noted at the time of putting the dead weights on the loading pan. Taking the cross-sensitivity due to F_X into account, the galvanometer deflection of the F_Z channel can be written as

Table 2.1 Performance of the Dynamometer under Simultaneous Action of Three Force Components

Load steps: 5 kg for F_X, 2 kg for F_Y, 10 kg for F_Z

S. No.	Galvanometer deflection of force channel Division		
	F_X	F_Y	F_Z
1	2.3	1.9	3.0
2	2.3	1.9	3.0
3	2.4	1.9	3.0
4	2.5	1.8	3.0
5	2.4	1.9	3.0
6	2.5	1.8	3.0
Mean value during unloading	2.4	1.87	3.0
Mean value and (standard deviation) during calibration	2.39(0.187)	1.92(0.29)	3.0(0.11)

$$G1 = C_{11}F_Z + C_{13}F_X$$

$$= 0.26x10 + 0.08x5 = 3.0$$

The estimated value, on the basis of calibration results, tallies exactly with the test observation.

In the second test the force component along and moment component about the Z-axis were simultaneously applied to the dynamometer. Table 2.2 records the galvanometer deflections for the two channels.

Table 2.2 Performance of the Dynamometer under Simultaneous Action of the Force Component Along and Moment Component About the Z-axis

Load steps: 10 kg for F_Z, 55 kg-cm for M_Z

S. No.	Galvanometer deflection of channel Division		
	F_Z	M_Z	
	(Unloading)	(Loading)	(Unloading)
1	2.6	2.6	2.9
2	2.6	2.2	3.0
3	2.5	2.1	3.0
4	2.6	2.25	3.0
5	2.6	2.4	3.0
6	2.6	2.5	2.7
Mean value	2.58	2.6375	
Mean value and (standard deviation) during calibration	2.60(0.11)	2.64(0.15)	

There is no cross-sensitivity between the two channels and the test results tally well with the calibration values.

During the third test the three force components and the moment component about the Y-axis were simultaneously applied to the dynamometer. The physical set-up for this test is shown in Figure 2.11; and the test results are mentioned in Table 2.3.

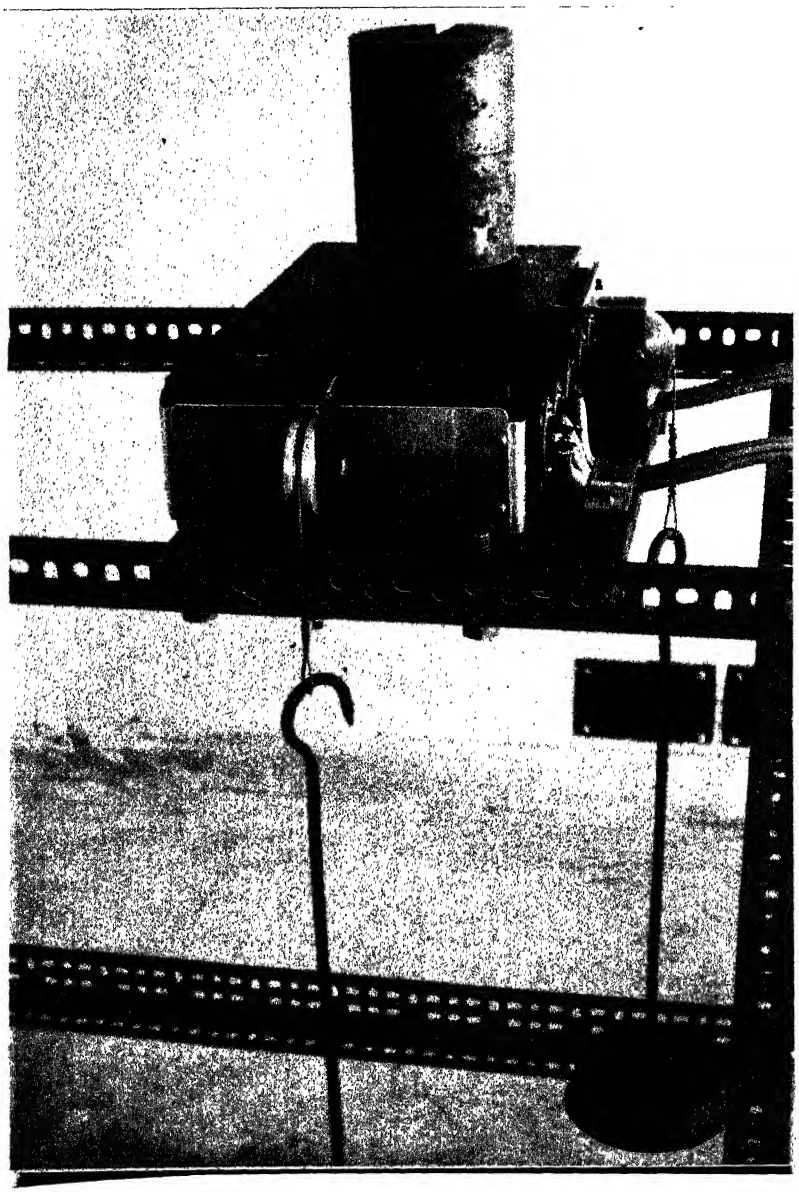

Fig. 2.11 Physical set-up for checking the performance of the dynamometer under action of three forces and one moment

Table 2.3 Performance of the Dynamometer under Simultaneous Action of Three Force Components and the Moment Component about Y-axis

Load steps: 5 kg for F_X; 5 kg for F_Y; 10 kg for F_Z; and 140 kg-cm for M_Y

S. No.	Galvanometer deflection of channel Division			
	F_X	F_Y	F_Z	M_Y
	Unloading	Unloading	Unloading	Unloading
1	2.35	4.0	3.0	0.5
2	2.25	4.1	2.9	0.6
3	2.25	4.2	2.8	0.5
Mean value during unloading	2.3	4.1	2.9	0.55
Expected value based on calibration results	2.39±0.126	4.24±0.5	3.0±0.07	0.656

The expected values of galvanometer deflections, based on calibration results, were calculated as mean value ± 0.675 x standard deviation (Holman, 1966). The cross-sensitivity of F_X on the F_Z channel was already considered in the first performance test; and a corresponding expected value for F_Z has been stated in Table 2.3. The expected calibration galvanometer deflection, corresponding to an equivalent 320 kg-cm of M_Y, was 1.49 ± 0.675 x 0.3387, division. Thus for the moment of 140 kg-cm, due to a single concentrated load, the expecte value of galvanometer deflection would be 0.656±0.1 divi

It will be noted from Figure 2.11 that all the three force components are applied along the negative directions and only the moment about Y-axis is positive. Thus the galvanometer deflection of the F_Y channel can be written as

$$-G2 = -C_{22}F_Y + C_{25}M_Y$$

or

$$G2 = C_{22}F_Y - C_{25}M_Y$$

$$= 0.96x5 - 0.00406x140$$

$$= 4.8 - 0.56 = 4.24$$

The standard deviation of galvanometer deflection for the F_Y channel is 0.29 for a load step of 2 kg, as shown in Table 2.1. Thus, according to the calibration results and for a loading of 5 kg, the expected value of galvanometer deflection may be stated as 4.24 ± 0.5. It may, therefore, be concluded that the test results tally well with the calibration values.

2.14 Computation of Foot-to-Ground Force Actions

The galvanometer deflections, on the force record obtained during the test runs, were measured and fed as input to a computer programme which was developed to obtain the calibrated values of the six force components

Since the vertical force component, which was mostly due to the weight of a subject, was the principal force action, it was essential that it was measured with the maximum possible accuracy. In order to ensure this, the galvanometer deflection of the vertical force channel was recorded immediately after the test runs, with the subject standing on the force plate. The calibrated value of the recorded galvanometer deflection was expected to give the weight of the subject. The magnitude of subject weight, as obtained by use of the force plate, was compared with the value noted by use of an accurate weighing balance. Taking the weighing balance reading as the correct value, a correction factor was calculated for each subject and was applied to the vertical force component during calibration. The values of this factor were 1.054, 0.9566 and 0.988 for subjects B, C and D, respectively.

It will be noted from the calibration coefficients mentioned in the previous section, that the F_Z channel is influenced by the magnitude of F_X; which itself is influenced by M_X. In its turn, the computation of M_X is based on the magnitude of F_Z, since the term (F_Z x distance between centres of rings C and D) has to be computed. In order to overcome this vicious circle, at an initial stage the cross-sensitivity due to M_X on F_X was not considered and the magnitude of F_Z was computed on the basis of cross-

sensitivity due to the approximate magnitude of F_X. This value of F_Z was then modified by use of the vertical force component correction factor. Next the magnitude of M_X was computed and its effect on the magnitude of F_X was found. Using the new value of F_X, the magnitude of F_Z was again computed. The computer programme adopted an iterative procedure till the difference between a new and the previous magnitude of F_Z was less than 0.001 kg. The magnitudes of the remaining force components were computed thereafter.

It was noted for the moment, induced due to positi of centre of foot-pressure, M_Y that the calibration coefficients for positive as well as negative moment did not hold good when the centre of foot-pressure was very close to the centre of the force plate. This was, possibly, due to a large stiffness of the structure to this moment component. Therefore, a graphical plotting of the moment cycle and extrapolation of such points was resorted to. Since the useful data points, for calculating the maximum resultant knee joint force, were quite away from the extrapolated points, the accuracy of results was not effected.

The calibrated values of the foot-to-ground force components, together with the time taken for the stance phase, are reported for all the test runs in Table A-1 to A-12 of Appendix A. A representative graph indicating

Ch... 5628
Acc. No. ...

variation of the six force components with time, during the stance phase, is shown in Figure 2.12. These force components were recorded during test run No. 3 of subject B. Also shown in this figure is the variation of M_Z during the stance phase for test run No. 3 of subject C. This additional curve has been given to indicate the possibility of a cyclic variation of M_Z during the stance phase.

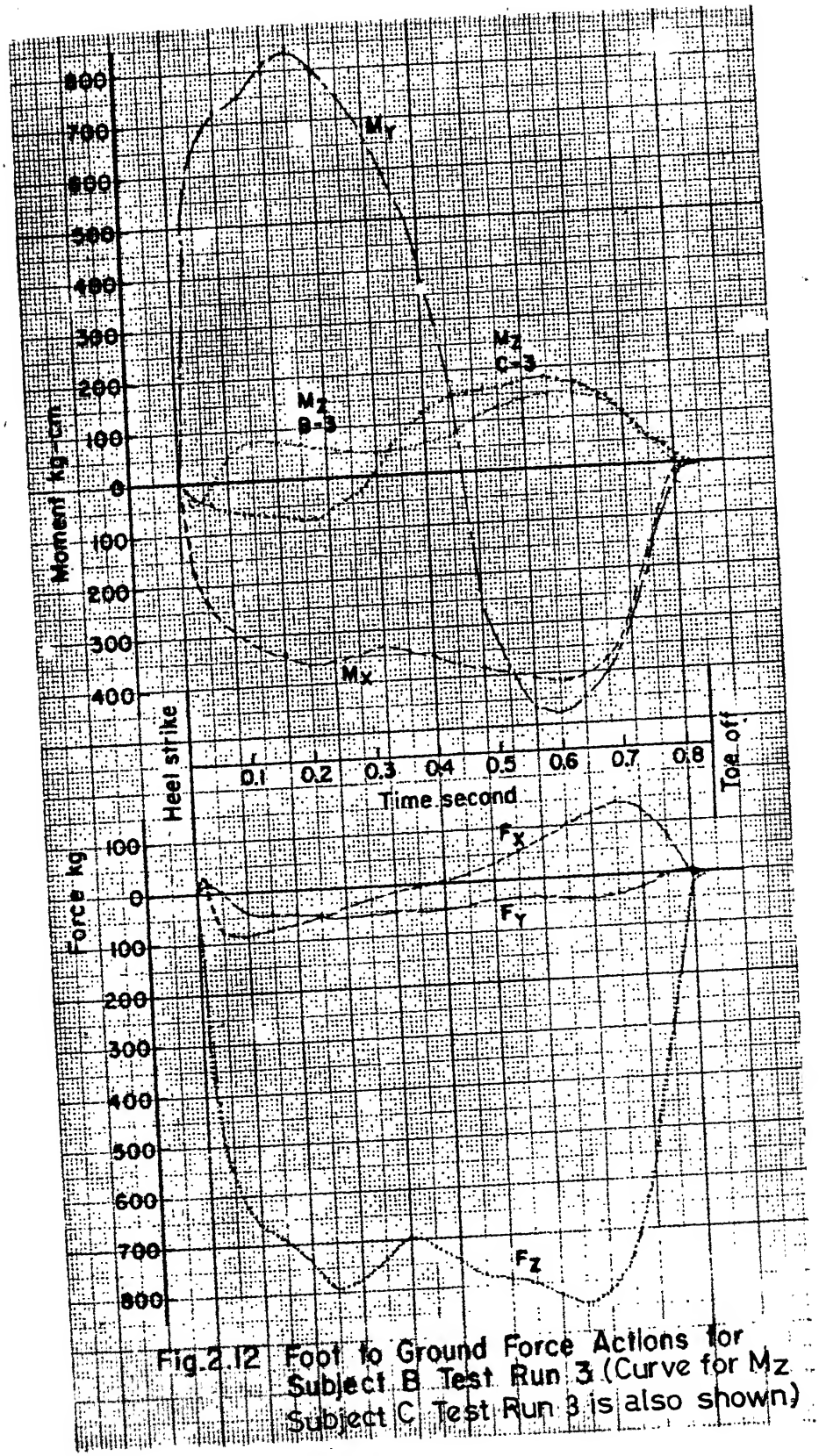

Fig.2.12 Foot to Ground Force Actions for Subject B Test Run 3 (Curve for Mz Subject C Test Run 3 is also shown)

CHAPTER 3

FINITE ELEMENT ANALYSIS OF THE OCTAGONAL RING

3.1 Introduction

The empirical formulae for the deformation characteristics of an octagonal ring, having its inclined face at an orientation of 50° from the horizontal, have already been mentioned in Section 2.3. The accuracy of these formulae has not been theoretically verified so far. The finite element analysis was taken up to fill the gap of information in this respect.

3.2 Element Used for Idealization

The cross-section of the octagonal ring is subjected to inplane forces, which may be either vertical or horizontal, and is in a state of plane stress. The finite element idealization of the cross-section was, therefore, made by using the plane stress triangular element having six degrees of freedom. The triangular shape of the element was found adequate to take care of the circular inner boundary and the sharp-cornered outer boundary of the octagonal ring.

The plane stress triangular element is shown in Figure 3.1, where the x and y components of displacement

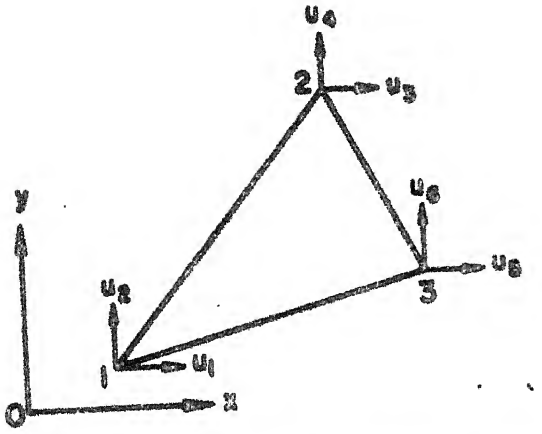

Fig.3.1 Plane Stress Triangular Element in the Local Co-ordinate System

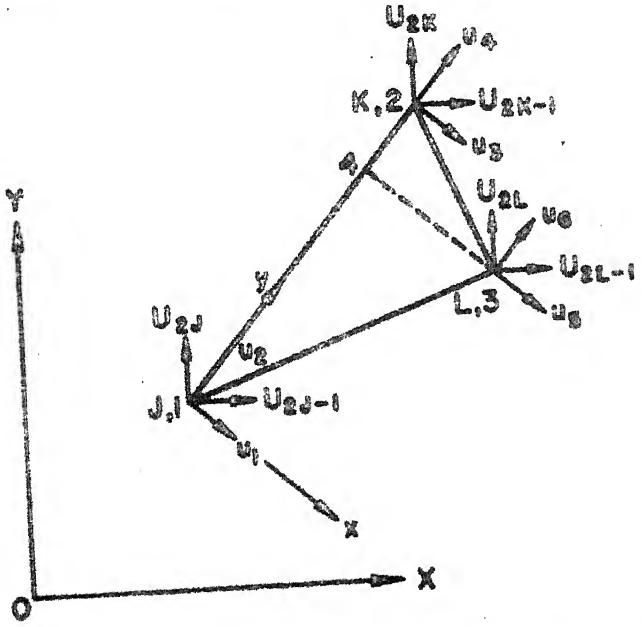

Fig.3.2 Plane Stress Triangular Element in the Local as well as Global Co-ordinate Systems

of the three vertices of the triangle are expressed as $u_1, \ldots, u_6$. The displacement functions, which are assumed linear may be expressed in terms of six arbitrary coefficient $c_1, \ldots, c_6$ as

$$u_x = c_1x + c_2y + c_3 , \quad u_y = c_4x + c_5y + c_6 \tag{3.1}$$

The coefficients can be found if the displacements of the three vertices of the triangle are known. The x and y components of displacement within the element can be expresse in terms of known quantities, some of which have been expressed in subscripted form, as stated below

$$x_{ij} = x_i - x_j , \quad y_{ij} = y_i - y_j \tag{3.2}$$

A_{123} = Area of the triangle 123

$$= \frac{1}{2} (x_{32}y_{21} - x_{21}y_{32}) \tag{3.3}$$

$$\begin{aligned} u_x = \frac{1}{2A_{123}} [&(y_{32}(x - x_2) - x_{32}(y - y_2))u_1 \\ &+ (- y_{31}(x - x_3) + x_{31}(y - y_3))u_3 \\ &+ (y_{21}(x - x_1) - x_{21}(y - y_1))u_5] \end{aligned} \tag{3.4}$$

$$\begin{aligned} u_y = \frac{1}{2A_{123}} [&(y_{32}(x - x_2) - x_{32}(y - y_2))u_2 \\ &+ (- y_{31}(x - x_3) + x_{31}(y - y_3))u_4 \\ &+ (y_{21}(x - x_1) - x_{21}(y - y_1))u_6] \end{aligned} \tag{3.5}$$

The strain components for the element may be computed by differentiating the above two equations, and may be expressed in explicit form as follows:

$$\bar{e} = \begin{Bmatrix} e_{xx} \\ e_{yy} \\ e_{xy} \end{Bmatrix} = \begin{Bmatrix} \frac{\partial u_x}{\partial x} \\ \frac{\partial u_y}{\partial y} \\ \frac{\partial u_x}{\partial y} + \frac{\partial u_y}{\partial x} \end{Bmatrix}$$

$$= \frac{1}{2A_{123}} \begin{bmatrix} y_{32} & 0 & -y_{31} & 0 & y_{21} & 0 \\ 0 & -x_{32} & 0 & x_{31} & 0 & -x_{21} \\ -x_{32} & y_{32} & x_{31} & -y_{31} & -x_{21} & y_{21} \end{bmatrix} \begin{Bmatrix} u_1 \\ u_2 \\ u_3 \\ u_4 \\ u_5 \\ u_6 \end{Bmatrix} \quad (3.7)$$

or, $\bar{e} = [B]\,\bar{u}$; (3.8)

where, the strain matrix [B], has been stated in explicit form in equation (3.6). The stress-strain relations, in case of plane stress, can be expressed as follows:

$$\begin{Bmatrix} \sigma_{xx} \\ \sigma_{yy} \\ \sigma_{xy} \end{Bmatrix} = \frac{E}{(1 - \nu^2)} \begin{bmatrix} 1 & \nu & 0 \\ \nu & 1 & 0 \\ 0 & 0 & \frac{1-\nu}{2} \end{bmatrix} \begin{Bmatrix} e_{xx} \\ e_{yy} \\ e_{xy} \end{Bmatrix}$$

or $\sigma = [D]\bar{e}$; (3

where [D] is the elasticity matrix and has been expressed i the explicit form in equation (3.8). For an element of thickness t and area A, the element stiffness matrix, [k], can be found by evaluating the area integral, as indicated below

$$[k] = t \int\int_A [B]^T [D][B] \, dA \quad (3$$

It is sometimes convenient to separate the element stiffnes matrix into two components - one due to normal stress, $[k_n]$ and the other due to shear stress, $[k_s]$. Thus,

$$[k] = [k_n] + [k_s] \quad (3$$

For an element of constant thickness, t, the values of thes two components of the stiffness matrix can be written in explicit form (Przemieniecki, 1968) as

$$[k_n] = \frac{E.t}{4A_{123}(1 - \nu^2)} [N] \quad (3$$

$$[k_s] = \frac{E.t}{8A_{123}(1 + \nu)} [S] \quad (3$$

where the [N] and [S] matrices are given by

$$[N] = \begin{bmatrix} y_{32}^2 & & & & & \\ -y_{32}x_{32} & x_{32}^2 & & & & \\ -y_{32}y_{31} & x_{32}y_{31} & y_{31}^2 & \text{Symmetric} & & \\ y_{32}x_{31} & -x_{32}x_{31} & -y_{31}x_{31} & x_{31}^2 & & \\ y_{32}y_{21} & -x_{32}y_{21} & -y_{31}y_{21} & x_{31}y_{21} & y_{21}^2 & \\ -y_{32}x_{21} & x_{32}x_{21} & y_{31}x_{21} & -x_{31}x_{21} & -y_{21}x_{21} & x_{21}^2 \end{bmatrix} \quad (3.$$

$$[S] = \begin{bmatrix} x_{32}^2 & & & & & \\ -x_{32}y_{32} & y_{32}^2 & & & & \\ -x_{32}x_{31} & y_{32}x_{31} & x_{31}^2 & \text{Symmetric} & & \\ x_{32}y_{31} & -y_{32}y_{31} & -x_{31}y_{31} & y_{31}^2 & & \\ x_{32}x_{21} & -y_{32}x_{21} & -x_{31}x_{21} & y_{31}x_{21} & x_{21}^2 & \\ -x_{32}y_{21} & y_{32}y_{21} & x_{31}y_{21} & -y_{31}y_{21} & -x_{21}y_{21} & y_{21}^2 \end{bmatrix} \quad (3.$$

Although the element stiffness matrix of equation (3.10) has been derived with reference to an arbitrary coordin system, it is convenient to set-up a local coordinate system for each element separately and thereafter transform it to the common global system of coordinates. In Figure 3.2, the global coordinate system is represented by the X and Y axes having their origin at O; and the node numbers of the

vertices of the triangle are represented by letters J, K and L. Let x and y represent the orientation of axes for the local coordinate system, where the y axis is chosen along the edge 1-2 of the triangle and the x axis is taken perpendicular to 1-2, pointing from 1 towards 3. The choice of origin at 1 would simplify the computations since x_1 and y_1 would both be zero. The x coordinate of node 2 would be zero while the y coordinate would be given by the distance between 1 and 2. Using subscripted notation, this distance may be conveniently expressed in terms of the global coordinates of the node numbers as follows:

$$d_{12} = (X_{KJ}^2 + Y_{KJ}^2)^{1/2} \qquad (3.$$

The direction cosines of the y axis can also be expressed as

$$l_{12} = \frac{X_{KJ}}{d_{12}} \qquad \text{and} \qquad m_{12} = \frac{Y_{KJ}}{d_{12}} \qquad (3.$$

In order to obtain the coordinates of node 3 in the local system, a line is drawn perpendicular to the edge 1-2 from point 3, intersecting it at 4. The x and y coordinates of 3 would then be given by the distances d_{43} and d_{14}, respectively. To express these distances in the global system, let the global coordinates of point 4 be expressed as $(X_J + l_{12}d_{14})$ and $(Y_J + m_{12}d_{14})$. Also let the direction cosines of the x axis be represented by l_{43} and m_{43}, such that

$$l_{43} = \frac{X_{34}}{d_{43}} = \frac{X_{LJ} - l_{12}d_{14}}{d_{43}} \qquad (3.1$$

and $$m_{43} = \frac{Y_{34}}{d_{43}} = \frac{Y_{LJ} - m_{12}d_{14}}{d_{43}} \qquad (3.1$$

From the condition of orthogonality between the x and y orientations, we can write

$$l_{12}l_{43} + m_{12}m_{43} = 0$$

or $$l_{12}(X_{LJ} - l_{12}d_{14}) + m_{12}(Y_{LJ} - m_{12}d_{14}) = 0 \qquad (3.2$$

Using the relationship $l_{12}^2 + m_{12}^2 = 1$, and solving equation (3.20) for d_{14}, we get

$$d_{14} = l_{12}X_{LJ} + m_{12}Y_{LJ} \qquad (3.2$$

Using the relation $d_{43}^2 = d_{13}^2 - d_{14}^2$, d_{43} can be expressed as

$$d_{43} = (X_{LJ}^2 + Y_{LJ}^2 - d_{14}^2)^{1/2} \qquad (3.2$$

The direction cosines of the x axis, as given by equations (3.18) and (3.19), can now be evaluated from the knowledge of the global coordinates of the vertices of the triangle. The element stiffness matrix in the global coordinate system, $[\bar{k}]$, can now be expressed as

$$[\bar{k}] = [\lambda]^T [k] [\lambda] \ , \qquad (3.2$$

where the transformation matrix, $[\lambda]$, is given by

$$\begin{bmatrix} l_{43} & m_{43} & 0 & 0 & 0 & 0 \\ l_{12} & m_{12} & 0 & 0 & 0 & 0 \\ 0 & 0 & l_{43} & m_{43} & 0 & 0 \\ 0 & 0 & l_{12} & m_{12} & 0 & 0 \\ 0 & 0 & 0 & 0 & l_{43} & m_{43} \\ 0 & 0 & 0 & 0 & l_{12} & m_{12} \end{bmatrix} \quad (3.$$

The element stiffness matrices, computed in accordance with equation (3.23), have to be assembled by using the standard procedure of structural analysis to obtai the global stiffness matrix of the whole structure, K . The equilibrium equations of the structure, after incorporat the boundary conditions, can be expressed as

$$[K]\{U\} = \{P\} \quad , \quad (3.$$

where {P} and {U} denote the load and displacement vectors, respectively. The set of equations, represented by (3.25), are solved by using the Cholesky decomposition method which takes care of the symmetry and banded nature of the matrix

3.3 Idealization of the Ring and Numerical Results

For a ring under diametral compression, on account of symmetry of geometry and loading, only one quarter of the

cross-section need be considered for the purpose of finite element idealization. Figure 3.3 shows a quarter portion of the section of the octagonal ring, under vertical loading, idealized by using plane stress triangular elements. By virtue of the conditions of symmetry, the X-component of displacements along AB and the Y-component of displacements along CD may be taken to be zero.

A convergence study of the plane stress triangular elements was made by using four different idealizations of the octagonal ring, subjected to a vertical load. A summary of the numerical results is presented in Table 3.1; and a graphical representation is shown in Figure 3.4.

For the same magnitudes of the physical constants and dimensions of the ring, the deflection of the ring was found to be 0.03386 cm by using the empirical formula of Cook. Thus the value for deflection obtained by finite element method, using 560 elements in a quarter of the ring, is 13.76% higher than the one given by Cook's formula. However, since the finite element satisfies all the converge criteria (Zienkiewicz, 1971), the displacement results are expected to converge monotonically from below. As such, the true deflection of the ring would be somewhat higher than the value given by using the finite element method.

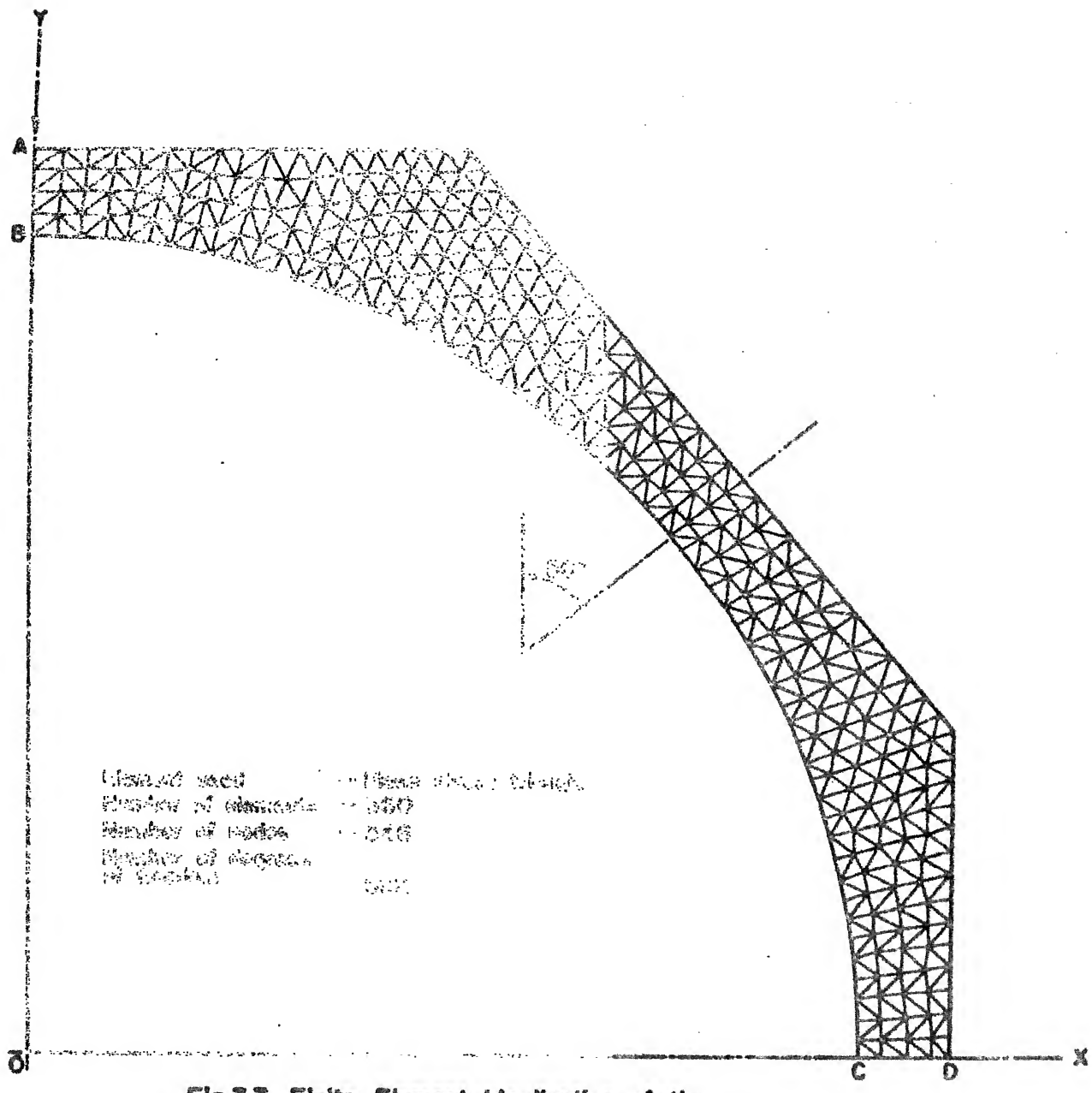

Fig.3.3 Finite Element Idealization of the Octagonal Ring under vertical loading

Table 3.1 Numerical Results for the Deflection of the Ring Under a Central Vertical Load

Load applied = 100 kg

Young's modulus for steel = 2.11×10^6 kg/cm^2

Poisson's ratio = 0.3

Size across octagonal faces = 80 cm

Diameter of inner surface = 72 cm

Width of ring = 1.2 cm

Idealization No.	No. of degrees of freedom	No. of elements in a quarter of the octagonal ring	Deflection of the ring under the load cm
1	112	56	0.007551
2	162	104	0.02313
3	564	434	0.03537
4	692	560	0.03852

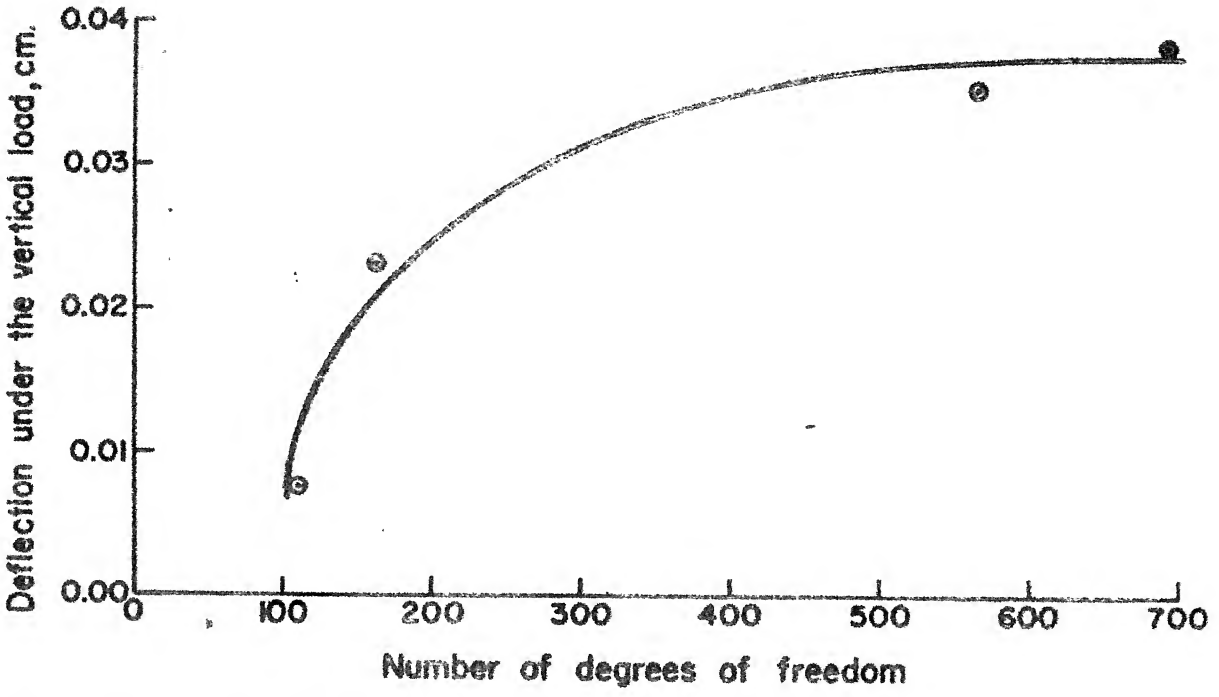

Fig. 3.4 Convergence Study of the Plane Stress Triangular Element for Idealization of the Octagonal Ring

This indicates that by using the empirical formula of Cook we get an underestimate of the value of deflection.

Although the displacement formulation, used for the finite element, does not predict the stresses and strains as accurately as the displacements, the magnitude of tensile strain at the centre of the vertical faces of the octagonal ring was also computed. With reference to Figure 3.3, the computation of strain was made at the point D by using equations (3.5) and (3.6). The eight triangular elements which have their nodes on CD, are shown in the upper portion of Figure 3.5. The strains calculated for different elements were assigned at the centroids of the triangles, and the magnitudes of strain were plotted along CD (Zienkiewicz, 1971) The method of least squares was then used to obtain the best fit line, which depicts the variation of strain along the section CD and is shown in the lower portion of Figure 3.5. The magnitude of strain at the point D is thus found to be 0.834×10^{-3}. As compared to the value calculated from Cook's empirical formula i.e. 0.6566×10^{-3}, the finite element result is 27.02% higher.

A similar trend of results is expected if the octagonal ring is subjected to horizontal loading. In this case, however, the loading is not symmetric and as such a quarter portion of the octagonal ring cannot be used for

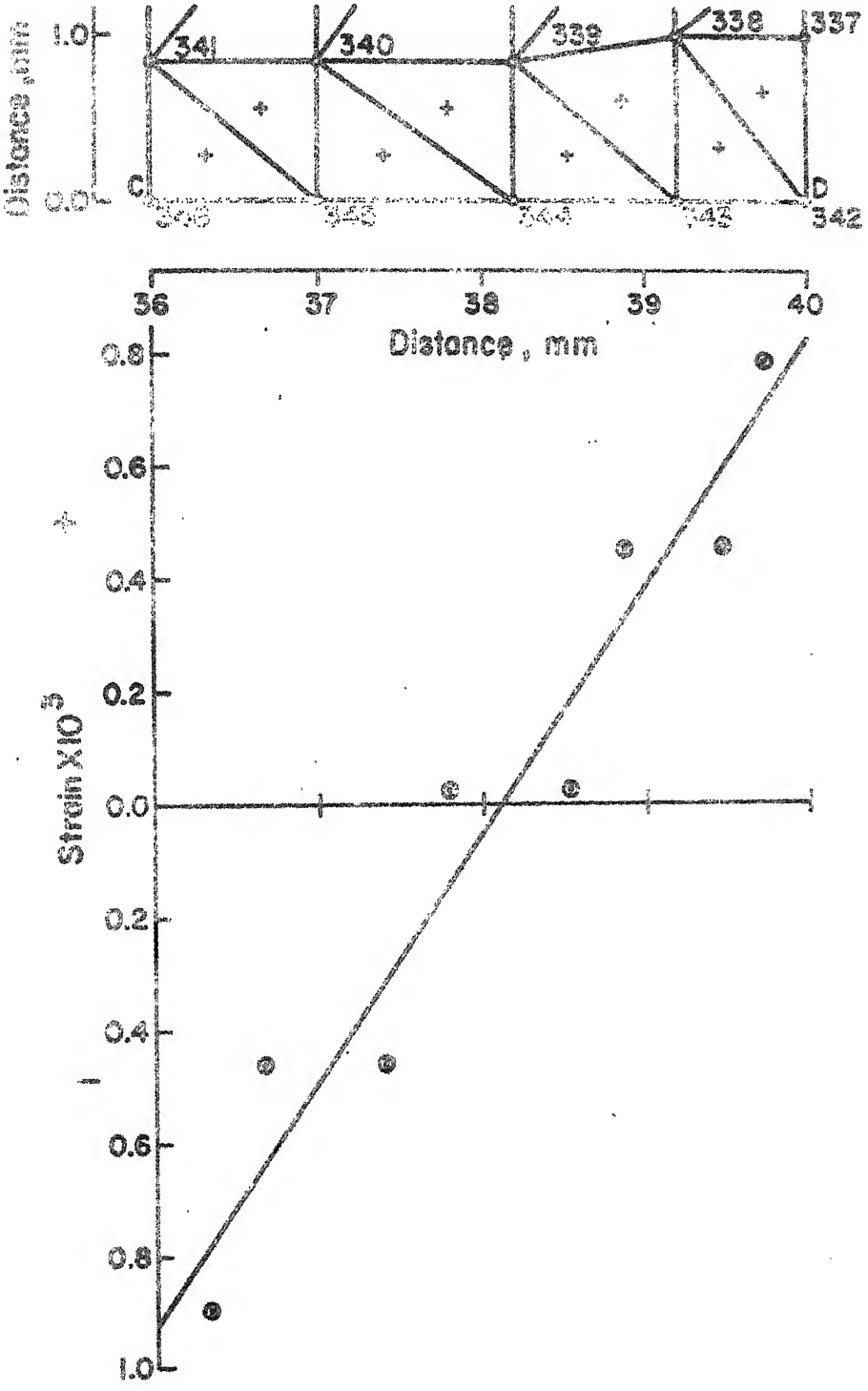

Fig.3.5 Strain along Section CD of the Octagonal Ring under vertical loading

idealization. With the use of a half ring and refinement of the mesh corresponding to 560 elements in a quarter of the ring, the computer storage requirement will be considerab higher. As such, the deformation characteristics of the ring under horizontal loading could not be investigated on the IBM-7044 computer.

CHAPTER 4

MEASUREMENT OF MOTION CHARACTERISTICS OF THE LIMB

4.1 Introduction

The dynamic analysis of a limb segment in motion requires consideration of the inertia forces, which come into play because of the mass of the limb segment and the accelerations to which it is subjected. In order to determine the magnitude of accelerations on the limb segment, it is evident that the corresponding displacements be first ascertained. The problem, therefore, resolves to the measurement of the coordinates of the centre of gravity of the limb segment. The cine-photographic technique had been first employed for such measurements by Bresler and Frankel (1950), and is still in vogue. In this technique, the motion of the limb in space is recorded simultaneously in the front and side views, by using two movie cameras. Anatomical landmarks are selected to enable the determination of the position of the centre of gravity of the limb segment; and adhesive markers are placed over them in order to distinguish their position in the two views. After the motion sequence of the subject is recorded, an illuminated graph is also photographed in the fields of view of the two movie cameras. The cine films are then projected,

frame by frame; and the positions of the markers with reference to the lines of the graph enable measurement of the reference coordinates. This scheme for measurement, though fundamental in nature, requires careful consideration of the details. Among such details are the selection of anatomical prominences to enable location of the centre of gravity of the limb segment; magnification of the image as the subject approaches the camera in the front view, synchronization of the two movie cameras; and consideration of the effect of parallax in photography and film projection. A detailed consideration of the various aspects, relating to the measurement of reference coordinates and computation of the motion characteristics, is presented in the following sections.

4.2 Description of the Anatomical Landmarks and the Physical Measurements for the Subjects

The position of the centre of gravity of the limb segment, upto the knee joint, can be estimated by noting the positions of the ankle and knee joints. Using the coefficient proposed by Contini and Drillis (1966), the position of the centre of gravity would be at a distance of 0.467 times the length of the shank, from the knee joint. In order to locate the position of the ankle and knee joints, markers were placed on the lateral malleolus of

fibula, the tubercle of tibia, and the lateral condyle of femur. The markers were also placed at appropriate positions in the front portion of the limb, having same height above floor as the bone prominences stated earlier. The markers were white in colour to enable easy distinction under the indoor lighting conditions, and had an adhesive inner surface Circular targets, in black ink, were also painted on the markers to help in locating the position of the bone prominences when the cine film was projected. The height of the marker centres, above floor, was noted for the vertical position of the leg. While the ankle joint was assumed at the same height as the centre of the lateral malleolus of fibula, the height of the knee joint was noted. The measurements taken in case of the three subjects are recorded in Table 4.1.

Table 4.1 Height of Markers on the Bone Prominences and the Knee Joint for the Test Subjects

Subject	Height of anatomical landmarks, cm			
	Lateral malleolus of fibula	Tubercle of tibia	Lateral condyle of femur	Approximate position
B	7.0	46.5	50.5	49.5
C	5.5	40.5	44.5	43.5
D	6.5	44.0	47.0	46.0

4.3 Details of the Cine Photographic Technique

Just as all the three dimensions of an object could be found from two orthographic views of engineering drawing, to capture the three dimensions of a moving object two movie cameras were located at right angles to each other. To record the test sequence, one of the cameras was placed at right angles to the plane of progression, while the other at right angles to the medial-lateral plane. In common terms, these were the side view and front view cameras. Since the reference coordinates were to be measured from the film record, it is essential that there was no magnification of image as the subject approached towards the front view camera. This was achieved, within tolerable limits, by use of a telephoto-lens on the front view camera. A telephoto-lens of 150 mm focal length was used and the distance between the lens centre and the centre of force plate was kept as 33 meter. It was found that for a marker of height 0.5 meter, the magnification in image was only 4.76%, as the marker was moved forward by a distance of 1.5 meter. The distance of the side view camera from the centre of the force plate was kept such that a complete walk cycle could be covered in the field of view. In order to locate the position of 'heel strike', on the force plate, simultaneously in the two views, two electronic clocks were

placed in the field of view of both the cameras. The smalle clock had a least count of 0.01 sec. However, since there was some doubt regarding the visibility of the indicating hand, a bigger clock with a least count of 0.03 sec. was also placed in the field of view.

After the initial synchronization of the two cine films, a one to one correspondence was expected in their frames if the two movie cameras were operating at the same speed. The movie cameras used were of 16 mm film size and 'Bolex' make. The two cameras were mechanically cranked and film speed was set at 48 frames/sec. In order to ensure uniformity of film speed, the shooting started from fully cranked position. The film speeds of the two cameras were checked by recording the electronic clock with least count of 0.01 sec., in the field of view of both the cameras separately and from a close distance. On development of the cine films, it was found that the actual speed of the side view camera was 51 frames/sec. for two successive seconds after starting from the fully cranked position. A similar speed check for the front view camera indicated that from an initial start of 50 frames per second, the film speed dropped down to 48 frames/sec. after 3 seconds. Since the side view camera was located at a distance of only about 5 meter, from the centre of force plate, it was started only just before the test run. The front view

camera, on the other hand, was started about 3 to 4 seconds earlier than the beginning of a test run. It was arranged so because the camera-man operating the front view camera, could not ascertain the beginning of test run in the field of view.

The difference in speed of the two cameras was compensated for by introducing additional data points in the front view record. The following procedure was adopted for what may be called as 'frame compensation'. After establishing that while recording the test sequence the front and side view cameras operated at 48 and 51 frames pe second, respectively; it was also determined that the difference in time taken by 16 frames at 48 frames per seco and 17 frames at 51 frames per second, was only 0.0001 secc If this difference in time could be accepted as reasonable, an additional frame could be added to the 16 frame sequence in order to compensate for the difference in speed of the two cameras. To be specific, for the test run B-4, a difference of 2 frames was noted between the number of frames, covering the stance phase of gait cycle, in the front and side view cine films. The compensation for the two frames was done by adding two additional data points, one after frame No. 16 and the other after frame No. 32 after 'heel strike', in the front view film. The additional

data points were given a value which was average of the two adjacent values. In most cases, including test run B-4, the first additional data point added, had the same value as the two adjacent data points. Thus no approximation was involved in this procedure.

The subject, bearing markers on the left lower extremity, moved on the walk platform against a dark background. Since the tests were conducted indoors, flood lights were used to illuminate the markers placed on the limb of the subject. An alphabet identifying the subject and the number of the test run, were written on cards taped to an angle iron frame, in the fields of view of both the cameras. Photographic records of the side and front views, during test run 3 of subject B, are shown in Figures 4.1 and 4.2, respectively.

To enable measurement of the coordinates of marker positions in different frames, a graph was also recorded in the fields of view of both the cameras, separately, after the test runs. The graph lines were made with white paint, on a 1.2 m x 2.4 m x 6 mm plywood board having a non-reflecting black surface. The graph board was held with its surface in a vertical plane, such that one of the vertical lines of the graph was placed over the centre of the force plate. Thus the graph provided the scales,

Figure 4.1 A side view record of the test sequence for subject B

Figure 4.2 A front view record of the test sequence fo
subject B

along two reference axes, in both the planes of motion i.e. the plane of progression and the medial-lateral plane. Since the graph lines occupied the fields of view completely the effect of parallox on the lines of the graph would be same as on the subject moving in the fields of view. Thus the measurements in the frames of the projected cine films, with reference to the lines of the graph, could be expected to be accurate. The best method for superimposing the graph on the motion sequence of the limb is by using the technique of double-exposure, i.e. after the test sequence, the films are rewound and exposed again to record the graph in the fields of view. However, on account of inexperience of the cameramen in double-exposure of the cine film while the telephoto-lens was used, only the graph alone could be photographed, separately. The superimposing of the graph on each frame of test sequence was done by a graphical technique, during projection of the cine films.

4.4 Details Regarding Projection of the Cine Films to Obtain the Displacement Patterns in the Two Fields of View

In order to superimpose the graph lines for the purpose of measurement, it was essneital that the position of the graph was accurately located in the frames. For the side view, the outline of the force plate provided a convenient object whose position did not change. In the front view, the slope of the walk platform out the angle iron frame, used to display the identification markings, were used for this purpose.

A 'stop action' projector of 'LAFAYETTE' make was used to project the cine films, frame by frame. The projections were made on the wall. A sheet of white paper fixed to a wooden support, by adhesive tape, was held on the surface of the wall for the purpose of obtaining the records. Firstly, a frame containing the view of the graph was projected; and the lines of the graph, as well as the stationary object selected for locating the frame, were marked on the sheet of paper. Thereafter the frames containing the test sequence were projected frame by frame. Each frame so projected was accurately located on the sheet of paper before noting the position of markers. The data points corresponding to some important events in the locomotion cycle, such as heel strike (H.S.), toe off other foot (T.O.F.), heel strike other foot (H.S.O.F.) and toe strike (T.S.), were marked to

distinguish them from the remaining ones. In most cases, a few data points, before heel strike and after toe strike were also noted. The scale of projection could be found by noting the spacing between the graph lines in the proximity of ankle and knee joints. On an average, the scales of film projection, for the front and side views, were 0.69 and 0.735 times the actual, respectively. Figures 4.3 and 4.4 show the typical displacement patterns obtained in the X-Z and Y-Z planes.

4.5 Computation of the Motion Characteristics

In the first place, the displacements of the ankle and knee joints along the reference axes, during the stance phase of the gait cycle, were calculated from the data obtained as a result of film projection. Scale factors were duly taken into account while converting the projection data into life-size values. At an initial stage of computation, the calculated heights of the ankle and knee joints, corresponding to the vertical position of the limb, were compared with the actual measurements for the subjects. The maximum percentage errors, in photographic measurements were found to be within 1% and 11% for the knee and ankle positions, respectively. The higher magnitude of percentage error in locating the ankle joint may be due to parallax, since the spacings between lines of the reference

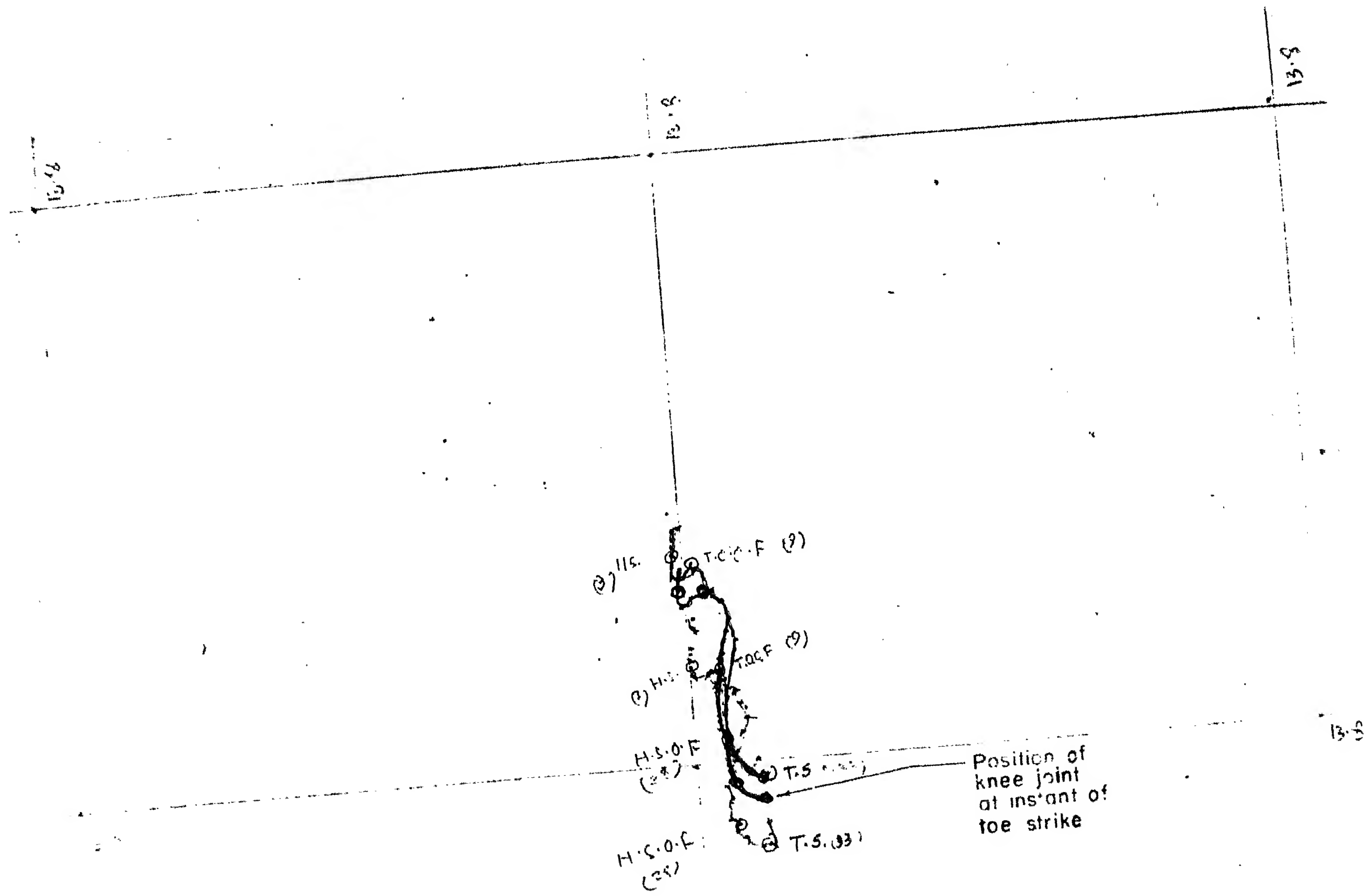

...ment pattern for locating knee joint
... Run 4)

graph was 20 cm and there were no finer divisions. The X and Z coordinates of the ankle and knee positions were calculated from the data of the displacement pattern in the X-Z plane; while the Y coordinates were calculated on the basis of data from the displacement pattern in the Y-Z plane. The reference coordinates for all the test runs have been mentioned in Tables B-1 to B-12 of Appendix B. These tables also provide details regarding the serial number of the frame and the frame numbers corresponding to important locomotion events such as heel strike, toe off other foot, heel strike other foot and toe strike.

The reference coordinates of the ankle and knee joints were then used to determine the coordinates of the centre of gravity of the limb segment, in accordance with the procedure outlined in Section 4.2. In order to obtain the acceleration of the centre of gravity, along a particular axis, a polynomial was fitted through the displacement data points. The degree of polynomial which gave least square error was finally chosen; and this was achieved by comparing the sum of the squares of errors in the computer programme itself. Once the degree of polynomial was settled, the second derivative could be evaluated from the polynomial coefficients. The error in fitting a polynomial through the displacement data was minimized for the useful data points by putting higher weightage for such points. In

order to check the pattern of displacement, computer graphs were obtained for the displacement of the centre of gravity of the limb segment along the X, Y and Z axes. These graphs were compared with those reported by Eberhart, Inman and Bresler (Klopsteg and Wilson, 1968), for the displacement of the ankle and knee joints along the axes. A good similarity was observed in such comparisons, which were carried out for the results of each test run. The angular rotations of the centre of gravity about the X and Y axes, ϕ_X and ϕ_Y, were obtained by computing the angular rotations of the axis of tibia. The direction of progression of a subject, during the walk cycle, was from negative to positive direction of the X-axis. The difference between the X coordinates of knee and ankle joints was positive before the axis of tibia become vertical; and was negative for the axis of tibia past the vertical position. The magnitude of ϕ_Y was positive in the former case, and negative in the later one. Therefore, ϕ_Y could be calculated, in both the cases, from the relation $\tan \phi_Y = (\frac{X_K - X_Z}{Z_K - Z_A})$. The rotation of the axis of tibia about the X-axis could be noted in the medial-lateral or the front view. Most of the time, the angular rotation, ϕ_X, was positive, while the difference between the Y coordinates of the knee and ankle joints was negative. Thus, ϕ_X could be computed as $\tan \phi_X = (- \frac{Y_K - Y_A}{Z_K - Z_A}$

The angular accelerations were determined in a manner similar to what has been stated about determining the linear accelerations, i.e. by fitting a polynomial, with the least square error, through the values of angular displacement.

CHAPTER 5

ANALYSIS OF THE RESULTANT KNEE JOINT FORCE

5.1 External Force Actions

The force actions to which the limb segment is subjected may conveniently be expressed with reference to an arbitrary coordinate system. A right handed coordinate system was adopted, with centre of the top surface of force plate as origin. The positive directions of the X, Y and Z axes of the reference coordinate system are shown in Figure 5.1. The figure depicts the foot of the left lower extremity in contact with the top surface of force plate during the stance phase. A free body diagram indicates the external force actions on the limb segment upto the knee joint.

The external force actions on the limb segment comprise of the ground-to-foot reactions, the gravitational force, and the inertia effects. The ground-to-foot reactions consist of the three forces along the reference axes i.e. F_X, F_Y and F_Z; and the three moments about the reference axes i.e. M_X, M_Y and M_Z. For convenience of analysis, the directions of all the six components are shown positive in Figure 5.1.

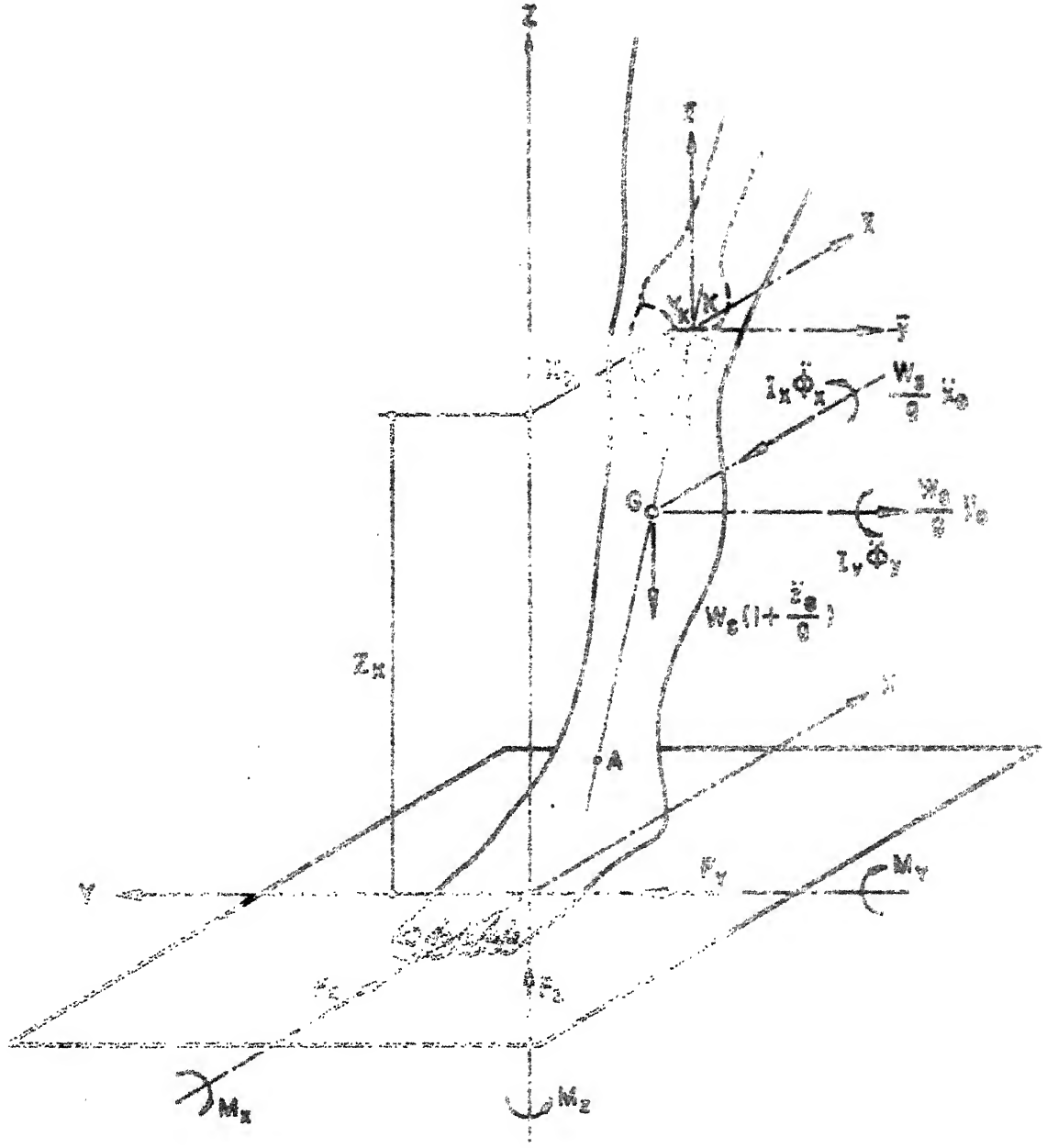

Fig.5.1 External force actions on the limb segment upto the knee joint

The gravitational force is due to the weight of the limb upto the knee joint; and is shown to be acting through the centre of gravity of the limb segment, denoted by G.

The inertia force components arise due to the inertia of the limb segment which is subjected to linear as well as angular accelerations. If the weight of the limb segment is denoted by W_S, the acceleration due to gravity by g, and the linear accelerations of the centre of gravity along directions parallel to the reference axes by $\ddot{x}_G$, $\ddot{y}_G$ and $\ddot{z}_G$, the inertia forces can be expressed as $W_S\ddot{x}_G/g$, $W_S\ddot{y}_G/g$ and $W_S\ddot{z}_G/g$, respectively. Similarly, if the angular accelerations about axes parallel to the X and Y axes and passing through G are denoted by $\ddot{\phi}_x$ and $\ddot{\phi}_y$, and the respective moments of inertia of the limb segment by I_x and I_y, the inertia moments can be expressed as $I_x\ddot{\phi}_x$ and $I_y\ddot{\phi}_y$, respectively. Since there is no rotation of the leg about its longitudinal axis during the stance phase, no inertia moment need be considered about an axis parallel to the Z-axis.

The weight of the limb segment, the position of the centre of gravity, and the radius of gyration about an axis perpendicular to the longitudinal axis of the shank, were calculated by using the coefficients evaluated by Contini and Drillis (1966). These coefficients were determined as a result of tests conducted, on twelve live male subjects having

their age between 20 to 39 years, at ~~the~~ New York University. By making use of the coefficients, the weight of shank and foot of one leg would be 0.062 times the body weight; and the distance of the centre of gravity of the shank would be 0.467 times the length of shank, from the knee position. The radius of gyration, for rotation about an axis through the mass centre and perpendicular to the longitudinal axis of the shank would be 0.29 times the length of the shank. Since the axis of shank is inclined to the vertical, in most cases, the effective radii of gyration would have to be correspondingly reduced. Thus, if k_x and k_y denote the radii of gyration about axes passing through G and parallel to the X and Y axes, and ϕ_x and ϕ_y denote the rotations of the axis of shank about axes parallel to the Y and X axes, then

$$k_x = 0.29 \text{ times length of the shank} \cdot \cos \phi_y$$

and $$k_y = 0.29 \text{ times length of the shank} \cdot \cos \phi_x$$

5.2 Forces and Moments at the Knee Joint

If the coordinates of the ankle and knee joints in the reference frame of axes (X, Y and Z) are denoted by the respective suffix; and a set of axes ($\bar{x}$, $\bar{y}$ and $\bar{z}$), parallel to the reference axes, are considered to be passing through the knee joint, K, the forces and moments acting at the knee joint may be summed up as follows:

Force along the $\bar{x}$-axis $= F_X - \frac{W_S}{g} \ddot{x}_G$

Force along the $\bar{y}$-axis $= F_Y - \frac{W_S}{g} \ddot{y}_G$

Force along the $\bar{z}$-axis $= F_Z - W_S(1 + \frac{\ddot{z}_G}{g})$

Moment about the $\bar{x}$-axis $= M_X - I_x \ddot{\phi}_x + F_Y Z_K - F_Z Y_K +$

$$W_S(1 + \frac{\ddot{z}_G}{g})(Y_K - Y_G) - \frac{W_S}{g} \ddot{y}_G (Z_K - Z_G$$

Moment about the $\bar{y}$-axis $= M_Y - I_y \ddot{\phi}_y - F_X Z_K + F_Z X_K +$

$$\frac{W_S}{g} \ddot{x}_G (Z_K - Z_G) - W_S(1 + \frac{\ddot{z}_G}{g})(X_K - X_G$$

Moment about the $\bar{z}$-axis $= M_Z + F_X Y_K - F_Y X_K - \frac{W_S}{g} \ddot{x}_G (Y_K - Y_G)$

$$+ \frac{W_S}{g} \ddot{y}_G (X_K - X_G)$$

The values of the force components mentioned above were calculated by use of a computer programme for which the ground-to-foot reactions and the displacement characteristics data were fed as input. The length of the shank was determined from the value of $(Z_K - Z_A)$ for the vertical position of the shank. The value of the radii of gyration k_x and k_y happens to be the same for the vertical position of the shank, and was also fed as input to the computer programme.

The effective radii of gyration, corresponding to a specific rotation ϕ_x or ϕ_y, were calculated in the computer programme itself. The values of the physical dimensional factors for the subjects, which were used in the computations, are listed in Table 5.1.

Table 5.1 Physical Dimensional Factors for Computation of External Force Actions at the Knee Joint

Subject	Body weight, W (kg)	Weight of shank and foot, $W_S = 0.062W$ (kg)	Length of Shank (cm)	Radii of gyration k_x or k_y, for vertical position of shank (cm)
B	74	4.588	42.5	12.325
C	63	3.906	36.75	10.657
D	57	3.534	39.0	11.31

5.3 Consideration of Body Forces

The forces acting within the body of the limb segment are due to action of the muscles. The contraction of a muscle is associated with the development of a tensile force, the line of action of which may be assumed to be that connecting the point of origin to the point of insertion of the muscle. While the external forces transmitted by the knee joint cause a corresponding bearing load between the surfaces of contact, the external moments are balanced by

the action of muscles and ligaments spanning the joint. At the knee joint, there is no musculature which can provide a balancing moment about the X and Z axes. There exists only a passive ligamentous structure which transmits the external moments from the tibia to the femur, without altering the magnitude of the resultant knee joint force. The moment about the Y-axis, which results in the flexion and extension of the tibia relative to the femur, happens to be the most significant one.

5.4 Musculature Providing Moment Balance

A comparison between the myoelectric signals from the leg muscles during a walk cycle and the corresponding force actions at the knee joint was made by Paul (1971). He used surface electrodes to collect the EMG signals from a selected group of muscles; and the force plate cum cinephotographic technique for determining the moment transmitted between the leg segments. The results indicated that there was no direct relationship between the muscle force and the EMG signal, but the later could be usefully employed to indicate the phasing of cyclical activity. Based on values reported by Bresler and Frankel (1950) and previously unreported values calculated by Morrison, a graph showing the variation of knee moment with time was reported. A

compilation of the EMG results of University of California (1953), Close and Todd (1959), Joseph and Battye (1966) and that of his own experiments was also made. By comparing the EMG results with the variation of extending/flexing knee moment during the stance phase, it was concluded that the three peaks in the knee moment curve required activity of the hamstrings, quadriceps, and the muscle gastrocnemius for obtaining a moment balance at the knee joint. No attempt was, therefore, made to obtain the EMG record of the subjects during the present investigation. The extending/flexing knee moment was computed in the regions of the second and third peaks during the stance phase, and then assigned to the activity of quadriceps and muscle gastrocnemius respectively. Although the quadriceps consist of the rectus femoris and the three vasties, the group as a whole was assumed to have a single line of action at the point of insertion with the patella ligament.

5.5 Balancing Moment Due to Force in the Patella Ligament When the Axis of Tibia is Prior to the Vertical Position

Figure 5.2(a) depicts the point of attachment, M, of the patella ligament to the tibia, before the axis of tibia becomes vertical. The line of action of the ligament force, P, is shown to be making an angle of 15° with the axis of tibia, which happens to be a normal anatomical feature.

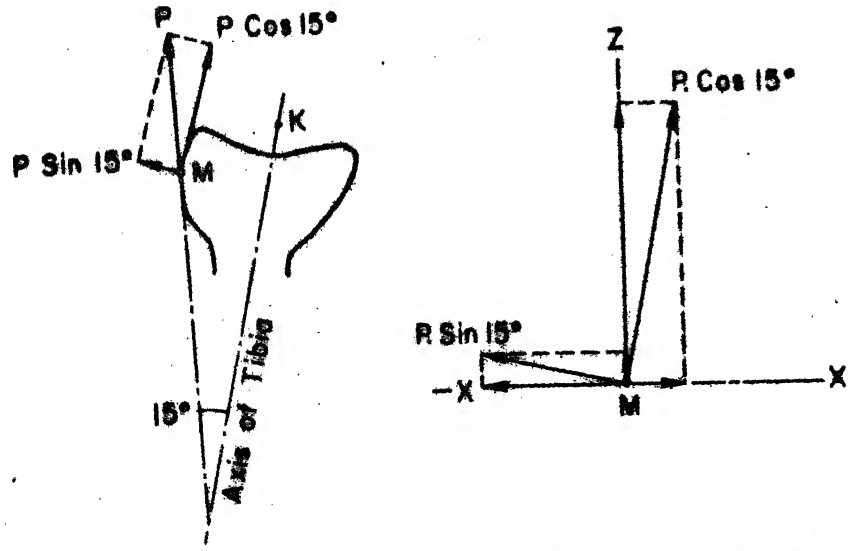

(a) When the axis of Tibia is prior to the vertical position

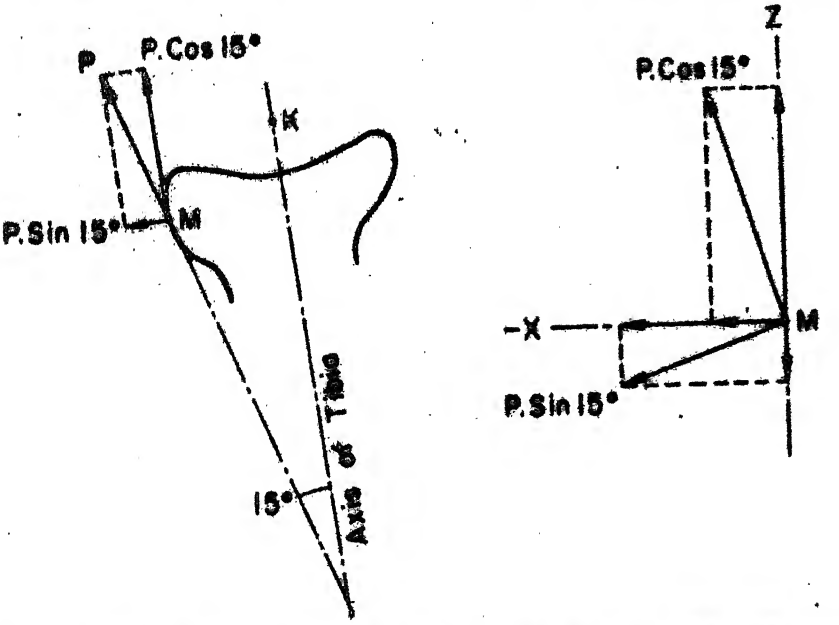

(b) When the axis of Tibia is past the vertical position

Fig.5.2 Force in the Patella Ligament, P, and its components

The ligament force can be resolved along and perpendicular to the axis of tibia as shown in Figure 5.2(a). The force components along directions parallel to the reference axes, X, Y and Z, may be calculated if the respective direction cosines are known. Let the force component along the axis of tibia have the direction cosines DCX, DCY, and DCZ; and the component normal to the axis of tibia have the direction cosines DCXN, DCYN, and DCZN, respectively. The methods used for determining the direction cosines, for the present case and the one discussed in Section 5.6, are mentioned in Sections 5.11 and 5.12.

The resolution of the force components along the orientations of X and Z axes is also depicted separately in Figure 5.2(a). The moment due to these components about an axis parallel to the Y-axis and passing through the knee joint, K, can be worked out as follows:

$$P \cos 15^\circ \; - DCX(Z_K - Z_M) + DCZ(X_K - X_M) \; +$$

$$P \sin 15^\circ \; DCXN(Z_K - Z_M) - DCZN(X_K - X_M)$$

5.6 Balancing Moment Due to Force in the Patella Ligament When the Axis of Tibia is Past the Vertical Position

Figure 5.2(b) depicts the force components acting on the tibia, due to tension in the patella ligament, when the axi of tibia is past the vertical position; and also the resolutio

of the force components along the orientations of X and Z axes. In this case, the moment caused by these force components about an axis parallel to the Y-axis and passing through the knee joint, K, can be written as follows:

$$P \cos 15^\circ \quad DCX(Z_K - Z_M) + DCZ(X_K - X_M) \quad +$$

$$P \sin 15^\circ \quad DCXN(Z_K - Z_M) - DCZN(X_K - X_M)$$

5.7 Balancing Moment Due to Activity of Muscle Gastrocnemius

Figure 5.3(a) shows the femur in contact with the tibia and the point of attachment, M, of the muscle gastrocnemius to the femur. The position of the knee joint, K, and the resolution of the muscle force into the X and Z components is also shown in this figure. The line of action of the muscle force has been assumed parallel to the axis of tibia, although the muscle itself has a curved profile. The exploded view, shown in Figure 5.3(b), depicts the reaction of the femur on the tibia and the direction of the muscle force with respect to tibia. The X and Z components of the muscle force, with respect to the tibia, are also shown separately in this figure.

The moment caused by the components of the muscle force, about an axis parallel to the Y-axis and passing through K, can be expressed as follows:

$$GS \quad DCX(Z_M - Z_K) + DCZ(X_M - X_K)$$

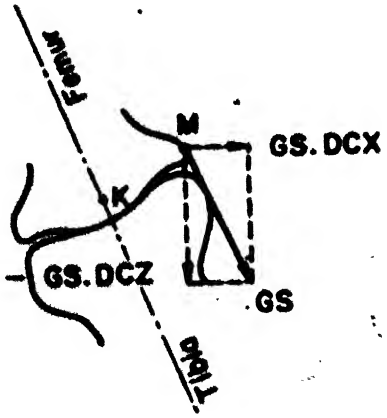

Fig.5.3 (a)

Force due to muscle Gastrocnemius on the Femur and its components

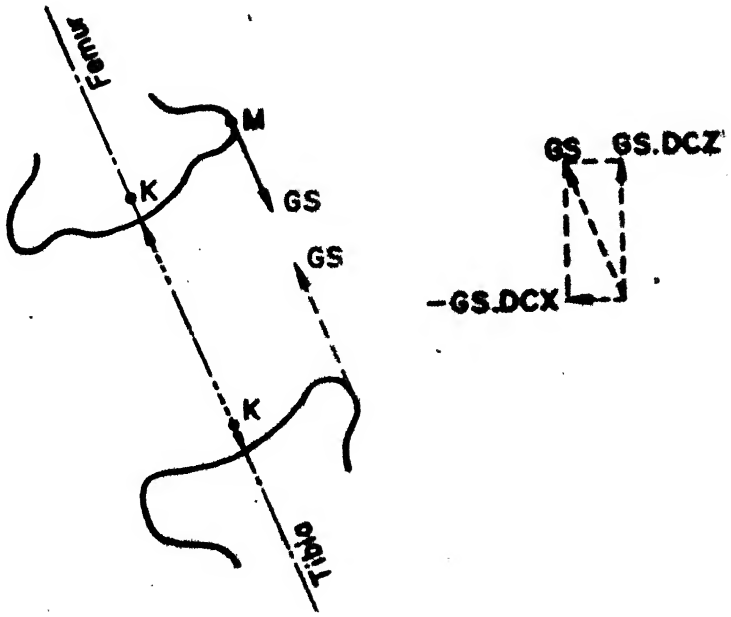

Fig.5.3 (b)

Direction of force due to muscle Gastrocnemius on Tibia and its components

5.8 Evaluation of Muscle Force

The expressions for balancing moment mentioned in Sections 5.5, 5.6 and 5.7 can be evaluated by equating them to the corresponding known value of the external moment at the knee joint. The value of the patella ligament force P or the muscle gastrocnemius force GS can be found if the X and Z coordinates of the point of attachment M, of the patella ligament to the tibia or the muscle gastrocnemius to the femur, are known. The relevant coordinates of point M, at a particular instant, were determined from a graphical layout of the point of attachment on the displacement record of the limb in the X-Z plane. To locate the point of attachment of the patella ligament to the tibia the X and Z coordinates of point M, with respect to the tubercle of tibia, were noted for the fully extended vertical position of the limb by external measurement. Similarly, to locate the point of attachment of the muscle gastrocnemius to the femur, the X coordinate of point M with respect to the femur condyle was noted for the fully extended position of the limb.

The scale factors were duly considered while locating the point M on the displacement record of the limb in the X-Z plane, and in converting back the values of the coordinates for use in computations. The external measurements taken to locate the point of attachment M, for each of the subjects, are listed in Table 5.2.

Table 5.2 Measurements for Locating the Point of Attachment of the Muscle or Ligament to the Appropriate Bone

Subject	Point of attachment of patella ligament to the tibia, from the tubercle of tibia		Point of attachment of muscle gastrocnemius to the femur, from the condyle of femur
	X-coordinate (cm)	Z-coordinate (cm)	X-coordinate (cm)
B	2.4	2.3	2.7
C	2.35	1.8	2.0
D	3.0	2.0	2.5

5.9 Muscle Force Components Along the Reference Axes

With reference to Figure 5.2(a), the force components due to tension in the patella ligament are the following:

X-component: (P cos 15° DCX - P sin 15° DCXN)

Y-component: -(P cos 15° DCY + P sin 15° DCYN)

Z-component: (P cos 15° DCZ + P sin 15° DCZN)

Considering Figure 5.2(b), the force components due to tension in the patella ligament are the following:

X-component: -(P cos 15° DCX + P sin 15° DCXN)

Y-component: -(P cos 15° DCY - P sin 15° DCYN)

Z-component: (P cos 15° DCZ - P sin 15° DCZN)

Referring to Figure 5.3(b), the force components, with respect to the tibia, due to action of the muscle gastrocnemius are the following:

X-component: -GS DCX

Y-component: -GS DCY

Z-component: GS DCZ

5.10 Resultant Force at the Knee Joint

The external force components have already been considered in Section 5.2. In order to make the analysis complete, it is only necessary to add the respective muscle force components along the reference axes, as mentioned in Section 5.9. The resultant knee joint force can be found by squaring and adding the net value of the components along the reference axes, and taking the square root of the sum.

5.11 The Direction Cosines When the Axis of Tibia is Prior to the Vertical Position

In the three dimensional view shown in Figure 5.4(a), the resultant vector OA has components x, -y and z along the reference axes with origin at O. The trace of OA on the Y-Z plane is represented by another vector OB; while OC is a vector perpendicular to OA and lying in the plane formed by OA and OB.

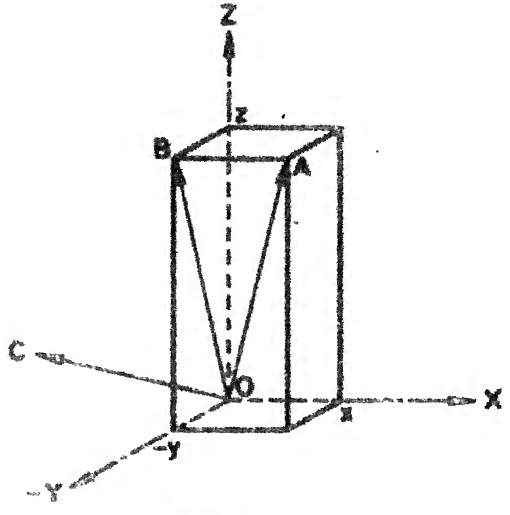

Fig.5.4 (a)

Three dimensional view when the axis of Tibia, OA, is prior to the vertical position

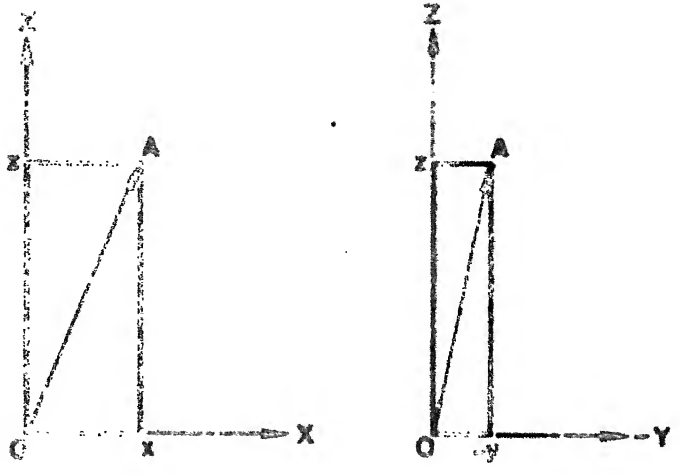

Fig.5.4 (b)

Axis of Tibia, OA, depicted in the X-Z and Y-Z planes (inclinations are exaggerated)

The direction cosines of OA are simple to calculate. Let these be represented by DCX, DCY, and DCZ, along the reference axes, respectively. If the magnitude of OA is represented by $V = (x^2 + y^2 + z^2)^{1/2}$, the direction cosines are given by

$$DCX = \frac{x}{V} \; ; \qquad DCY = -\frac{y}{V} \; ; \quad \text{and} \quad DCZ = \frac{z}{V}$$

The direction cosines of OC can be found mathematically (Selby, 1969) if the direction cosines of OB are known and certain equations, involving the known direction cosines, are satisfied. Let the direction cosines of OA be represented by

$$a_1 = L = \frac{x}{V} \; ; \quad b_1 = M = -\frac{y}{V} \; ; \quad \text{and} \quad c_1 = N = \frac{z}{V}$$

The direction cosines of OB are also simple to calculate and are given by

$$a_2 = 0 \; ; \qquad b_2 = -\frac{y}{(y^2 + z^2)^{1/2}} \; ; \quad \text{and} \quad c_2 = \frac{z}{(y^2 + z^2)^{1}}$$

Then, the direction cosines of OC, represented by l, m, and n, can be found if the following three equations are simultaneously satisfied:

$$l^2 + m^2 + n^2 = 1 \qquad (5.1$$

$$lL + mM + nN = 0 \qquad (5.2$$

$$\text{and} \quad l(b_1c_2 - c_1b_2) + m(c_1a_2 - a_1c_2) + n(a_1b_2 - a_2b_1) = 0 \qquad (5.$$

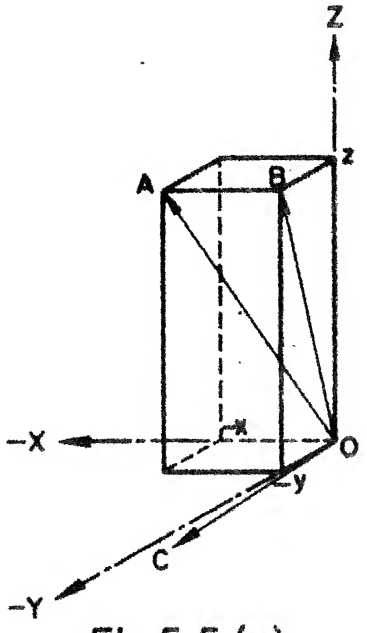

Fig.5.5 (a)

Three dimensional view when the axis of Tibia, OA, is past the vertical position

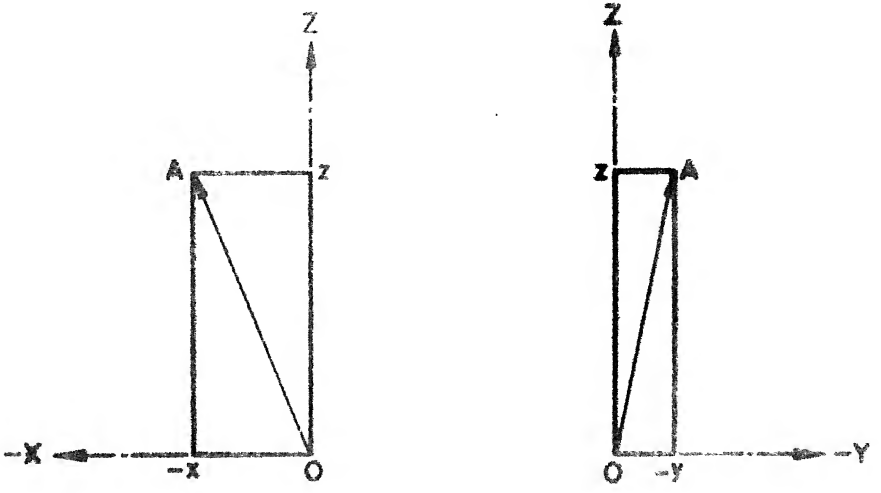

Fig.5.5(b)

Axis of Tibia, AO, depicted in the X-Z and Y-Z planes (inclinations are exaggerated)

The following are the values of l, m and n, which satisfy the above three equations:

$$l = DCXN = -\frac{(y^2 + z^2)^{1/2}}{V}\ ;\quad m = DCYN = -\frac{xy}{V(y^2 + z^2)^{1/}}$$

$$\text{and}\quad n = DCZN = \frac{xz}{V(y^2 + z^2)^{1/2}}$$

5.12 The Direction Cosines When the Axis of Tibia is Past the Vertical Position

In this case the components of the resultant vector OA, along the reference axes, are -x, -y and z, as shown in Figure 5.5(a) and the position of OA in the xz and yz planes is illustrated in Figure 5.5(b). Proceeding in a manner similar to Section 5.11, the direction cosines of OA are given by $DCX = -\frac{x}{V}$; $DCY = -\frac{y}{V}$; and $DCZ = \frac{z}{V}$.

The direction cosines of OB are given by

$$a_2 = 0;\quad b_2 = -\frac{y}{(y^2 + z^2)^{1/2}}\ ;\quad \text{and}\quad c_2 = \frac{z}{(y^2 + z^2)^{1/2}}$$

In this case, the values of l, m and n, which satisfy the three equations 5.1, 5.2 and 5.3, are given by

$$l = DCXN = -\frac{(y^2 + z^2)^{1/2}}{V}\ ;\quad m = DCYN = \frac{xy}{V(y^2 + z^2)^{1/2}}$$

$$\text{and}\quad n = DCZN = -\frac{xz}{V(y^2 + z^2)^{1/2}}$$

In the analysis discussed in the present as well as in the previous section, the vector CA represents the orientation of the axis of tibia, while the vector OC represents an orientation normal to the axis of tibia and pointing towards the front portion of the leg. For any given position of the limb in the reference frame of axes, both these orientations can be conveniently expressed in term of the X, Y and Z coordinates of the ankle and knee joints. Since the absolute values of the direction cosines for the vectors OA and OC are same in Sections 5.11 and 5.12, these were first evaluated in the computer programme. The positive or negative sign was taken care of in the analysis while computing the effect of a particular component.

CHAPTER 6

EXPERIMENTAL RESULTS AND DISCUSSIONS

6.1 About the Subjects and Test Conditions

Three normal adult male subjects, having their age between 24 to 37 years, were tested during level walking. The subjects walked without shoes on a walk platform, which was fabricated for the purpose of experimentation. They wore minimum clothing so as to provide an unobstructed view of the adhesive markers, placed over anatomical landmarks of the left lower extremity. Before conducting the experiment, the subjects were instructed to walk at their natural gait during a number of trial runs; and their natural step length was noted. Later on, the starting position and initial step length was marked with chalk on the walk platform to provide the initial starting condition. With some adjustments in the starting position, the subjects could walk at their natural gait such that the left foot always fell on the force plate. The force plate was suitably accommodated along the walk-path; and its top surface was kept in level with that of the walk platform. The foregoing procedure enabled to obtain a constant stride length for a subject, during all the test runs, without altering the natural gait. The length of the walk platform

was about six meters; and the subjects could complete two gait cycles before proceeding for the one which was recorded. The performance of a subject was evaluated on the basis of four test runs. The experiments were conducted indoors, under moderate temperature conditions between 26-28°C.

6.2 Computation of Results

The calibrated values of ground-to-foot reactions, the motion characteristics of the limb segment, and the physical dimensions of the test subjects were fed as input to a computer programme which, in the first stage, calculated the external forces and moments acting at the knee joint. In the second stage of the programme, the extending/flexing knee moment was assigned to a specific muscle group and the muscle force, as well as its ratio to the weight of the subject, was calculated. Taking the muscle force into account, this stage was also used to calculate the components of knee joint force along the reference axes, the resultant force at the knee joint, and the ratio between the resultant force and the weight of a subject.

6.3 Results and Discussions

The relevant experimental results for all the four test runs performed by each of the three subjects B,

C and D are compiled in tabular form in Appendix - C. The details mentioned therein are the identification of the test run, the data point number during force calibration, the stance phase timing in percentage, the musculature active during the period, the ratio between the resultant knee joint force and the body weight, and the value of muscle force corresponding to the maximum value of the ratio.

The ratio between the resultant knee joint force and body weight of a subject was plotted as a function of stance phase timing, for all the four test runs, and a summary curve depicting the average behaviour of each subject was obtained. If a drastically different behaviour pattern was noted during an individual test run, which did not agree with the majority of test results for that particular subject, such test run was not considered in obtaining the summary curve. A graphical representation, of the results of individual test runs as well as the summary curve for the three subjects, is shown in Figures 6.1, 6.2 and 6.3. The peak values of the ratio between the resultant knee joint force and body weight of a subject and the timings of these peak values during the stance phase, as obtained from the summary curves, are shown in Table 6.1. It will be noted that the peak value of the resultant knee joint force occurs during activity of quadriceps femoris for subjects B and D, and muscle gastrocnemius for subject C.

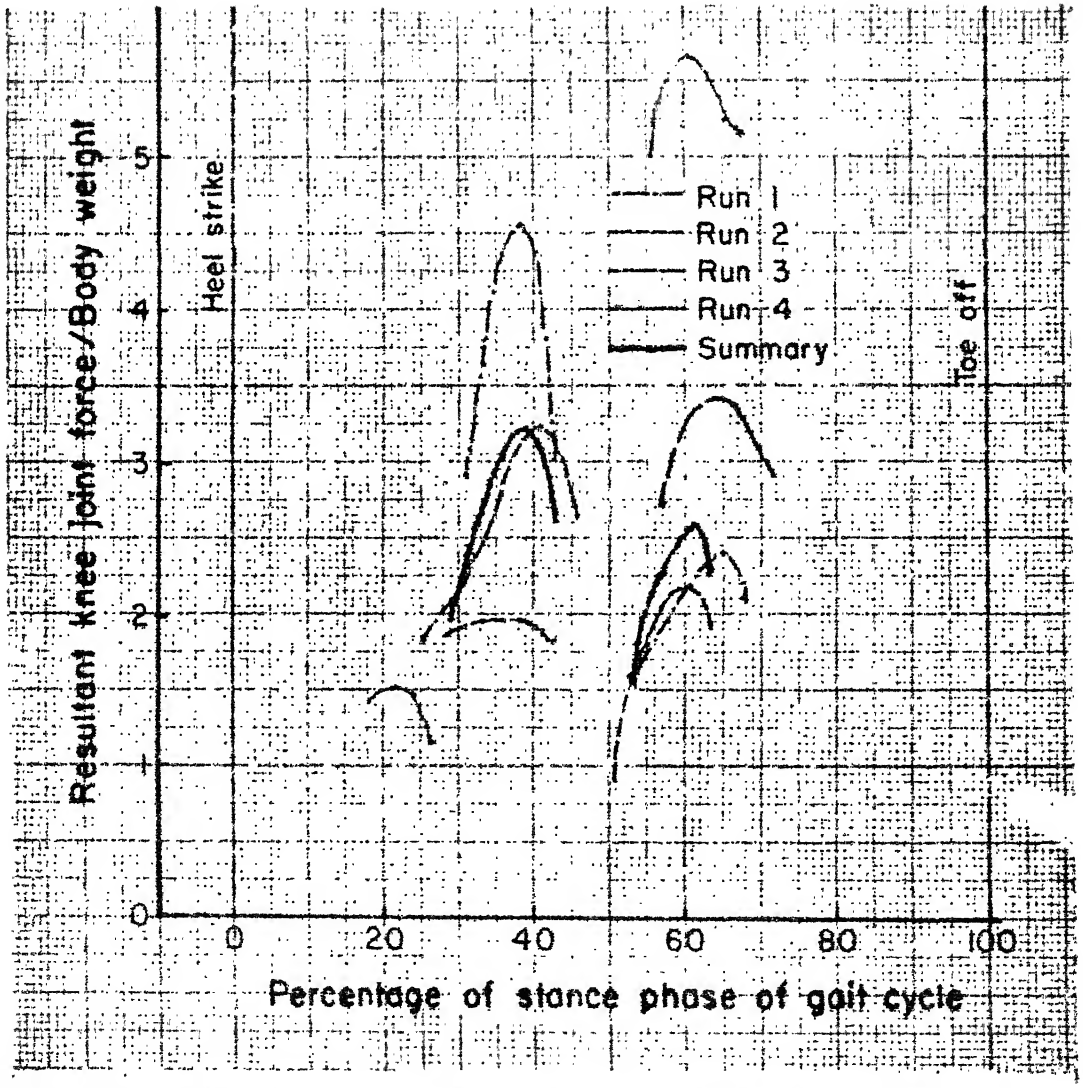

Fig.6.1 Variation of Resultant Knee Joint Force with Time for Subject B

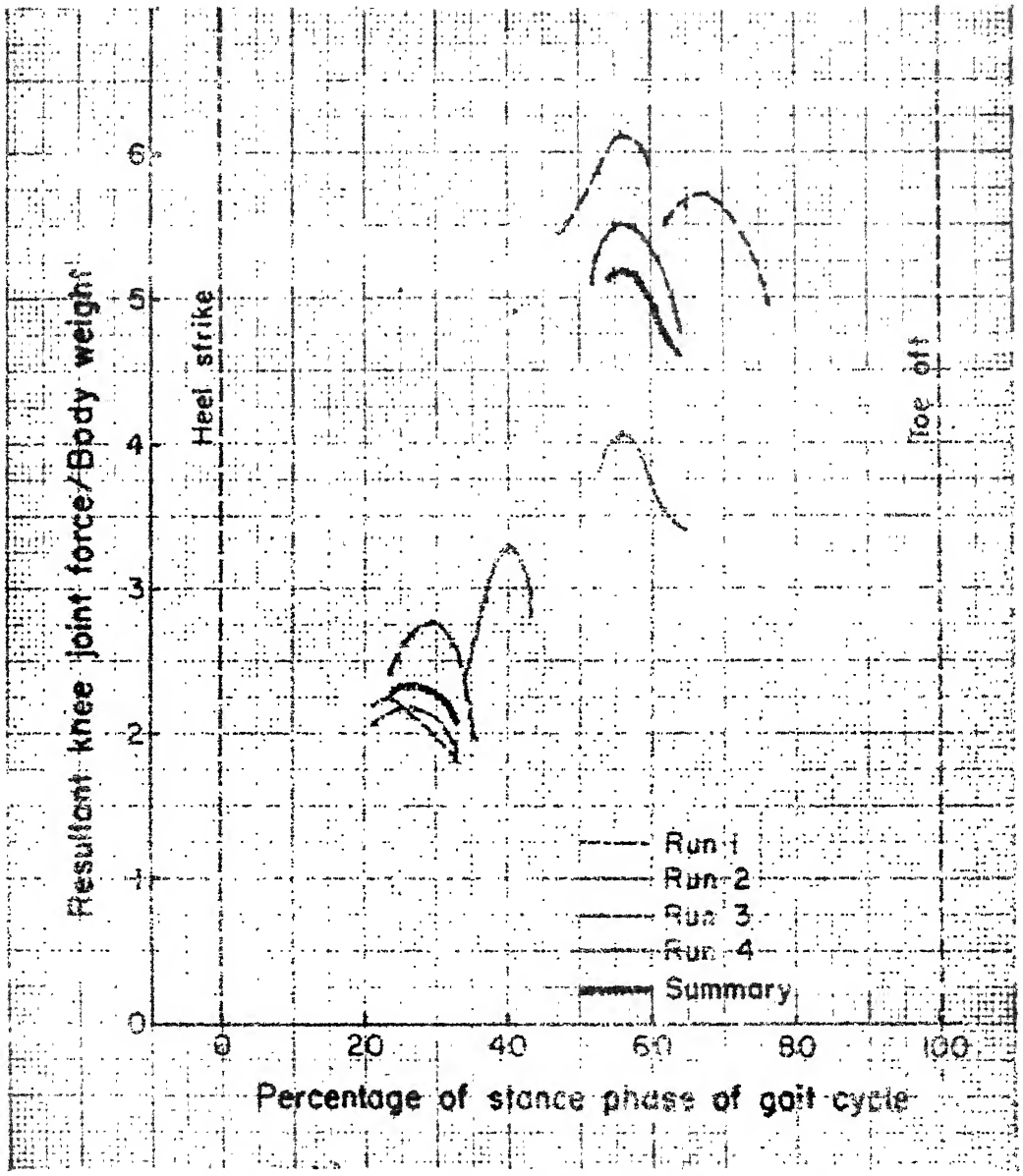

Fig.6.2 Variation of Resultant Knee Joint Force with Time for Subject C

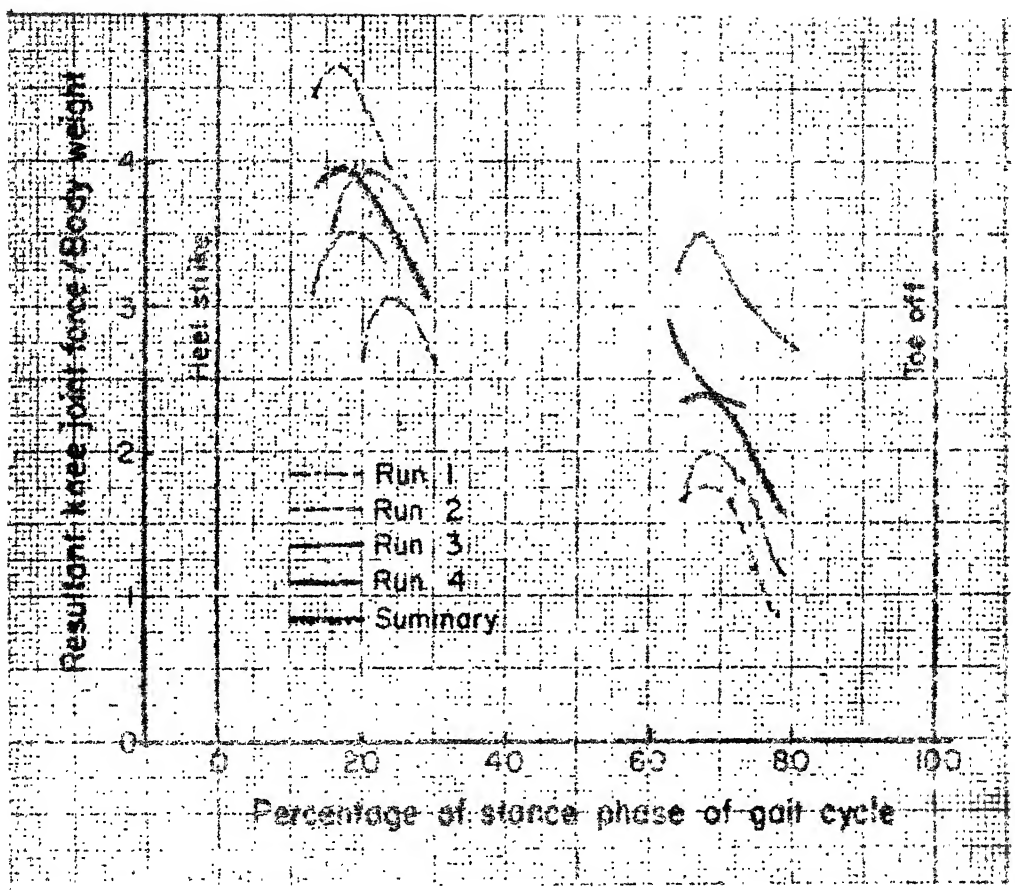

Fig.6.3 Variation of Resultant Knee Joint Force with Time for Subject D

Table 6.1 Peak Values of Resultant Knee Joint Force Obtained from the Summary Curves

Subject	Ratio of maximum knee joint force and body weight during stance phase				Maximum knee joint force lb.
	Quadriceps femoris active		Muscle gastrocnemius active		
	Magnitude of ratio	Timing as percent of stance phase	Magnitude of ratio	Timing as percent of stance phase	
B	3.22	38.5	2.6	61.5	524.22
C	2.35	27.0	5.2	56.5	720.72
D	3.96	17.5	2.41	67.5	496.58
Average value subjects B and D	3.59	28.0	2.505	64.5	

It is, therefore, found that the maximum knee joint force can occur during activity of either of the two muscle groups, and a single muscle group cannot be identified.

The magnitude of the knee joint force, corresponding to the peak of a summary curve, has also been mentioned in Table 6.1. For the purpose of comparison of the results with those of earlier investigators, the force magnitudes

have been stated in pounds. Paul (1970), using the data obtained by him and Morrison, had proposed a linear relationship between the average maximum knee joint force and a physical dimensional factor, WL/H, as shown in Figure 6.4. The values of this physical dimensional factor were also calculated for the subjects of present investigation. These values, together with the physical dimensions of the test subjects, are mentioned in Table 6.2.

Table 6.2 Physical Dimensions of the Test Subjects

Subject	Age yr	Weight, W kg	Height, H cm	Length of stride, L cm	Value of factor, WL/H lb
B	37	74	179.0	125.0	113.69
C	31	63	157.0	96.0	84.74
D	24	57	167.5	135.0	101.06

Two of the data points of present investigation, which were in the range covered by Paul and Morrison, are also shown in Figure 6.4. Incidentally, the two data points lie higher up but on a straight line having almost same slope as for the straight line proposed by Paul. It was found that the two points are higher up by about 65% from the straight line

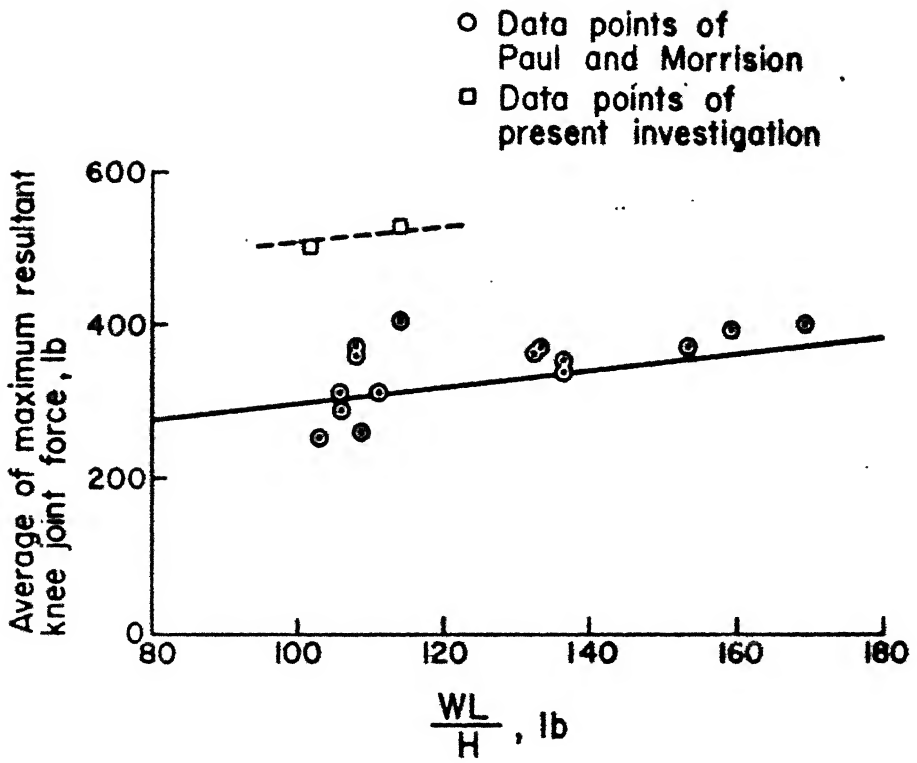

Fig. 6.4 Variation of Average Maximum Resultant Knee joint Force with Body weight W, Stride length L and Height H

fit of Paul. It was also noted that one of the data points of even the previous investigators was higher up by about 30% from the straight line fit. Keeping in view that the element of error in the overall result could be to the extent of 35% (Paul and Poulson, 1974), it can be concluded that the general trend of results, for the present investigation, compares well with that of previous investigators. The third data point, having the value of the factor $^{W}L/H$ equal to 84.74 lb., had the joint force considerably higher from the straight line fit. This type of behaviour was considered abnormal; and in the absence of any other data point in this range, no further comments can be offered about it. The overall conclusions regarding the magnitude of maximum loading were, therefore, drawn on the basis of results obtained for the other two subjects i.e. B and D.

It will be noted that from Table 6.1 that the average value of the ratio between maximum resultant knee joint force and body weight is 3.59. Also the average timings for the maximum knee joint force, due to action of the quadriceps femoris and muscle gastrocnemius, are 28% and 64.5% of the stance phase, respectively. In comparison, according to the summary curve of Harrington (1974), the magnitude of the ratio is 3.5 and the timings are 30% and 80%, respectively. The difference between the timings, for maximum knee joint force due to activity of muscle

gastrocnemius, may be attributed to the variable nature of human behaviour.

The ratio between the maximum muscle force and body weight of a subject has been compiled, for all the test runs, in Table 6.3. The average values of this ratio, for the quadriceps femoris and muscle gastrocnemius, are 2.33 and 1.92, respectively. In the absence of any information in this regard from previous investigations, these values could not be compared.

Table 6.3 Maximum Muscle Force During the Test Runs

Test No.	Ratio of maximum muscle force and body weight	
	Quadriceps femoris active	Gastrocnemius active
B-1	3.649	1.272
B-2	2.335	1.121
B-3	1.059	2.291
B-4	0.511	4.498
C-1	1.322	3.066
C-2	1.348	4.574
C-3	1.912	5.046
C-4	2.383	4.378
D-1	1.997	0.973
D-2	3.598	0.716
D-3	2.997	1.889
D-4	2.482	2.602
Average value subjects B and D	2.33	1.92

CHAPTER 7

CONCLUSIONS AND SCOPE FOR FURTHER WORK

7.1 Conclusions

An experimental evaluation of the maximum knee joint loading was made for three normal adult males, walking without shoes on a level surface. The left lower extremity was considered for the purpose of analysis; and the tests were conducted at the natural stride length of the subjects, which was maintained constant. The following conclusions can be made on the basis of test results:

1. A single muscle or muscle group, which causes maximum resultant knee joint force during level walking, cannot be identified, though in a majority of cases the maximum loading of the knee joint occurs during activity of quadriceps femoris.
2. The ratio between the average value of maximum resultant knee joint force and the subject weight is of the order of 3.59.
3. The ratio between the average values of maximum muscle forces and the subject weight, during activity of quadriceps femoris and muscle gastrocnemius, are 2.33 and 1.92, respectively.

4. The average value of the maximum resultant knee joint force varies linearly as a function of the subject weight and stride length; and there is no significant effect on the knee joint force due to change in climatic conditions.

As regards the finite element analysis, which was used to varify the deformation characteristics of the octagonal rings used in the dynamometer, it may be stated that it provides a more accurate solution than the empirical formulae available so far.

7.2 Scope for Further Work

A dynamic analysis of the left lower extremity, using the force plate cum cine-photographic technique, can be made with a change in one or more of the variables of the problem. The variables of the problem are

(i) Age group of subjects: Evaluation can be made for children as well as old subjects.

(ii) Sex of subjects: Female subjects may be evaluated.

(iii) Physical status of subjects: Subjects with limb deformities may be evaluated.

(iv) Whether shoes have been put on or not: The subject may walk with shoes; and the shoes may be with different types of heels.

(v) Condition of surface for walking: It may be up or down a slope; climing up or descending down the stairs; walking in sand or on a very smooth surface.

(vi) Stride length: It may be fast walking or running.

(vii) Activities other than walking: These may include sport activities such as jumping, skating etc.

(viii) Temperature conditions during the tests: Extreme conditions of temperature may be provided during tests.

(ix) The joint under consideration: Ankle or hip joints may as well be considered.

Further work is also possible by a change in the techniques of measurement, besides refining the ones used during the present investigation. The cine-photographic technique, for motion measurement, is time consuming. Collection of kinematic data by T.V. cameras and automatic data processing may be used. Similarly, in place of the force plate, the evaluation of ground-to-foot reactions may be made by use of transducers placed in the sole of the foot. In addition, transducers or techniques, such as infra-red photography, may be used to determine the muscle forces.

A change in the technique of analysis is also possible. Mathematical modelling, which has so far been used to determine the joint force under quasi-static conditions, can be used to determine the joint force under completely dynamic conditions.

A further possibility exists by consideration of joints other than that of the lower extremity. The upper extremity and the motion of other segments of human body, such as motion of the jaw during mastication, may be considered.

There is, thus, enough scope for further work; and a vast field remains to be explored.

REFERENCES

Bernstein, N.A., et al., "Biodynamics of Locomotion", VIEM, Moscow, USSR, Vol. 1, 1935.

Bernstein, N.A., et al., "Determination of masses and centroids of segments of human body on live objects", VIEM, Moscow, USSR, 1936.

Bigland, B. and Lippold, O.C.J., "The relation between force, velocity and integrated electrical activity in human muscles", J. Physiol., Vol. 123, 1954, p. 214.

Braune, W. and Fischr, O., "Uber den Schwerpunkt des menschlichen Korpers mit Ruecksicht auf die Aursruestung des deutschen Infanteriesten" (concerning the centre of gravity of the human body with reference to the equipment of the German infantryman), Abhandlungen der Koenigl. Saechs. Gesellschaft der Wissenschaft, Vol. 15, 1872.

Bresler, B. and Frankel, J.P., "The forces and moments in the leg during level walking", Trans. ASME, Vol. 72, 1950, p. 27.

Close, J.R. and Todd, F.N., "The phasic activity of the muscles of the lower extremity and the effect of tendon transfer", J. Bone Jt. Surg., Vol. 41A, 1959, p. 189.

Contini, R. and Drillis, R.J., "Body Segment Mass Properties" Technical Report No. 1166.03, New York University, 1966.

Cook, N.H. and Rabinowicz, E., "Physical Measurement and Analysis", Addison-Wesley Pub. Co., Inc., USA, 1963.

Cunningham, D.M. and Brown, G.W., "Two devices for measuring the forces acting on the human body during walking", Proc. SESA, Vol. 9, No. 2, 1952, p. 75.

Elftman, H., "A cinematic study of the distribution of pressure in the human foot", Anatomical Record, Vol. 59, 1934, p. 481.

Elftman, H., "The function of arms in walking", Human Biol., Vol. 2, 1939, p. 529.

Elftman, H., "The rotation of body in walking", Arbeitsphysiologie, Vol. 10, 1939, p. 477.

Elftman, H., "The force exerted by the ground in walking", Arbeitsphysiologie, Vol. 10, 1939, p. 485.

Elftman, H., "Forces and energy changes in the leg during walking", Am. J. Physiol., Vol. 125, 1939, p. 339.

Elftman, H., "The function of muscles in locomotion", Am. J. Physiol., Vol. 125, 1939, p. 357.

Elftman, H., "The action of the muscles in the body", Biol. Symposia, Vol. 3, 1941, p. 191.

Frank, A.A. and Vukobratovic, M., "On the synthesis of biped locomotion machines", 8th Int. Conf. Medical and Biol., Engng., Evanston, Illinois, 1969.

Harrington, I.J., "The effect of congenital and pathological conditions on the load action transmitted at the knee joint", Conf., Instn. Mech. Engrs., Paper C-204/74, 1974.

Holman, J.P., "Experimental methods for engineers", McGraw-Hill Book Co., USA, 1966.

Joseph, J. and Battaye, C.K., "An investigation by telemetering of the activity of some muscles in walking", Med. and Biol. Engng., Vol. 4, 1966, p. 125.

Klopsteg, P.E. and Wilson, P.D., et al., "Human limbs and their substitutes", Hafner Pub. Co., New York, 1968.

Lamoreux, L.W., "Kinematic measurements in the study of human walking", Bull. Prosth. Res., BPR 10-15, 1971, p. 3.

Levi, R., "Multicomponent calibration of machine tool dynamometers", J. Engg. for Industry, Trans. ASME, Vol. 94, Nov. 1972, p. 1067.

Lippold, O.C.J., "The relation between integrated action potentials in a human muscle and its isometric tension", J. Physiol., Vol. 117, 1952, p. 492.

Loewen, E.G. and Cook, N.H., "Metal cutting measurements and their interpretation", SESA Proc., Vol. XIII, No. 2, 1955 (Photoelastic analysis of octagonal rings).

Marey, E.J., "Terrestrial locomotion of bipeds and quadrupeds", J. de l'Anat. et de la Physiol., Vol. 9, 1873, p. 42.

Marey, E.J. and Demny, G., "Experimental studies of human locomotion", Comptes Rendus Acad. des Ses., Vol. 105, 1887, p. 544.

Morrison, J.H., "Bio-engineering analysis of force actions transmitted by the knee joint", Bio-med. Engng., Vol. 4, 1968, p. 164.

Morrison, J.H., "The mechanics of knee joint in relation to normal walking", J. Biomechanics, Vol. 3, 1970, p. 51.

Newman, W.N. and Sproull, R.F., "Principles of Interactive Computer Graphics", McGraw-Hill, New York, 1973.

Paul, J.P., "Forces transmitted by joints in the human body", Proc. Inst. Mech. Engrs., Vol. 181, Pt. 3J, 1967, p. 8.

Paul, J.P., "The effect of walking speed on the force actions transmitted at the hip and knee joints", Proc. Royal Soc. Med., Vol. 63, 1970, p. 200.

Paul, J.P., "Comparison of EMG signals from leg muscles with the corresponding force actions calculated from walkpath measurements", Conf. Human Locomotor Engng., Inst. Mech. Engrs., Univ. of Sussex, 1971.

Paul, J.P. and Poulson, J., "The analysis of forces transmitted by joints in the human body", Proc. 5th Intern. Conf. Exptl. Stress Analysis, CISM, UDINE, ITALY, 1974, Section 3, p. 34.

Przemieniecki, J.S., "Theory of matrix structural Analysis", McGraw-Hill Inc., USA, 1968.

Rydell, N., "Forces in the hip joint II, Intravital Studies" in 'Biomechanics and related bio-engineering topics' (ed. Kenedi, R.M.), Pergamon Press, London, 1965.

Rydell, N., "Forces acting on the femoral head prosthesis", Thesis, 1966, Trycheri A.B., Litotyp Goteburg, Sweden.

Ryker, N.J. and Bartholomew, N.J., "Determination of acceleration by use of accelerometers", Prosth. Dev. Res. Proj., University of California, Berkeley, 1951.

Seireg, A. and Arvikar, R.J., "A mathematical model for evaluation of forces in lower extremities of the musculo-skeletal system", J. Biomechanics, Vol. 6, 1973, p. 313.

Seireg, A. and Arvikar, R.J., "The prediction of muscular load sharing and joint forces in the lower extremities during walking", J. Biomechanics, Vol. 8, 1975, p. 89.

Selby, S.M. (Editor), "C.R.C. Standard Mathematical Tables", The Chemical Rubber Co., Cleveland, 1969, p. 371.

Spolek, G.A., Day, E.E., Lippert, F.G. and Kirkpatrick, G.S. "Ambulatory-force measurement using an instrumented-shoe system", Exptl. Mechanics, Vol. 15(7), 1975, p. 271.

Townsend, M.A. and Seireg, A., "The synthesis of biped locomotion", J. Biomechanics, Vol. 5, 1972a, p. 71.

Townsend, M.A. and Seireg, A., "Optimal trajectories and controls for systems of coupled rigid bodies", J. Engng. Industry, Vol. 94 (B-2), 1972b, p. 472.

Townsend, M.A. and Seireg, A., "Effect of model complexity and gait criterion on the synthesis of bipedal locomotion", IEEE Trans. Bio-med. Engng., Vol. 20 (6), 1973, p. 433.

University of California, Berkeley, "Fundamental studies of human locomotion and other information relating to artificial limbs", Report to National Research Council, Advisory Committee on Artificial Limbs, Vol. 1 and 2, June 1947.

University of California, Berkeley, "The pattern of muscular activity in the lower extremity during walking", Prosth. Devices Res. Rep., Ser. 2, Iss. 25, 1953.

Weber, W. and Weber, E., "Mechanics of human locomotion", Gottingen, Germany, 1836.

Williams, R. and Seireg, A., "Interactive computer modeling of the musculo-skeletal system", IEEE Trans. Biomed. Engng., Vol. 24 (3), 1977, p. 213.

Winter, D.A., Hobson, D.A. and Greenlaw, R.K., "A micro-switch shoe for use in locomotion studies", J. Biomechanics, Vol. 5, 1972, p. 553.

Winter, D.A., Quanbury, A.O., Hobson, D.A., Sidwall, H.G., Reimer, G., Trenholm, B.G., Steinke, T. and Shlosser, H., "Kinematics of normal locomotion - a statistical study based on T.V. data", J. Biomechanics, Vol. 7, 1974, p. 479.

Zienkiewicz, O.C., "The Finite Element Method in Engineering Science", McGraw-Hill Pub. Co. Ltd., England, 1971.

APPENDIX - A

OBSERVATIONS AND RESULTS FOR CALIBRATION OF THE DYNAMOMETER, AND CALIBRATED VALUES OF FOOT-TO-GROUND FORCE COMPONENTS FOR ALL THE TEST RUNS

Table A-(i) Calibration of Dynamometer for Horizontal Load along Negative X Direction

Load step: 5 kg Maximum load: 25 kg

S. No.	Galvanometer deflection of channel, Division			
	Loading		Unloading	
	F_X	F_Z	F_X	F_Z
1	2.125	0.5	2.125	0.4
2	2.375	0.4	2.4	0.4
3	2.5	0.4	2.6	0.4
4	2.4	0.4	2.6	0.4
5	2.4	0.4	2.6	0.4
1	2.2	0.4	2.0	0.4
2	2.5	0.5	2.25	0.4
3	2.5	0.5	2.6	0.5
4	2.5	0.4	2.75	0.5
5	2.3	0.3	2.6	0.5
1	2.0	0.3	2.3	0.25
2	2.4	0.4	2.4	0.25
3	2.25	0.4	2.4	0.4
4	2.4	0.3	2.5	0.4

Force component	Mean value (Division)	Standard deviation (Division)
F_X	2.39	0.1873
F_Z	0.40	0.071

Table A-(ii) Calibration of Dynamometer for Horizontal Load along Negative Y Direction

Load step: 2 kg Maximum load: 12 kg

S. No.	Galvanometer deflection of F_Y channel, Division	
	Loading	Unloading
1	1.8	2.25
2	1.6	2.25
3	1.8	2.25
4	2.1	2.0
5	2.1	1.5
6	1.85	1.25
1	2.2	2.15
2	2.1	2.3
3	2.2	2.1
4	2.0	1.9
5	1.5	1.5
6	1.7	1.6
1	2.0	2.25
2	1.9	2.35
3	2.1	2.0
4	1.9	1.7
5	1.75	1.4

Mean value: 1.92 division

Standard deviation: 0.29 division

Table A-(iii) Calibration of the Dynamometer for Vertical Load along Negative Z Direction

Load step: 10 kg Maximum load: 80 kg

S. No.	Galvanometer deflection of F_Z channel, Division	
	Loading	Unloading
1	2.6	2.75
2	2.6	2.6
3	2.75	2.5
4	2.6	2.6
5	2.7	2.6
6	2.5	2.6
7	2.5	2.5
8	2.5	2.65
1	2.6	2.6
2	2.6	2.6
3	2.6	2.6
4	2.75	2.6
5	2.5	2.6
6	2.6	2.2
7	2.4	2.6
8	2.4	2.4
1	2.6	2.75
2	2.6	2.75
3	2.75	2.75
4	2.7	2.75
5	2.6	2.6
6	2.4	2.75
7	2.4	2.5
8	2.4	2.75

Mean value: 2.6 division

Standard deviation: 0.11 division

Table A-(iv)a Calibration of the Dynamometer for Moment About the X-axis (Positive)

Moment step: 80 kg-cm Maximum moment: 480 kg-cm

S. No.	Galvanometer deflection of channel, Division					
	Loading			Unloading		
	M_X	F_X	M_Z	M_X	F_X	M_Z
1	2.875	1.2	1.25	2.5	0.9	1.0
2	3.2	1.1	1.25	3.2	0.75	1.0
3	3.25	0.75	1.0	2.8	0.5	1.0
4	3.25	0.5	1.0	2.9	0.3	0.8
5	3.3	0.62	1.0	2.9	0.4	1.0
6	3.6	0.62	1.0	3.2	0.4	1.0
1	2.75	0.9	1.1	2.95	0.8	1.0
2	3.3	0.7	1.1	2.5	0.5	0.95
3	3.0	0.6	1.1	3.0	0.5	1.0
4	3.0	0.3	1.1	2.8	0.5	0.75
5	3.1	0.7	1.0	3.0	0.35	1.0
6	3.0	0.5	-	2.0	0.4	-
1	2.85	0.9	1.2	2.75	0.75	1.2
2	3.0	0.7	1.2	2.4	0.6	1.2
3	3.25	0.6	1.2	3.25	0.4	1.2
4	3.2	0.6	1.2	2.8	0.4	0.75
5	3.0	0.4	0.9	3.0	0.35	0.9
6	3.0	-	0.55	2.0	-	0.5

Force component	Mean value (Division)	Standard deviation (Division)
$M_X(+)$	3.03	0.1742
$F_X(+)$	0.57	0.181
$M_Z(+)$	1.04 .	0.1404

Table A-(iv)b Calibration of Dynamometer for Moment about X-axis (Negative)

Moment step: 80 kg-cm Maximum moment: 480 kg-cm

S.No.	Galvanometer deflection of channel, Division									
	Loading					Unloading				
	M_X	F_X	F_Z	M_Y	M_Z	M_X	F_X	F_Z	M_Y	M_Z
1	2.4	-	0.4	0.7	1.2	2.0	0.5	0.5	0.75	1.4
2	2.3	0.25	0.35	1.0	1.15	2.2	0.3	0.35	0.8	1.0
3	2.4	0.25	0.3	1.2	1.0	2.4	0.6	0.55	0.8	1.0
4	2.2	0.6	0.3	0.7	1.0	2.0	0.7	0.3	0.3	0.8
5	2.0	1.0	0.5	0.35	1.0	2.35	1.0	0.9	0.25	1.0
6	2.35	0.6	0.35	0.2	1.0	1.9	0.5	0.3	-	0.8
1	2.5	-	0.3	1.0	1.2	2.9	0.5	0.25	0.6	1.6
2	2.2	0.25	0.5	1.1	0.8	2.3	0.6	0.35	0.95	1.0
3	2.4	0.25	0.5	1.1	1.0	2.4	0.4	0.6	1.0	1.0
4	2.3	0.6	0.6	0.4	1.2	1.7	0.8	0.45	-	0.8
5	2.2	0.7	0.6	0.65	1.0	2.4	0.8	0.4	-	1.0
6	2.3	0.7	0.5	0.45	1.0	1.6	0.55	0.15	-	0.75
1	2.4	-	0.25	1.0	1.0	2.9	0.6	0.625	0.65	1.3
2	2.5	0.4	0.4	0.8	1.4	2.4	0.6	0.65	0.8	1.2
3	2.4	0.4	0.7	1.0	1.0	2.4	0.9	1.0	0.375	1.2
4	2.2	0.8	0.65	0.3	1.2	1.65	0.5	0.4	0.4	0.5
5	2.0	0.8	0.6	-	1.0	2.0	0.7	0.625	0.3	1.0
6	2.4	-	0.5	0.75	1.0	2.4	0.75	-	0.5	1.0

Force component	Mean value (Division)	Standard deviation (Division)
M_X (-)	2.28	0.1682
F_X (-)	0.61	0.1499
F_Z (+)	0.46	0.1343
M_Y (+)	0.70	0.2838
M_Z (-)	1.04	0.1593

Table A-(v)a Calibration of Dynamometer for Moment about Y-axis (Positive)

Moment step: 160 kg-cm Maximum moment: 960 kg-cm

S.No.	Galvanometer deflection of channel, Division					
	Loading			Unloading		
	F_Y	M_Y	M_Z	F_Y	M_Y	M_Z
1	1.0	2.0	0.6	0.75	1.8	0.6
2	1.0	2.1	0.65	1.0	1.625	-
3	1.25	1.5	0.5	0.75	1.625	0.5
4	1.75	1.25	0.3	1.5	1.3	0.5
5	1.75	1.0	-	1.625	1.1	0.625
6	1.7	1.8	0.75	1.25	1.1	0.25
1	1.35	2.2	0.4	1.25	1.75	0.25
2	1.3	1.875	0.4	1.2	1.625	-
3	1.5	2.1	0.7	1.1	1.5	0.3
4	0.9	1.6	0.4	1.2	1.4	-
5	1.25	1.25	0.3	1.375	1.2	0.9
6	1.6	1.3	1.0	1.1	0.875	0.6
1	1.7	1.75	0.375	1.4	1.75	0.25
2	1.5	1.4	0.4	1.1	1.75	-
3	1.25	1.5	0.5	1.1	1.3	-
4	1.2	1.5	-	1.2	1.4	0.25
5	1.4	1.25	-	1.625	1.0	1.0
6	1.625	1.3	1.1	1.1	1.0	0.7

Force component	Mean value (Division)	Standard deviation (Division)
F_Y (+)	1.30	0.2708
M_Y (+)	1.49	0.3387
M_Z (+)	0.54	0.2444

Table A-(v)b Calibration of Dynamometer for Moment about Y-axis (Negative)

Moment step: 160 kg-cm Maximum moment: 800 kg-cm

S.No.	Galvanometer deflection of channel, Division					
	Loading			Unloading		
	F_Y	M_Y	M_Z	F_Y	M_Y	M_Z
1	0.6	2.25	1.5	0.75	1.6	1.75
2	0.5	1.75	2.0	0.6	1.85	1.0
3	0.5	1.65	1.5	0.75	1.85	1.5
4	0.4	1.75	1.5	0.6	1.8	1.5
5	0.5	1.75	1.8	0.6	1.5	0.7
1	0.5	1.3	1.5	-	1.5	2.0
2	0.6	1.1	1.5	0.6	1.0	1.5
3	0.4	1.05	1.35	0.7	1.2	1.5
4	0.5	1.15	1.5	0.75	1.1	1.5
5	0.7	1.2	1.7	0.4	0.9	0.8
1	0.5	1.15	1.45	0.62	0.65	1.2
2	0.6	1.2	1.5	0.6	0.55	1.0
3	0.62	1.2	1.5	0.7	1.0	1.25
4	0.62	1.1	1.45	0.6	1.0	1.25
5	0.6	1.05	1.30	0.6	0.8	0.75

Force component	Mean value (Division)	Standard deviation (Division)
F_Y (-)	0.61	0.0792
M_Y (-)	1.35	0.3087
M_Z (-)	1.49	0.2344

Table A-(vi) Calibration of Dynamometer for Moment about Z-axis (Negative)

Moment step: 55 kg-cm Maximum moment: 275 kg-cm

S. No.	Galvanometer deflection of M_Z channel Division	
	Loading	Unloading
1	2.5	2.6
2	2.75	3.0
3	2.75	2.75
4	2.75	2.7
5	2.5	2.2
1	2.4	2.75
2	2.5	2.5
3	2.6	2.7
4	2.5	2.5
5	2.5	1.75
1	2.5	2.75
2	2.75	2.7
3	2.6	3.0
4	2.75	2.75
5	2.5	2.5

Mean value: 2.64 division

Standard deviation: 0.1536 division

Table A-1 Calibrated Values of Foot-to-Ground Force Componen

Subject B, Test Run 1

Stance Phase Time - 0.815 second

S.No.	Time after heel strike second	Forces kg			Moments kg-cm		
		F_X	F_Y	F_Z	M_X	M_Y	M_Z
1	0.19	-4.448	-8.352	-75.423	-334.306	835.772	99.26
2	0.21	-3.738	-8.630	-76.787	-344.630	846.007	102.38
3	0.23	-2.856	-8.606	-77.342	-350.355	828.056	99.62
4	0.25	-2.044	-8.361	-76.354	-347.257	819.250	96.39
5	0.27	-1.671	-8.164	-74.787	-341.568	791.233	88.27
6	0.31	-0.989	-7.191	-70.321	-322.064	715.177	74.75
7	0.35	-0.301	-6.986	-69.822	-329.628	570.000	68.28
8	0.39	0.705	-3.393	-74.248	-350.960	290.000	131.41
9	0.43	2.443	-3.873	-77.692	-372.074	-180.000	126.39
10	0.47	3.996	-4.038	-81.114	-396.318	-388.000	126.13
11	0.51	6.464	-4.139	-83.576	-417.214	-539.053	124.40
12	0.53	8.105	-4.495	-85.026	-426.359	-556.398	124.19
13	0.55	9.049	-4.726	-84.931	-426.675	-557.981	129.60
14	0.57	10.212	-4.999	-84.514	-428.172	-551.931	132.34

Table A-2 Calibrated Values of Foot-to-Ground Force Component

Subject B, Test Run 2

Stance Phase Time - 0.79 second

S.No.	Time after heel strike second	Forces kg			Moments kg-cm		
		F_X	F_Y	F_Z	M_X	M_Y	M_Z
1	0.16	-4.962	-6.119	-75.346	-342.033	831.176	75.473
2	0.18	-3.041	-6.916	-76.913	-353.407	847.095	80.621
3	0.20	-1.868	-7.151	-76.515	-356.219	828.923	85.806
4	0.24	-1.126	-7.064	-75.959	-357.395	808.203	74.193
5	0.28	-1.236	-6.665	-72.519	-343.620	744.767	64.658
6	0.32	-0.698	-6.375	-70.028	-332.325	676.013	59.813
7	0.36	-0.062	-6.747	-70.248	-333.465	460.000	51.609
8	0.40	1.250	-3.668	-74.456	-353.664	0.000	119.699
9	0.44	2.962	-4.176	-77.450	-371.631	-300.000	118.586
10	0.48	4.839	-4.698	-79.824	-383.941	-466.997	120.198
11	0.50	6.017	-4.892	-80.652	-387.424	-474.390	121.386
12	0.52	7.308	-4.943	-81.529	-391.974	-488.106	123.333
13	0.54	8.143	-5.144	-81.797	-391.739	-491.812	124.181
14	0.56	9.390	-5.175	-81.580	-390.614	-489.153	125.333

Table A-3 Calibrated Values of Foot-to-Ground Force Component

Subject B, Test Run 3

Stance Phase Time - 0.84 second

S.No.	Time after heel strike second	Forces kg			Moments kg-cm		
		F_X	F_Y	F_Z	M_X	M_Y	M_Z
1	0.00	0.000	0.000	0.000	0.000	0.000	0.000
2	0.02	-0.973	1.833	-41.228	-173.206	477.876	-41.237
3	0.04	-8.096	0.272	-55.200	-231.045	643.884	-27.774
4	0.08	-8.831	-4.113	-65.934	-302.968	726.217	51.992
5	0.12	-7.373	-4.638	-69.462	-321.672	751.741	79.670
6	0.16	-6.513	-4.807	-73.577	-337.731	798.047	71.886
7	0.20	-5.489	-5.388	-79.048	-361.230	843.060	71.405
8	0.24	-3.839	-5.834	-76.913	-358.285	794.546	60.209
9	0.28	-2.455	-5.622	-73.393	-348.150	744.286	54.351
10	0.32	-1.132	-5.253	-69.360	-330.482	687.968	45.602
11	0.36	-0.602	-5.191	-71.416	-344.399	550.000	54.413
12	0.40	0.357	-5.025	-74.845	-359.746	400.000	63.84
13	0.44	1.675	-4.615	-77.468	-374.158	180.000	71.432
14	0.48	3.065	-3.671	-78.851	-384.582	-250.000	104.969
15	0.52	5.598	-3.673	-79.705	-387.387	-380.000	122.64
16	0.56	7.856	-4.026	-82.300	-408.162	-464.743	137.842
17	0.60	10.432	-4.365	-84.043	-416.384	-477.404	144.350
18	0.64	12.442	-4.526	-81.737	-406.047	-448.719	144.335
19	0.68	14.275	-3.733	-74.859	-373.627	-402.151	133.867
20	0.72	12.927	-2.112	-56.949	-283.178	-300.675	106.56
21	0.76	7.954	-0.468	-29.200	-144.945	-157.850	59.930
22	0.80	-0.683	0.158	-2.461	-12.764	36.468	5.65
23	0.84	0.000	0.000	0.000	0.000	0.000	0.00

Table A-4 Calibrated Values of Foot-to-Ground Force Component

Subject B, Test Run 4

Stance Phase Time - 0.83 second

S.No.	Time after heel strike second	Forces kg			Moments kg-cm		
		F_X	F_Y	F_Z	M_X	M_Y	M_Z
1	0.12	-6.628	-1.919	-70.840	-349.531	798.498	67.218
2	0.14	-6.021	-1.507	-73.186	-360.077	818.122	82.541
3	0.16	-5.515	-1.745	-73.326	-357.956	812.807	88.690
4	0.18	-4.039	-2.212	-74.633	-359.455	830.934	100.757
5	0.20	-2.614	-2.682	-74.226	-354.504	818.874	106.760
6	0.22	-1.160	-2.528	-74.683	-353.216	754.000	105.004
7	0.26	0.429	-1.776	-74.669	-342.582	666.000	99.065
8	0.30	1.131	-2.083	-72.570	-325.604	490.000	104.540
9	0.46	7.603	-0.483	-83.570	-350.156	-496.000	157.132
10	0.50	9.534	-1.282	-86.699	-356.231	-640.000	153.378
11	0.54	11.440	-1.934	-88.972	-359.082	-731.312	148.714
12	0.56	12.781	-2.173	-91.053	-369.875	-741.984	151.211
13	0.58	14.293	-2.273	-92.526	-375.888	-757.486	153.008
14	0.60	15.330	-2.291	-91.835	-374.744	-748.392	151.971
15	0.62	16.304	-2.424	-89.612	-365.654	-720.525	148.037
16	0.66	17.424	-2.528	-83.699	-348.794	-668.197	139.117

Table A-5 Calibrated Values of Foot-to-Ground Force Components

Subject C, Test Run 1

Stance Phase Time - 0.70 second

S.No.	Time after heel strike second	Forces kg			Moments kg-cm		
		F_X	F_Y	F_Z	M_X	M_Y	M_Z
1	0.13	-2.653	-5.547	-57.502	-257.743	541.834	-62.243
2	0.15	-1.440	-6.207	-58.310	-265.560	543.913	-61.257
3	0.17	-0.790	-6.156	-56.875	-268.375	519.695	-65.234
4	0.19	-0.810	-6.266	-54.818	-265.815	475.000	-64.767
5	0.21	-0.745	-5.792	-55.292	-274.016	415.000	-57.794
6	0.23	-0.458	-5.668	-56.215	-283.744	345.000	-52.360
7	0.25	0.085	-5.864	-57.645	-299.387	255.000	-44.713
8	0.35	-0.615	-5.043	-63.286	335.412	-325.000	-32.859
9	0.37	0.918	-5.245	-63.737	334.628	-380.000	-25.154
10	0.39	2.199	-5.426	-64.114	336.766	-415.248	-15.750
11	0.41	3.215	-5.517	-64.597	340.841	-421.815	-9.415
12	0.43	4.119	-5.668	-65.231	345.773	-424.509	-5.655
13	0.45	5.148	-5.770	-65.534	348.158	-425.660	1.946
14	0.47	6.310	-5.987	-65.140	346.594	-420.305	6.326

Table A-6 Calibrated Values of Foot-to-Ground Force Component

Subject C, Test Run 2

Stance Phase Time - 0.71 second

S.No.	Time after heel strike second	Forces kg			Moments kg-cm		
		F_X	F_Y	F_Z	M_X	M_Y	M_Z
1	0.17	-2.169	-9.194	-56.531	-187.231	474.463	-199.635
2	0.19	-1.079	-9.802	-58.519	-205.796	495.130	-218.680
3	0.21	-0.208	-10.123	-58.085	-210.073	484.858	-215.657
4	0.23	0.711	-9.769	-58.649	-220.377	462.719	-198.901
5	0.25	1.121	-9.274	-59.081	-232.451	420.000	-179.769
6	0.27	1.696	-8.719	-58.767	-238.994	350.000	-158.807
7	0.29	1.732	-8.506	-57.906	-243.492	280.000	-136.896
8	0.42	4.873	-6.827	-65.555	-322.701	-285.000	60.974
9	0.44	6.446	-7.300	-68.002	-336.294	-348.000	78.666
10	0.46	7.985	-7.553	-69.952	-345.660	-393.083	87.012
11	0.48	9.620	-7.771	-71.698	-353.963	-414.681	96.481
12	0.50	10.706	-8.004	-72.806	-358.930	-428.460	104.740
13	0.52	12.289	-8.182	-73.290	-360.639	-443.495	110.596
14	0.54	13.325	-8.062	-73.214	-359.426	-451.677	110.184

Table A-7 Calibrated Values of Foot-to-Ground Force Components

Subject C, Test Run 3

Stance Phase Time - 0.68 second

S.No.	Time after heel strike second	Forces kg			Moments kg-cm		
		F_X	F_Y	F_Z	M_X	M_Y	M_Z
1	0.0	0.000	0.000	0.000	0.000	0.000	0.000
2	0.02	-0.218	-1.752	-28.650	-71.084	352.635	-27.753
3	0.04	-5.619	-3.535	-32.699	-82.412	343.229	-38.389
4	0.08	-5.661	-7.085	-40.177	-129.641	351.298	-57.276
5	0.12	-2.954	-7.794	-44.914	-154.383	365.156	-68.996
6	0.16	-0.111	-8.853	-54.471	-196.107	443.165	-78.584
7	0.18	0.138	-8.975	-55.655	-214.150	447.392	-74.206
8	0.20	0.068	-8.568	-55.312	-218.496	425.000	-60.331
9	0.24	0.093	-7.262	-58.758	-247.945	190.000	-21.011
10	0.28	0.836	-6.012	-62.167	-288.649	-435.000	62.524
11	0.32	1.732	-6.384	-65.477	-315.749	-510.000	120.863
12	0.36	4.765	-6.812	-68.600	-335.331	-608.700	150.274
13	0.38	5.267	-6.978	-68.720	-332.684	-630.292	155.655
14	0.40	6.327	-7.167	-69.050	-334.408	-653.611	162.838
15	0.44	8.523	-7.515	-69.512	-334.367	-674.734	171.131
16	0.48	11.300	-7.622	-69.784	-334.968	-725.724	180.324
17	0.52	13.680	-7.523	-68.542	-325.210	-723.224	168.343
18	0.56	15.270	-6.860	-61.814	-288.442	-676.858	138.034
19	0.60	11.887	-3.079	-39.609	-179.031	-547.920	72.172
20	0.64	3.505	0.071	-11.637	-46.043	-403.320	37.536
21	0.68	0.000	0.000	0.000	0.000	0.000	0.000

Table A-8 Calibrated Values of Foot-to-Ground Force Components

Subject C, Test Run 4

Stance Phase Time - 0.675 second

S.No.	Time after heel strike second	Forces kg			Moments kg-cm		
		F_X	F_Y	F_Z	M_X	M_Y	M_Z
1	0.19	1.844	-8.887	-59.650	-231.332	500.394	-113.323
2	0.21	3.174	-9.220	-60.509	-240.724	492.798	-112.826
3	0.23	3.513	-9.077	-62.069	-257.053	508.456	-97.623
4	0.25	3.449	-8.644	-62.104	-262.143	516.841	-84.728
5	0.27	3.137	-8.283	-60.267	-262.366	505.335	-70.752
6	0.29	2.916	-8.431	-59.681	-274.032	375.000	-49.570
7	0.31	2.817	-8.684	-60.442	-287.819	0.000	-22.892
8	0.35	3.925	-6.085	-66.325	-334.900	-440.000	106.197
9	0.37	6.195	-6.889	-69.990	-357.310	-518.096	127.797
10	0.39	8.008	-7.511	-72.547	-374.756	-545.388	145.306
11	0.41	9.526	-7.962	-73.985	-381.444	-580.994	154.873
12	0.43	10.052	-8.064	-74.696	-381.888	-608.349	165.920
13	0.45	11.658	-8.099	-75.586	-386.534	-642.970	174.073
14	0.47	12.983	-8.351	-75.378	-382.177	-647.203	177.018

Table A-9 Calibrated Values of Foot-to-Ground Force Components

Subject D, Test Run 1

Stance Phase Time - 0.60 second

S.No.	Time after heel strike second	Forces kg			Moments kg-cm		
		F_X	F_Y	F_Z	M_X	M_Y	M_Z
1	0.10	-5.215	-4.834	-54.503	-264.402	650.308	61.934
2	0.12	-4.812	-5.687	-59.642	-288.727	704.422	64.370
3	0.14	-3.568	-5.294	-62.048	-300.448	734.531	61.776
4	0.16	-1.591	-4.564	-59.260	-285.922	685.146	56.334
5	0.18	-0.235	-4.109	-54.440	-259.175	606.000	49.554
6	-39	3.493	-2.359	-55.286	-267.665	-290.000	112.210
7	0.41	4.669	-2.592	-60.145	-297.062	-376.000	125.878
8	0.43	6.498	-2.774	-65.617	-329.655	-439.113	136.809
9	0.45	8.672	-2.936	-69.954	-353.068	-489.051	143.156
10	0.47	10.248	-3.656	-72.486	-367.078	-519.853	145.957
11	0.49	12.048	-4.452	-70.639	-356.638	-512.271	139.641
12	0.51	13.592	-4.113	-65.467	-327.242	-473.288	126.671

Table A-10 Calibrated Values of Foot-to-Ground Force Components

Subject D, Test Run 2

Stance Phase Time - 0.59 second

S.No.	Time after heel strike second	Forces kg			Moments kg-cm		
		F_X	F_Y	F_Z	M_X	M_Y	M_Z
1	0.06	-10.813	-2.544	-55.721	-270.746	724.748	57.055
2	0.08	-8.044	-4.933	-60.526	-303.131	760.118	81.032
3	0.10	-6.846	-6.411	-62.619	-322.195	776.943	101.773
4	0.12	-4.778	-5.926	-61.885	-319.186	760.880	97.763
5	0.14	-2.741	-5.499	-60.719	-312.294	746.089	84.849
6	0.38	-0.283	-2.392	-57.864	318.839	-579.360	46.343
7	0.40	0.955	-3.168	-61.470	335.281	-634.335	41.115
8	0.42	2.119	-3.873	-64.104	347.546	-673.120	31.757
9	0.44	3.168	-4.577	-66.513	361.209	-711.812	20.117
10	0.46	4.069	-4.784	-66.977	366.516	-738.884	15.774
11	0.48	5.098	-4.594	-66.910	368.809	-755.764	10.850
12	0.50	6.546	-4.055	-64.120	356.997	-738.581	12.867

Table A-11 Calibrated Values of Foot-to-Ground Force Components

Subject D, Test Run 3

Stance Phase Time - 0.62 second

S.No.	Time after heel strike second	Forces kg			Moments kg-cm		
		F_X	F_Y	F_Z	M_X	M_Y	M_Z
1	0.10	-8.920	-3.183	-51.628	284.807	567.880	-6.419
2	0.12	-8.230	-3.959	-55.448	304.467	603.718	-10.340
3	0.14	-7.273	-3.619	-57.449	316.484	609.447	-20.501
4	0.16	-6.171	-3.008	-55.884	308.945	588.163	-23.942
5	0.18	-5.052	-2.811	-51.664	285.012	541.518	-15.938
6	0.39	2.528	0.257	-57.009	292.590	-523.240	101.747
7	0.41	3.440	-0.056	-60.896	310.626	-549.415	102.884
8	0.43	4.890	-0.431	-64.186	326.617	-570.445	94.425
9	0.45	6.305	-1.172	-66.517	333.148	-590.276	90.256
10	0.47	7.775	-1.839	-67.344	332.488	-595.587	87.735
11	0.49	8.611	-2.274	-66.648	332.554	-586.125	74.309
12	0.51	9.682	-2.235	-64.883	329.232	-579.922	68.949

Table A-12 Calibrated Values of Foot-to-Ground Force Component

Subject D, Test Run 4

Stance Phase Time - 0.61 second

S.No.	Time after heel strike second	Forces kg			Moments kg-cm		
		F_X	F_Y	F_Z	M_X	M_Y	M_Z
1	0.06	-6.189	-0.307	-47.749	-247.164	565.138	13.631
2	0.08	-13.370	-0.798	-54.265	306.452	558.096	-34.007
3	0.10	-12.377	-2.513	-59.887	327.640	594.274	-10.021
4	0.12	-11.350	-3.197	-60.200	330.081	595.838	-1.032
5	0.14	-9.496	-2.444	-58.293	319.936	577.966	-7.364
6	0.37	0.226	0.189	-52.319	278.694	-345.000	61.777
7	0.39	0.454	-0.388	-52.578	276.153	-425.000	69.180
8	0.41	1.060	-0.943	-53.902	278.984	-495.824	75.930
9	0.43	1.990	-1.121	-57.605	294.636	-537.282	80.957
10	0.45	3.621	-1.314	-61.901	314.322	-545.292	74.901
11	0.47	5.372	-1.463	-65.853	332.058	-575.318	71.244
12	0.49	7.126	-1.844	-67.146	335.381	-592.903	68.333

APPENDIX - B

REFERENCE COORDINATES FOR THE ANKLE AND KNEE JOINTS, DURING STANCE PHASE, FOR ALL THE TEST RUNS

Table B-1 Reference Coordinates for Subject B, Test Run 1

S.No.	Locomotion event during stance phase	X-coordinate, cm		Y-coordinate, cm		Z-coordinate, cm	
		Ankle XA	Knee XK	Ankle YA	Kneee YK	Ankle ZA	Knee ZK
1		13.54	28.33	1.38	2.54	10.98	49.87
2		12.38	26.21	1.52	2.46	9.96	49.73
3*	Heel strike	11.97	23.89	1.38	2.46	8.73	49.20
4		11.22	21.84	1.38	2.10	7.92	48.25
5		9.73	20.61	1.30	1.88	8.53	48.52
6		8.37	18.29	1.23	1.59	7.92	48.79
7		8.37	16.38	1.16	1.16	7.92	48.93
8		8.37	14.88	1.16	0.80	7.92	49.06
9		8.37	13.52	1.45	0.51	7.92	49.47
10		7.76	12.56	1.45	0.22	7.24	49.47
11*	Toe off other	7.76	11.40	1.45	0.00	7.24	49.47
12	foot	7.76	10.44	1.96	-0.29	7.24	49.47
13		7.76	9.56	2.10	-0.51	7.24	49.47
14		7.76	8.81	2.10	-0.65	7.24	49.47
15		7.76	8.05	2.10	-0.65	7.24	49.20
16		7.76	6.83	2.10	-0.87	7.24	49.20
17		7.76	5.87	2.10	-1.01	7.24	49.47
18		7.76	[illegible].64	2.10	-1.09	7.24	49.20
19		7.76	3.75	2.10	-1.23	7.24	49.06
20		7.76	3.07	2.10	-1.23	7.24	49.20
21		7.76	2.05	2.10	-1.23	7.24	48.93
22		7.76	1.02	2.10	-1.23	7.24	48.93
23		7.76	0.00	2.10	-1.23	7.24	48.79
24		7.76	-0.82	2.10	-1.23	7.24	48.59
25		7.55	-1.71	2.10	-1.23	7.92	48.66
26		7.55	-2.80	2.10	-1.23	7.92	48.59
27		7.55	-3.82	2.10	-1.23	7.92	48.59
28		7.48	-5.05	2.10	-1.23	8.19	48.39
29		7.41	-5.73	2.10	-1.23	8.46	48.39
30		7.41	-6.69	2.10	-1.23	8.60	48.39
31		7.21	-7.78	2.10	-1.23	8.73	47.98
32		7.01	-8.74	2.10	-1.23	9.01	48.12
33		6.67	-10.17	2.10	-1.23	9.41	48.12
34		6.53	-11.40	2.17	-1.23	9.69	48.12
35*	Heel strike	6.19	-12.83	2.10	-1.23	10.09	47.98
36	other foot	5.71	-14.54	2.03	-1.09	10.77	47.98
37		5.44	-16.25	1.96	-1.01	10.57	47.85
38		5.10	-18.57	1.96	-0.94	12.07	47.58
39		4.22	-21.16	1.88	-0.87	13.49	47.38
40		3.40	-24.03	1.52	-0.87	14.18	47.11
41		1.36	-27.78	1.16	-0.87	15.54	46.91
42		-1.09	-32.08	0.80	-0.80	17.51	46.50
43		-3.81	-36.25	0.58	-0.80	19.01	46.23
44*	Toe strike	-6.94	-40.34	0.43	-1.01	20.84	45.96
45		-10.48	-45.26	0.43	-1.52	22.07	46.10

Table B-2 Reference Coordinates for Subject B, Test Run 2

S.No.	Locomotion event during stance phase	X-coordinate, cm		Y-coordinate, cm		Z-coordinate, cm	
		Ankle XA	Knee XK	Ankle YA	Knee YK	Ankle ZA	Knee ZK
1		14.01	28.19	0.00	0.80	10.03	49.87
2		12.86	25.73	0.00	0.65	9.35	49.47
3*	Heel strike	12.24	23.34	0.29	0.72	8.73	48.79
4		10.54	21.71	0.87	0.80	8.19	48.39
5		9.80	19.86	1.01	0.80	8.32	48.79
6		9.52	17.75	1.16	0.80	8.12	48.93
7		9.12	16.11	0.87	0.14	7.92	49.06
8		8.98	14.47	1.16	-0.29	7.71	49.20
9		8.98	13.38	1.38	-0.58	7.51	49.47
10*	Toe off other	8.57	12.22	1.67	-0.58	7.51	49.47
11	foot	8.57	11.47	1.67	-0.80	7.51	49.47
12		8.57	10.58	1.67	-1.09	7.51	49.47
13		8.57	9.69	1.67	-1.45	7.51	49.53
14		8.57	8.74	1.96	-1.45	7.51	49.20
15		8.57	7.92	1.96	-1.30	7.51	49.47
16		8.57	6.35	2.10	-1.52	7.64	49.47
17		8.57	5.46	2.10	-1.38	7.64	49.20
18		8.16	4.23	2.10	-1.38	7.78	49.20
19		8.16	3.14	2.10	-1.23	7.78	49.20
20		8.16	2.05	2.25	-1.01	7.78	49.20
21		8.16	1.09	2.46	-1.01	7.78	49.20
22		8.16	0.27	2.46	-0.94	7.78	48.86
23		8.16	-0.55	2.46	-0.94	7.78	48.86
24		8.16	-1.50	2.46	-0.94	7.78	48.86
25		8.16	-2.39	2.46	-0.94	7.78	48.52
26		7.89	-3.14	2.46	-0.94	8.05	48.52
27		7.89	-4.37	2.46	-0.94	8.32	48.52
28		7.76	-5.39	2.46	-0.94	8.60	48.52
29		7.62	-6.69	2.46	-0.72	8.80	48.52
30		7.48	-7.71	2.46	-0.72	8.87	48.52
31		7.35	-9.01	2.46	-0.72	9.41	48.25
32		6.94	-10.51	2.46	-0.72	9.89	48.25
33		6.73	-11.95	2.46	-0.72	10.16	48.25
34		6.53	-13.52	2.17	-0.72	10.71	48.25
35		6.12	-15.22	2.17	-0.72	11.39	48.25
36*	Heel strike	5.85	-16.79	2.10	-0.43	12.00	47.85
37	other foot	5.65	-18.43	2.06	-0.29	12.95	47.98
38		4.63	-20.82	2.03	-0.14	13.77	47.92
39		3.54	-24.03	1.67	-0.14	14.86	47.71
40		1.97	-27.30	1.67	-0.14	16.28	47.45
41		-0.41	-31.40	1.30	0.07	17.78	47.11
42		-3.27	-35.49	1.30	0.07	19.35	46.64
43		-6.53	-40.27	0.94	0.07	21.11	46.57
44*	Toe strike	-10.88	-45.32	0.94	0.07	22.81	46.64
45		-14.42	-49.42	1.38	-0.07	23.90	46.91

Table B-3 Reference Coordinates for Subject B, Test Run 3

S.No.	Locomotion event during stance phase	X-coordinate, cm		Y-coordinate, cm		Z-coordinate, cm	
		Ankle XA	Knee XK	Ankle YA	Knee YK	Ankle ZA	Knee ZK
1		15.03	30.99	0.36	0.72	10.71	49.33
2		13.74	28.67	0.65	0.72	9.35	48.52
3*	Heel strike	13.06	26.48	0.51	0.72	8.32	48.05
4		12.38	24.44	0.94	0.58	7.92	47.65
5		10.88	22.39	1.16	0.72	8.19	48.12
6		10.34	20.20	1.01	0.58	7.78	48.52
7		10.00	18.16	1.01	-0.51	7.51	48.59
8		9.52	16.38	1.01	-0.65	7.17	48.79
9		9.52	15.29	1.01	-0.36	7.17	49.20
10*	Toe off other	9.52	14.13	1.01	-0.72	7.17	48.93
11	foot	9.52	12.90	1.96	-0.94	7.17	49.06
12		9.52	11.95	1.96	-0.94	7.17	49.06
13		9.52	10.99	1.96	-1.52	7.17	48.99
14		9.52	10.44	1.96	-1.52	7.17	49.33
15		9.52	9.62	1.96	-1.52	7.17	48.93
16		9.52	8.67	1.96	-1.52	7.17	49.13
17		9.52	7.85	1.96	-1.67	7.17	49.20
18		9.52	7.24	1.96	-1.67	7.17	48.66
19		9.52	6.48	1.96	-1.67	7.17	49.06
20		9.52	5.53	1.96	-1.67	7.17	49.06
21		9.52	4.57	1.96	-1.67	7.17	48.86
22		9.52	3.41	1.96	-1.88	7.17	48.86
23		9.52	2.39	1.96	-1.88	7.17	48.86
24		9.52	1.37	1.96	-1.88	7.17	48.66
25		9.52	0.41	1.96	-1.88	7.17	48.66
26		9.52	-0.14	1.96	-1.81	7.17	48.52
27		9.52	-1.23	1.96	-1.67	7.17	48.52
28		9.25	-1.91	1.96	-1.67	7.37	48.19
29		9.25	-3.00	1.96	-1.59	7.51	48.19
30		9.25	-3.89	1.96	-1.67	7.64	48.19
31		9.25	-5.12	1.96	-1.52	7.78	47.85
32		8.91	-6.42	1.96	-1.59	7.85	47.65
33		8.84	-7.58	1.96	-1.59	8.05	47.65
34		8.78	-8.60	1.96	-1.59	8.46	47.65
35		8.44	-9.90	1.96	-1.38	9.01	47.38
36*	Heel strike	8.10	-11.47	1.88	-1.30	10.09	47.38
37	other foot	7.76	-12.90	1.81	-1.23	10.37	47.38
38		7.69	-14.74	1.74	-1.09	11.05	47.31
39		7.07	-17.06	1.59	-1.09	12.07	47.18
40		5.92	-19.93	1.30	-1.09	13.36	47.18
41		4.90	-22.94	1.01	-1,09	14.79	47.11
42		2.38	-26.89	0.65	-1.01	16.35	46.64
43		0.14	-31.33	0.80	-1.01	17.98	46.37
44		-2.72	-35.49	1.16	-1.01	19.07	46.23
45*	Toe strike	-6.26	-39.80	1.23	-1.16	21.11	46.37

Table B-4 Reference Coordinates for Subject B, Test Run 4

S.No.	Locomotion event during stance phase	X-coordinate, cm		Y-coordinate, cm		Z-coordinate, cm	
		Ankle XA	Knee XK	Ankle YA	Knee YK	Ankle ZA	Knee ZK
1		19.73	30.51	-1.59	-1.74	9.96	50.54
2		17.48	28.67	-1.45	-1.81	10.09	50.27
3*	Heel strike	13.40	26.76	-1.52	-1.81	9.62	49.73
4		12.52	24.91	-1.38	-2.25	8.32	48.79
5		12.11	23.21	-1.52	-2.54	7.98	48.79
6		10.68	21.71	-1.45	-2.97	7.71	48.12
7		9.86	19.86	-1.38	-3.12	7.58	48.39
8		9.46	17.95	-1.30	-3.33	7.30	48.39
9		8.84	16.04	-1.30	-3.55	7.30	48.79
10*	Toe off other	8.50	14.33	-1.01	-3.84	7.30	48.79
11	foot	8.50	12.90	-1.01	-3.99	7.30	49.20
12		8.50	11.88	-1.01	-4.28	7.30	49.06
13		8.50	10.99	-1.01	-4.28	7.30	49.06
14		8.50	10.24	-1.01	-4.28	7.30	49.33
15		8.50	9.35	-1.01	-4.71	7.30	49.33
16		8.50	8.74	-1.01	-4.71	7.30	49.47
17		8.50	7.78	-1.01	-4.71	7.30	49.60
18		8.50	6.96	-1.01	-4.71	7.30	49.06
19		8.50	6.01	-1.01	-4.71	7.30	49.33
20		8.50	5.19	-1.01	-4.71	7.30	49.33
21		8.50	4.37	-1.01	-4.71	7.30	49.20
22		8.50	3.55	-1.01	-4.71	7.30	49.20
23		8.50	2.53	-1.01	-4.86	7.30	49.06
24		8.50	1.64	-1.01	-4.86	7.30	49.06
25		8.50	0.61	-1.01	-4.86	7.30	49.13
26		8.50	-0.20	-1.01	-4.86	7.30	48.79
27		8.50	-1.23	-1.01	-4.86	7.30	48.79
28		8.50	-2.05	-0.87	-4.64	7.30	48.52
29		8.50	-3.00	-0.87	-4.86	7.30	48.19
30		8.50	-4.37	-0.87	-4.86	7.30	48.19
31		7.96	-5.53	-0.87	-5.22	7.37	48.19
32		7.96	-6.62	-0.72	-5.07	7.37	47.71
33		7.82	-7.78	-0.72	-4.71	7.64	47.85
34		7.82	-9.08	-0.72	-4.78	7.64	47.45
35		7.41	-10.51	-0.94	-4.71	9.01	47.85
36*	Heel strike	7.01	-12.01	-0.94	-4.42	9.41	47.31
37	other foot	6.73	-13.65	-0.94	-4.13	9.69	47.31
38		6.67	-15.15	-0.94	-4.13	10.23	47.31
39		6.26	-17.34	-1.52	-3.62	11.05	47.18
40		5.78	-19.45	-1.81	-3.77	12.20	47.31
41		4.35	-22.32	-1.96	-3.77	13.36	46.91
42		2.99	-25.39	-1.96	-3.77	14.72	46.91
43		0.82	-29.49	-1.96	-3.77	16.15	46.44
44		-1.63	-33.72	-2.03	-3.99	17.78	46.10
45*	Toe strike	-4.76	-37.95	-2.25	-4.20	19.89	46.64

Table B-5 Reference Coordinates for Subject C, Test Run 1

S.No.	Locomotion event during stance phase	X-coordinate, cm		Y-coordinate, cm		Z-coordinate, cm	
		Ankle XA	Knee XK	Ankle YA	Knee YK	Ankle ZA	Knee ZK
1		17.63	27.21	2.17	1.88	8.75	43.94
2		13.29	25.51	2.17	1.88	8.55	43.27
3		10.17	23.06	2.17	1.96	8.07	42.87
4*	Heel strike	8.68	20.07	2.46	1.88	7.47	42.73
5		7.66	17.55	2.17	1.30	6.93	42.13
6		6.78	14.97	2.17	0.87	6.59	42.46
7		5.83	12.52	2.10	0.87	6.05	42.46
8		5.56	10.00	1.81	-0.00	6.39	42.87
9		5.56	8.64	2.03	-0.00	6.39	42.80
10		5.56	7.48	2.25	-0.29	6.39	42.87
11*	Toe off other	5.56	6.53	2.25	-0.51	6.39	42.87
12	foot	5.56	5.51	2.25	-0.51	6.39	42.87
13		5.63	4.90	2.25	-0.72	6.32	42.87
14		5.63	4.15	2.25	-0.80	6.32	42.87
15		5.63	3.47	2.25	-0.80	6.32	43.14
16		5.63	2.86	2.25	-0.80	6.32	43.00
17		5.42	2.18	2.25	-0.80	6.86	43.00
18		5.42	1.36	2.25	-0.80	6.86	43.00
19		5.42	0.34	2.25	-0.80	7.06	43.27
20		5.42	-0.41	2.25	-0.80	7.06	43.54
21		5.42	-1.09	2.25	-0.84	7.26	43.40
22		5.15	-1.97	2.25	-0.87	7.40	43.81
23		4.88	-3.13	2.25	-0.87	8.01	44.21
24		4.75	-4.08	2.25	-0.87	8.61	44.48
25		4.68	-5.31	2.25	-0.87	9.02	44.82
26		4.34	-6.33	1.81	-0.87	9.49	44.62
27		3.93	-7.96	1.81	-0.87	10.03	45.09
28		3.66	-9.32	1.96	-1.01	10.78	45.69
29		2.64	-11.09	1.81	-1.01	11.11	45.29
30		2.37	-13.06	1.23	-1.16	11.93	45.90
31		1.83	-14.97	1.01	-1.52	12.40	45.53
32*	Heel strike	0.61	-17.48	0.43	-1.81	13.21	45.76
33	other foot	-0.34	-20.27	0.14	-2.61	14.36	45.96
34		-2.24	-23.95	0.22	-3.91	14.97	45.69
35		-4.27	-27.62	0.07	-4.35	16.59	45.56
36		-6.85	-31.90	0.29	-4.64	18.21	44.95
37		-10.78	-37.07	0.36	-5.00	20.03	44.48
38*	Toe strike	-14.24	-42.24	0.51	-4.64	21.52	44.95
39		-18.78	-47.69	0.43	-4.35	23.41	44.89
40		-23.05	-52.52	0.36	-4.20	24.22	45.49

Table B-6 Reference Coordinates for Subject C, Test Run 2

S.No.	Locomotion event during stance phase	X-coordinate, cm		Y-coordinate, cm		Z-coordinate, cm	
		Ankle XA	Knee XK	Ankle YA	Knee YK	Ankle ZA	Knee ZK
1		11.05	25.03	4.13	5.65	8.95	42.87
2		9.22	22.93	4.13	5.58	8.61	42.66
3		8.14	20.41	4.06	5.51	7.60	42.26
4*	Heel strike	7.39	18.37	4.35	5.36	7.40	41.92
5		6.17	16.60	3.84	4.78	6.99	41.92
6		6.17	14.42	3.99	4.20	6.99	42.19
7		5.63	12.79	3.84	3.99	6.66	42.19
8		5.63	10.82	3.84	3.33	6.66	42.46
9		5.22	9.52	3.62	2.97	6.32	42.53
10		4.88	8.50	3.62	2.39	6.18	42.46
11		4.27	7.76	3.55	2.17	6.25	42.80
12*	Toe off other	4.27	7.28	3.48	2.03	6.25	42.66
13	foot	4.88	6.39	3.62	1.67	6.45	42.66
14		4.88	6.05	3.62	1.67	6.45	43.00
15		4.88	5.51	3.62	1.67	6.45	42.60
16		4.88	5.03	3.62	1.52	6.45	43.07
17		4.88	4.29	3.62	1.52	6.45	43.00
18		4.88	3.33	3.62	1.38	6.45	43.07
19		4.75	2.31	3.62	1.38	6.79	42.80
20		4.61	1.36	3.62	1.38	6.69	42.93
21		4.61	0.27	3.62	1.38	6.79	43.00
22		4.47	-0.48	3.62	1.38	6.79	43.00
23		4.47	-1.43	3.62	1.38	6.79	43.07
24		4.34	-1.90	3.62	1.38	6.79	42.80
25		4.34	-2.72	3.62	1.38	7.20	43.27
26		4.14	-3.81	3.62	1.38	7.60	43.34
27		3.86	-4.90	3.62	1.38	8.01	43.40
28		3.66	-6.19	3.62	1.38	8.48	43.81
29		3.25	-7.62	3.62	1.38	9.09	43.81
30		3.25	-9.18	3.62	1.38	9.09	44.08
31		2.64	-10.82	3.26	1.38	10.03	44.35
32		2.31	-12.79	3.26	0.43	10.64	44.08
33*	Heel strike	1.69	-15.31	3.26	-0.14	11.66	44.55
34	other foot	0.61	-17.89	2.97	-0.14	12.74	44.41
35		-0.47	-20.95	2.97	-0.72	13.89	44.75
36		-2.37	-24.35	2.97	-1.16	14.83	44.48
37		-4.81	-28.71	2.97	-1.16	16.66	44.21
38		-7.39	-33.54	2.83	-1.59	18.55	44.35
39		-11.32	-38.57	2.46	-1.96	20.37	44.08
40*	Toe strike	-15.39	-43.33	2.68	-2.46	21.86	44.08

Table B-7 Reference Coordinates for Subject C, Test Run 3

S.No.	Locomotion event during stance phase	X-coordinate, cm		Y-coordinate, cm		Z-coordinate, cm	
		Ankle XA	Knee XK	Ankle YA	Knee YK	Ankle ZA	Knee ZK
1.		11.59	22.93	3.48	3.55	8.75	43.94
2		9.22	21.22	3.55	3.77	8.82	43.67
3		7.12	18.78	3.55	3.99	8.34	43.14
4*	Heel strike	5.90	16.19	3.41	3.84	7.74	42.66
5		5.15	13.88	3.70	3.55	6.66	42.39
6		4.20	11.70	3.62	3.04	6.66	42.39
7		3.53	8.98	3.55	1.81	6.45	42.87
8		3.19	6.73	3.55	1.81	6.32	42.80
9		3.19	5.31	3.55	1.81	6.32	42.93
10		3.19	4.69	3.55	1.38	6.32	42.93
11		3.19	3.81	3.55	1.38	6.32	43.07
12*	Toe off other	3.19	3.40	3.62	1.16	6.32	42.80
13	foot	3.19	2.65	3.70	1.16	6.32	42.80
14		3.19	2.18	3.70	1.16	6.32	42.60
15		3.19	1.16	3.70	1.09	6.32	42.80
16		3.19	0.14	3.70	1.09	6.32	43.07
17		3.19	-0.34	3.70	1.30	6.32	42.87
18		2.71	-0.95	3.70	1.30	6.66	42.87
19		2.71	-1.84	3.70	1.30	6.66	43.00
20		2.71	-2.52	3.70	1.38	6.66	43.07
21		2.71	-3.20	3.70	1.45	6.66	43.07
22		2.71	-4.15	3.70	1.45	7.26	43.27
23		2.58	-5.03	3.70	1.45	7.60	43.47
24		2.31	-6.12	3.70	1.45	8.14	43.74
25		2.17	-7.07	3.70	1.45	8.55	43.81
26		1.90	-8.44	3.70	1.45	9.09	44.15
27		1.63	-9.66	3.70	1.45	9.56	44.01
28		1.22	-10.95	3.70	1.30	10.17	44.68
29		0.61	-12.65	3.26	1.30	10.71	44.75
30		0.27	-14.35	3.26	1.30	11.05	44.89
31*	Heel strike	-0.20	-15.99	3.26	0.87	11.79	45.16
32	other foot	-0.95	-18.23	3.41	0.58	12.60	45.22
33		-1.76	-20.34	3.12	0.58	13.28	44.89
34		-3.25	-23.40	3.12	0.51	14.43	45.36
35		-5.29	-27.14	3.04	0.51	15.37	45.02
36		-7.05	-30.88	3.04	0.51	16.39	44.48
37		-9.90	-35.31	2.97	0.29	18.21	44.08
38*	Toe strike	-12.88	-39.59	3.19	0.07	19.83	44.01
39		-16.81	-45.10	3.41	-0.07	21.66	45.09
40		-20.95	-49.46	3.41	-0.14	22.40	44.89

Table B-8 Reference Coordinates for Subject C, Test Run 4

S.No.	Locomotion event during stance phase	X-coordinate, cm		Y-coordinate, cm		Z-coordinate, cm	
		Ankle XA	Knee XK	Ankle YA	Knee YK	Ankle ZA	Knee ZK
1		12.88	23.13	2.97	2.75	9.22	44.48
2		9.56	21.02	2.90	3.04	8.95	43.94
3		7.59	19.86	2.90	3.19	8.75	43.47
4*	Heel strike	6.58	17.55	3.04	3.26	7.80	42.80
5		6.10	15.37	3.12	2.61	7.06	42.39
6		5.02	13.33	3.12	2.61	6.72	42.19
7		5.02	11.56	3.12	2.03	6.72	42.53
8		4.14	9.39	3.12	2.03	6.45	42.53
9		4.14	8.03	3.26	2.03	6.45	42.87
10		4.14	6.94	3.26	1.67	6.45	43.14
11		4.14	5.99	3.26	1.67	6.45	42.87
12		4.14	5.24	3.33	1.52	6.45	42.93
13*	Toe off other	4.14	4.69	3.41	1.52	6.45	43.00
14	foot	4.14	3.81	3.41	1.52	6.45	43.14
15		4.14	3.13	3.41	1.23	6.45	43.14
16		3.80	2.04	3.41	1.23	6.66	43.14
17		3.80	0.82	3.41	1.23	6.66	43.07
18		3.80	0.00	3.41	1.23	6.66	43.07
19		3.80	-1.09	3.41	1.23	6.66	43.07
20		3.80	-1.84	3.41	1.23	6.66	43.00
21		3.80	-2.99	3.41	1.23	6.66	42.93
22		3.80	-4.01	3.33	1.23	6.66	43.00
23		3.66	-4.97	3.19	1.16	7.13	43.14
24		3.12	-6.39	3.19	1.16	8.01	43.40
25		2.64	-7.55	3.19	1.16	8.61	43.54
26		2.37	-8.71	3.12	0.87	9.22	43.67
27		2.24	-10.27	3.12	0.87	9.63	44.01
28		1.90	-11.63	2.90	0.87	10.10	44.21
29		1.42	-13.40	2.54	0.22	10.71	44.41
30		0.68	-15.24	2.25	0.22	11.59	44.62
31		0.00	-17.62	2.17	-0.43	12.26	44.62
32*	Heel strike	-1.08	-20.00	2.17	-0.43	13.01	44.55
33	other foot	-2.31	-22.99	2.10	-1.45	13.95	44.55
34		-4.07	-25.99	2.10	-1.45	15.30	44.95
35		-6.44	-30.20	2.54	-2.46	16.39	44.21
36		-8.81	-34.56	2.32	-1.59	18.28	44.21
37		-11.93	-39.05	2.17	-1.45	19.90	43.94
38*	Toe strike	-15.93	-44.63	2.03	-1.30	21.52	43.81
39		-20.14	-48.71	1.88	-1.16	23.21	44.41
40		-24.47	-54.29	1.74	-1.01	23.95	44.01

Table B-9 Reference Coordinates for Subject D, Test Run 1

S.No.	Locomotion event during stance phase	X-coordinate, cm		Y-coordinate, cm		Z-coordinate, cm	
		Ankle XA	Knee XK	Ankle YA	Knee YK	Ankle ZA	Knee ZK
1		13.72	28.91	0.94	1.16	9.21	45.84
2		10.59	26.46	1.09	1.30	8.32	45.17
3*	Heel strike	9.37	23.06	1.30	1.45	6.96	45.03
4		8.76	19.59	1.45	1.45	6.28	44.76
5		7.20	17.14	1.45	1.38	6.28	44.63
6		7.20	14.15	1.52	1.38	6.35	45.03
7		5.91	11.02	1.52	1.38	6.35	45.78
8		5.91	9.66	1.67	1.30	6.35	45.37
9		5.91	8.23	1.67	1.30	6.35	45.51
10*	Toe off other	5.91	7.07	1.88	1.30	6.35	45.28
11	foot	5.84	5.71	2.17	1.16	6.35	45.51
12		5.84	4.76	2.25	0.87	6.35	45.26
13		5.84	4.22	2.03	0.65	6.35	45.17
14		5.84	3.61	1.88	0.43	6.35	45.10
15		5.84	2.79	1.67	0.43	6.35	45.37
16		5.84	1.63	1.67	0.36	6.35	45.24
17		5.84	1.02	1.67	0.29	6.35	45.17
18		5.70	0.14	1.67	0.29	6.35	44.83
19		5.70	-1.09	1.67	0.22	6.35	44.90
20		5.70	-2.31	1.67	0.29	6.35	44.76
21		5.70	-3.95	1.67	0.36	6.35	44.56
22		5.30	-5.58	1.67	0.36	6.76	44.22
23		5.30	-6.87	1.67	0.36	6.76	43.93
24		5.23	-8.16	1.67	0.36	6.90	43.55
25		5.23	-9.90	1.67	0.36	6.90	43.48
26		4.96	-11.70	1.67	0.36	7.44	43.14
27		4.75	-13.61	1.67	0.36	7.98	43.41
28*	Heel strike	4.21	-15.78	1.67	0.29	8.87	43.21
29	other foot	3.12	-18.44	1.52	0.14	10.30	43.14
30		2.72	-20.82	1.38	0.00	11.05	42.94
31		0.54	-25.03	1.38	-0.29	13.36	43.55
32		-2.11	-29.12	1.30	-0.72	15.26	43.28
33*	Toe strike	-5.57	-33.54	1.38	-1.09	17.24	43.61
34		-9.51	-37.21	0.94	-1.38	18.80	43.34
35		-13.99	-40.61	0.87	-1.45	19.55	42.33

Table B-10 Reference Coordinates for Subject D, Test Run 2

S.No.	Locomotion event during stance phase	X-coordinate, cm		Y-coordinate, cm		Z-coordinate, cm	
		Ankle XA	Knee XK	Ankle YA	Knee YK	Ankle ZA	Knee ZK
1		13.17	28.50	0.22	0.00	8.73	45.51
2		9.64	25.44	0.22	0.19	8.32	45.03
3*	Heel strike	8.08	22.31	0.29	0.36	7.98	44.49
4		6.93	18.84	0.29	0.22	6.96	44.44
5		5.16	16.12	0.36	0.14	6.90	44.22
6		4.21	13.33	0.51	0.00	5.67	44.76
7		3.67	10.14	0.51	-0.14	5.47	44.97
8		3.67	8.44	0.65	-0.22	5.47	45.24
9		3.67	6.53	0.72	-0.29	5.47	45.55
10*	Toe off other	3.67	5.24	0.80	-0.36	6.22	45.55
11	foot	3.67	4.54	0.80	-0.36	6.22	45.55
12		3.67	3.95	0.80	-0.36	6.28	45.68
13		3.67	2.93	0.80	-0.36	6.35	45.90
14		3.67	2.04	0.80	-0.36	6.35	45.90
15		3.67	1.02	0.80	-0.36	6.42	45.37
16		3.67	0.54	0.80	-0.36	6.42	45.64
17		3.67	0.00	0.80	-0.29	6.42	45.30
18		3.67	-1.50	0.80	-0.14	6.42	45.36
19		3.67	-2.72	0.80	-0.07	6.42	45.17
20		3.67	-4.35	0.80	-0.07	6.42	45.17
21		3.67	-5.71	0.72	0.00	6.69	44.76
22		3.67	-7.01	0.72	0.14	6.69	44.90
23		3.33	-8.44	0.72	0.14	6.76	44.43
24		3.33	-9.86	0.72	0.07	6.76	44.29
25		3.33	-11.16	0.72	0.00	6.90	44.36
26		2.85	-13.06	0.72	-0.14	7.44	44.02
27		2.65	-14.61	0.72	-0.22	7.92	44.16
28*	Heel strike	2.24	-16.46	0.72	-0.14	8.60	43.95
29	other foot	1.29	-18.44	0.72	-0.14	9.55	43.68
30		0.75	-21.22	0.51	-0.36	10.57	43.75
31		-0.34	-23.74	0.29	-0.43	12.07	43.41
32		-2.17	-27.01	0.00	-0.58	13.63	44.09
33*	Toe strike	-4.41	-31.50	0.22	-0.72	15.47	44.09
34		-7.88	-36.73	0.80	-1.01	17.44	43.75
35		-12.77	-41.70	0.87	-1.30	20.23	43.68

Table B-11 Reference Coordinates for Subject D, Test Run 3

S.No.	Locomotion event during stance phase	X-coordinate, cm		Y-coordinate, cm		Z-coordinate, cm	
		Ankle XA	Knee XK	Ankle YA	Knee YK	Ankle ZA	Knee ZK
1		13.31	28.84	-0.29	0.00	8.19	44.49
2		11.07	25.71	-0.43	0.14	7.30	44.29
3*	Heel strike	10.46	22.31	0.29	0.36	6.69	44.36
4		8.83	18.98	0.14	0.29	6.22	44.22
5		7.74	15.99	0.36	0.29	6.69	44.97
6		7.13	13.13	0.65	0.14	6.69	45.17
7		7.13	10.61	0.65	-0.14	6.49	45.37
8		6.99	9.39	0.65	-0.14	6.49	45.17
9		6.59	7.28	0.65	-0.29	6.42	45.37
10*	Toe off other	6.59	6.05	0.58	-0.58	6.42	45.17
11	foot	6.59	5.37	0.65	-0.58	6.49	45.03
12		6.59	4.16	0.65	-0.72	6.49	45.03
13		6.59	3.54	0.65	-0.87	6.56	45.17
14		6.59	2.11	0.65	-0.87	6.56	44.90
15		6.59	1.43	0.65	-0.87	6.62	44.76
16		6.04	0.41	0.65	-0.87	6.62	44.76
17		5.98	-0.68	0.65	-0.87	6.69	44.70
18		5.84	-1.90	0.65	-0.87	6.83	44.49
19		5.84	-2.86	0.65	-0.87	6.83	44.22
20		5.84	-4.22	0.65	-0.87	6.83	43.95
21		5.77	-5.58	0.65	-0.90	7.37	43.89
22		5.77	-7.21	0.65	-0.94	7.51	43.82
23		5.77	-8.71	0.65	-1.01	7.58	43.41
24		5.70	-9.80	0.65	-1.16	7.71	43.01
25		5.16	-10.94	0.65	-1.30	7.85	43.21
26		5.09	-12.71	0.65	-1.38	8.60	43.01
27		5.09	-14.75	0.65	-1.45	8.60	43.01
28		4.69	-16.60	0.58	-1.81	9.41	43.01
29*	Heel strike	4.28	-18.98	0.58	-2.10	10.64	43.14
30	other foot	3.12	-21.43	-0.14	-2.39	11.93	42.87
31		1.09	-25.03	-0.72	-2.97	13.90	42.87
32		-1.97	-29.80	-0.87	-3.77	15.26	43.14
33		-5.37	-34.90	-1.01	-4.26	17.58	42.80
34*	Toe strike	-8.96	-39.73	-1.59	-4.57	19.62	43.34
35		-14.53	-45.03	-1.74	-4.78	20.71	43.89

Table B-12 Reference Coordinates for Subject D, Test Run 4

S.No.	Locomotion event during stance phase	X-coordinate, cm		Y-coordinate, cm		Z-coordinate, cm	
		Ankle XA	Knee XK	Ankle YA	Knee YK	Ankle ZA	Knee ZK
1		13.79	30.68	0.14	0.16	8.87	45.24
2		12.43	27.28	0.14	0.16	7.78	44.90
3*	Heel strike	11.82	23.88	0.14	0.16	6.42	44.49
4		10.19	20.61	0.14	0.07	6.15	44.63
5		9.03	14.90	0.14	0.00	6.28	44.63
6		8.69	15.65	0.16	-0.14	5.94	46.10
7		8.69	13.33	0.16	-0.22	5.94	45.30
8		8.56	12.24	0.14	-0.43	5.94	45.37
9*	Toe off other	8.56	10.18	0.14	-0.65	5.94	45.84
10	foot	8.56	9.12	0.00	-0.80	5.94	45.57
11		8.56	8.41	0.22	-0.94	5.94	45.37
12		8.56	8.03	0.29	-1.09	5.94	45.64
13		8.56	7.07	0.36	-1.30	5.94	45.51
14		8.49	6.67	0.58	-1.59	5.94	45.37
15		8.49	5.92	0.72	-1.38	5.94	45.55
16		8.49	5.17	0.58	-1.30	5.94	45.68
17		8.49	3.95	0.43	-1.23	5.94	45.22
18		8.49	2.79	0.29	-1.23	5.94	45.14
19		8.49	1.50	0.22	-1.16	5.94	45.37
20		8.49	-0.14	0.22	-1.16	5.94	45.03
21		8.49	-1.29	0.14	-1.16	6.22	44.76
22		8.49	-2.86	0.14	-1.16	6.22	44.63
23		8.08	-4.08	0.14	-1.16	6.69	44.36
24		8.08	-5.65	0.14	-1.16	6.69	43.95
25		7.61	-7.07	0.14	-1.17	7.10	43.55
26		7.61	-8.91	0.14	-1.17	7.10	43.41
27		7.13	-10.75	0.14	-1.17	7.71	43.28
28*	Heel strike	6.32	-13.06	0.14	-1.19	8.94	43.28
29	other foot	6.04	-15.24	-0.22	-1.38	9.75	43.48
30		5.23	-18.23	-0.29	-1.59	11.25	43.48
31		2.92	-21.90	-0.14	-1.88	13.09	43.52
32		0.95	-26.67	0.00	-2.17	14.58	43.34
33*	Toe strike	-2.65	-30.48	0.00	-2.25	17.03	43.55
34		-6.45	-36.33	0.29	-2.17	18.80	43.95
35		-11.21	-41.56	0.29	-2.10	20.16	43.95

APPENDIX - C

EXPERIMENTAL RESULTS ON KNEE JOINT LOADING FOR ALL THE TEST RUNS

Table C-1 Experimental Results for Subject B, Test Run 1

Data point No.	3	4	5	6	7	9	10	11	12	13
% of stance phase	28.2	30.67	33.13	38.04	42.94	52.76	57.67	62.58	65.03	67.48
Muscle active		QUADRICEPS FEMORIS					GASTROCNEMIUS			
Ratio between resultant knee joint force and body weight	2.86	2.905	3.62	4.546	3.008	1.592	1.902	2.315	2.403	2.115
Maximum muscle force (kg)				270.00					94.121	

Table C-2 Experimental Results for Subject B, Test Run 2

Data point No.	3	4	5	6	7	8	9	10	11
% of stance phase	25.32	30.38	35.44	40.5	45.57	50.63	55.7	60.76	63.29
Muscle active		QUADRICEPS FEMORIS					GASTROCNEMIUS		
Ratio between resultant knee joint force and body weight	1.827	2.212	2.779	3.224	2.645	0.903	1.919	2.177	1.933
Maximum muscle force (kg)				172.77				82.986	

Table C-3 Experimental Results for Subject B, Test Run 3

Data point No.	8	9	10	11	14	15	16	17
% of stance phase	28.57	33.3	38.09	42.86	57.14	61.9	66.67	71.43
Muscle active	QUADRICEPS FEMORIS				GASTROCNEMIUS			
Ratio between resultant knee joint force and body weight	1.862	1.953	1.964	1.833	2.729	3.364	3.374	2.916
Maximum muscle force (kg)	78.366				169.542			

Table C-4 Experimental Results for Subject B, Test Run 4

Data point No.	3	4	5	6	9	10	11	12
% of stance phase	19.28	21.69	24.1	26.5	55.42	60.24	65.1	67.47
Muscle active	QUADRICEPS FEMORIS				GASTROCNEMIUS			
Ratio between resultant knee joint force and body weight	1.446	1.509	1.465	1.154	5.017	5.657	5.242	5.166
Maximum muscle force (kg)	37.799				332.88			

Table C-5 Experimental Results for Subject C, Test Run 1

Data point No.	2	3	4	5	6	9	10	11	12	13
% of stance phase	21.43	24.29	27.14	30.0	32.86	52.86	55.71	58.57	61.43	64.29
Muscle active		QUADRICEPS FEMORIS					GASTROCNEMIUS			
Ratio between resultant knee joint force and body weight	2.065	2.155	2.165	2.089	1.878	3.823	4.06	3.901	3.545	3.399
Maximum muscle force (kg)			83.295				193.176			

Table C-6 Experimental Results for Subject C, Test Run 2

Data point No.	1	2	3	4	9	10	11	12	13
% of stance phase	23.94	26.76	29.58	32.39	61.97	64.79	67.61	73.24	76.06
Muscle active		QUADRICEPS FEMORIS				GASTROCNEMIUS			
Ratio between resultant knee joint force and body weight	2.229	2.124	1.989	1.837	5.523	5.627	5.702	5.354	4.961
Maximum muscle force (kg)	84.939					288.151			

Table C-7 Experimental Results for Subject C, Test Run 3

Data point No.	6	7	8	9	10	11	12	13	14
% of stance phase	23.53	26.47	29.41	35.29	41.18	47.06	52.94	55.88	58.82
Muscle active	QUADRICEPS FEMORIS					GASTROCNEMIUS			
Ratio between resultant knee joint force and body weight	2.422	2.676	2.76	1.966	4.895	5.437	5.86	6.118	6.031
Maximum muscle force (kg)			120.457					317.89	

Table C-8 Experimental Results for Subject C, Test Run 4

Data point No.	3	4	5	6	9	10	11	12	13
% of stance phase	34.07	37.04	40.0	42.96	51.85	54.81	57.78	60.74	63.7
Muscle active	QUADRICEPS FEMORIS					GASTROCNEMIUS			
Ratio between resultant knee joint force and body weight	2.397	2.925	3.299	2.819	5.112	5.513	5.488	5.271	4.768
Maximum muscle force (kg)			150.103			275.80			

Table C-9 Experimental Results for Subject D, Test Run 1

Data point No.	2	3	4	5	6	7	8	9	10
% of stance phase	20.0	23.3	26.6	30.0	65.0	68.3	71.6	75.0	78.3
Muscle active	QUADRICEPS FEMORIS					GASTROCNEMIUS			
Ratio between resultant knee joint force and body weight	2.881	3.06	2.982	2.643	1.66	1.994	1.881	1.648	1.157
Maximum muscle force (kg)		113.821				55.434			

Table C-10 Experimental Results for Subject D, Test Run 2

Data point No.	2	3	4	5	6	7	8	9	10
% of stance phase	13.5	16.9	20.3	23.7	64.4	67.79	71.18	74.57	77.96
Muscle active	QUADRICEPS FEMORIS					GASTROCNEMIUS			
Ratio between resultant knee joint force and body weight	4.435	4.664	4.342	3.962	1.669	1.763	1.672	1.191	0.867
Maximum muscle force (kg)		205.107				40.803			

Table C-11 Experimental Results for Subject D, Test Run 3

Data point No.	1	2	3	4	5	6	7	8	9	10
% of stance phase	16.1	19.3	22.58	25.8	29.0	62.9	66.1	69.3	72.58	75.8
Muscle active		QUADRICEPS FEMORIS					GASTROCNEMIUS			
Ratio between resultant knee joint force and body weight	3.464	3.917	3.798	3.896	3.458	2.86	2.558	2.413	2.358	1.86
Maximum muscle force (kg)		170.818				107.673				

Table C-12 Experimental Results for Subject D, Test Run 4

Data point No.	2	3	4	5	6	7	8	9	10
% of stance phase	13.1	16.39	19.67	22.95	67.2	70.49	73.77	77.0	80.3
Muscle active		QUADRICEPS FEMORIS					GASTROCNEMIUS		
Ratio between resultant knee joint force and body weight	3.086	3.49	3.491	3.309	3.115	3.241	3.505	3.287	3.085
Maximum muscle force (kg)			141.49				148.311		